[redacted]

LOCKHEED-GEORGIA COMPANY

A DIVISION OF LOCKHEED AIRCRAFT CORPORATION

ER 6785

COMPONENTS IRRADIATION TEST NO. 1

Transistors and SCR's

21 February 1964

Prepared For:

GEORGE C. MARSHALL SPACE FLIGHT CENTER

Prepared By:

Georgia Nuclear Laboratories

GEORGIA NUCLEAR LABORATORIES
Lockheed-Georgia Company - A Division of Lockheed Aircraft Corporation

If this document is supplied under the requirements of a United States Government contract, the following legend shall apply unless the letter U appears in the coding box:

This data is furnished under a United States Government contract and only those portions hereof which are marked (for example, by circling, underscoring or otherwise) and indicated as being subject to this legend shall not be released outside the Government (except to foreign governments, subject to these same limitations), nor be disclosed, used, or duplicated, for procurement or manufacturing purposes, except as otherwise authorized by contract, without the permission of Lockheed-Georgia Company, A Division of Lockheed Aircraft Corporation, Marietta, Georgia. This legend shall be marked on any reproduction hereon in whole or in part.

The "otherwise marking" and "indicated portions" as used above shall mean this statement and includes all details or manufacture contained herein respectively.

Code: U	Contract: NAS 8-5332

FOREWORD

This report is submitted to the Astrionics Laboratory of the George C. Marshall Space Flight Center, National Aeronautics and Space Administration, Huntsville, Alabama, in accordance with the requirements of Task Order No. ASTR-LGC-4 of Contract No. NAS 8-5332. The report describes radiation effects on four types of transistors and one type silicon controlled rectifier. The test was performed by the Georgia Nuclear Laboratories, Lockheed-Georgia Company.

TABLE OF CONTENTS

LIST OF TABLES AND FIGURES

LIST OF TABLES AND FIGURES
(Continued)

LIST OF TABLES AND FIGURES
(Continued)

LIST OF TABLES AND FIGURES
(Continued)

1.0 SUMMARY

All test specimens were subjected a radiation exposure of about 2.9×10^{14} n/cm^2 and at a constant temperature of 100°F. At the end of the irradiation period all SCR specimens had failed and the current gain of all transistor specimens had decreased to less than 35% of their original value. The transistor specimens consisted of both new units and units which had been subjected to previous environmental test. Considering only the new specimens, the following tabulation describes the radiation exposure at which the current gain of these type units had decreased to 50% of its original value. These values represent the mean of each of the specimen groups.

2N722	4.1×10^{12} n/cm^2	5.7×10^5 r
2N697	6.8×10^{12} n/cm^2	7.5×10^5 r
2N657A	2.3×10^{11} n/cm^2	1.9×10^5 r
2N1016D	1.15×10^{11} n/cm^2	1.5×10^5 r

Statistical analyses have indicated that prior environmental tests alter the effects of radiation on these devices. The principal alteration is in the statistical spread of the groups. Units which have been subjected to prior environmental tests tend to exhibit larger current gain spreads within the group. In the case of the 2N1016 significant changes were also noted in the means of the groups; however, the transistor specimens in each group were not completely identical and this could cause differences in the mean.

Analysis of the radiation induced failure distribution of these transistors

has shown that significant safety factors must be considered to assure their reliable operation in electronic circuits exposed to nuclear radiations.

The I_{cbo} measurements performed on all specimens during the irradiation showed that this parameter did not increase above the manufacturer's specification until the current gain of the transistor had degradated to an unusable value. For practical circuit applications normal bias point stabilization techniques should be sufficient to stabilize I_{cbo}.

The silicon control rectifier specimens irradiated in this test exhibit discontinuities which were apparently radiation induced at an exposure of 1.09×10^{8} n/cm^2. These discontinuities were evident on five of the SCR specimens. The SCR specimens which did not exhibit these discontinuities were grouped and operated into the order of 10^{12} n/cm^2 without serious degradation. Complete failure of the SCR specimens occurred between the exposures of 7.43×10^{12} n/cm^2, and 6.07×10^{5} r to 2.79×10^{13} n/cm^2 and 7.73×10^{5} r.

2.0 INTRODUCTION

The experiment described in this report is the second in a series of radiation effects tests on electronic equipment, circuits, and components contemplated for use on the RIFT vehicle. Since the use of equipment on this vehicle is contingent upon its ability to withstand the RIFT nuclear environment, the Astrionics Laboratory of the Marshall Space Flight Center has undertaken to assure that government furnished or specified equipment will survive this environment. The equipment is to be subjected to the expected RIFT nuclear environment as simulated at the Georgia Nuclear Laboratories. Measurements made on the equipment during the irradiation will describe its radiation tolerance.

The subject of this test is four types of transistors and one type silicon controlled rectifier.

3.0 TEST PROCEDURE

Five types of semi-conductor components, consisting of 72 transistors of 4 types and 15 silicon controlled rectifiers (SCR's) of 1 type, were exposed to 5.5×10^5 r, behind a neutron attenuator shield. The shield was then removed and the test resumed until an integrated neutron flux of 2.4×10^{14} n/cm^2 was accumulated. During the test, all specimens were mounted in a controlled temperature chamber held at $100^\circ \pm 3^\circ$F. Before, during, and after the irradiation, measurements of h_{FE} and I_{cbo} were made on all transistor specimens and measurements of V_{gf}, I_{gf}, I_h, I_r and V_{bo} were made on the SCR specimens. Other measurements made during the test included those necessary to define the nuclear and temperature environments.

3.1 TEST SPECIMENS

The semi-conductors were breadboard mounted by the Astrionics Laboratory of the George C. Marshall Space Flight Center, NASA, Huntsville, Alabama and submitted to GNL for irradiation. Instrumentation circuitry and mounting hardware were provided by GNL.

3.1.1 Specimen Description

The semi-conductor devices tested were (15) 2N657A transistors, (15) 2N697 transistors, (27) 2N722 transistors, (15) 2N1016 transistors, and (15) 2N1774 silicon controlled rectifiers (SCR). Some of the 87 specimens received had been previously subjected to environmental testing by MSFC-ASTR (Table 1). Even though many of the specimens were not new items, the parameters measured prior to irradiation

conformed to manufacturer's specifications (Tables 2 and 3).

Test specimens 2N657A (NPN), 2N697 (NPN), and 2N722 (PNP) are low power transistors, whereas the 2N1016 (NPN) transistors are high power types. The SCR specimens irradiated in this test are a low current type.

3.1.2 Specimen Mounting

When received at GNL, specimens were mounted on breadboards as follows:

TYPE COMPONENT	TYPE BREADBOARD
2N657A (NPN)	12" x 12" printed circuit fiberglass
2N697 (NPN)	12" x 12" printed circuit fiberglass
2N722 (PNP)	12" x 12" printed circuit fiberglass
2N1016 (NPN)	8" x 12" aluminum heat sink
SCR 2N 1774	8" x 12" aluminum heat sink

GNL received the specimen boards with the transistor leads soldered in place. Thin mica washers insulated the 2N1016 and SCR specimens from the aluminum heat sinks. No moisture inhibiting coating or epoxy was used on the circuit boards.

Each breadboard was mounted vertically on the test fixture to equalize flux distribution over the test specimens (Figure 1). The test fixture was placed in a controlled temperature chamber adjacent to the reactor with the SCR specimen board located where the maximum flux rates were expected.

3.2 TEST SPECIMEN MEASUREMENTS

A complete set of data was taken at ambient temperature (70°F) and

again at $100 \pm 3^{\circ}F$ to establish baseline data for the irradiation; all measurements were made with the test fixture in place at the Reactor Facility.

During the irradiation, a complete set of measurements was made on all specimens at least once every half hour; also a complete set of data was taken at each radiation rate from 2.1×10^{5} n/cm^2/sec to 6.5×10^{10} n/cm^2/sec. Immediately after cessation of the irradiation a complete set of post-irradiation data was taken. All transistor and silicon controlled rectifier specimens had failed at this time.

3.2.1 Transistors

The transistor parameters monitored during the experiment were h_{FE} and I_{cbo}. The bias conditions necessary for these measurements have been tabulated in Table 4. Current gain, h_{FE}, was calculated by measuring the base current, I_b, at a constant collector current, I_c. The following relationship was used to calculate h_{FE}:

$$h_{FE} \approx \frac{I_c}{I_b}$$

The collector to emitter voltage, V_{ce}, associated with each measurement is also tabulated in Table 4.

To verify the test system integrity, measurements of leakage current were also made on an unused breadboard position. All leakage values measured were negligible when compared to the I_{cbo} specimen measurements. Therefore, board leakage was not considered in the data reduction.

3.2.2 Silicon Controlled Rectifiers

The silicon controlled rectifier parameters monitored during the experiment were: gate firing voltage, V_{gf}, gate firing current, I_{gf}, holding current, I_h, breakover voltage, V_{bo}, and reverse current, I_r. The bias conditions necessary for performing these measurements have been tabulated in Table 5 . V_{gf}, I_{gf} and I_h were measured for ten specimens; V_{bo} and I_r were measured for the remaining five specimens.

3.3 TEST SPECIMEN INSTRUMENTATIONS

All measurements were performed at the Reactor Facility operations area, approximately 300 cable feet from the test specimens at the reactor. (Appendix B contains a description of the Georgia Nuclear Laboratories Facility). Individual leads were connected to each specimen and the specimens were commutated in the operations area.

The transistor monitoring equipment yielded a digital, typewriter tabulation of base currents. The SCR measurements were performed manually.

3.3.1 Transistor Measurement Circuit

The circuit shown in Figure 2 was used to measure I_{cbo} and h_{FE} parameters of all transistor specimens. Since the emitter leads of all specimens on each breadboard were commoned, only the base and collector terminals were connected to the operations area commutator by permanent cabling. A five-conductor instrumentation cable was connected to the emitter circuit of each breadboard to provide isolation between boards and to reduce the emitter

lead resistance.

The test circuit was designed to automatically vary the base bias current (I_b) to obtain the specified collector current (Table 4). The base current (I_b) was measured with an L & N Data Logging System, which tabulated the data (Figure 3).

Feedback loop operation of the test circuit, Figure 2, held the quiescent point to a constant I_c. The collector current feedback is obtained as the difference between the IxR drop across Resistor R_3 and the bucking voltage of the mercury cell. The difference existing between the two voltages is amplified and used to establish the base bias current. Improvements in system stability were achieved by damping circuits in both the feedback amplifier and Data Logging System inputs.

Reference to the test diagram in Figure 2 indicates the two switches which were actuated to perform the I_{cbo} measurement. Specimen reverse current (I_{cbo}) was measured by opening the emitter switch and reversing the Data Logging System polarity. The feedback loop was also shorted out.

3.3.2 Silicon Control Rectifier Measurement Circuit

The silicon controlled rectifier parameters were measured by the circuits shown in Figures 4 and 5. The circuit of Figure 4 is designed to measure the minimum gate firing voltage, V_{gf}; the minimum gate firing current, I_{gf} and the minimum holding current, I_h, while the circuit of Figure 5 is designed to measure the reverse current, I_r and the minimum breakover voltage, V_{bo}.

All SCR specimens were connected through instrumentation cables to special commutators located near the reactor. The commutators were connected through a common cable to the operations area. Common cathode terminals on the (10) specimen group permitted connection to the Operations Area with a single instrumentation cable.

The Harrison Labs model 865-B power supply was used as a constant voltage and current source. Anode voltage was set at 30 v and the gate voltage or current was manually increased until the SCR fired. The increasing gate voltage was monitored on a 4 channel Sanborn Recorder. A similar scheme was used to measure I_{gf} and the data was recorded on the Sanborn (Figures 4, 5, and 6). After the second firing, the anode voltage was decreased until forward conduction ceased. The forward current was continuously monitored and the discontinuity noted when forward conduction ceased was recorded as the minimum holding current (I_h).

Figure 5 shows the circuit used to monitor the minimum breakover voltage and reverse current. The breakover voltage was measured by gradually increasing the anode supply voltage from 0 to 480 v while monitoring the series circuit current. When breakover occurred, the voltage (V_{vo}) was recorded.

The reverse current was measured by a micromicroammeter at a reverse bias of 200 v dc. (Table 5).

3.4 TEST SEQUENCE

3.4.1 Pre-Irradiation Tests

The measurements described in Paragraph 3.2 were accomplished twice at

each environment temperature prior to the irradiation. Two complete sets of measurements were made at ambient temperature and again after the temperature chamber had stabilized.

3.4.2 During Irradiation Tests

The measurements described in Paragraph 3.2 were accomplished in complete sets approximately 1/4 hour apart. All measurements were made with the specimens in the temperature chamber at $100^{\circ} \pm 3^{\circ}F$.

3.4.3 Post-Irradiation Tests

The measurements described in Paragraph 3.2 were accomplished immediately upon cessation of the irradiation and periodically after the irradiation. The post-irradiation tests were made on all specimens in the temperature chamber at $100^{\circ} \pm 3^{\circ}F$ and later at ambient.

3.5 TEST ENVIRONMENT

The semiconductor components breadboards were kept in containers at atmospheric pressure and ambient temperature (approximately $73^{\circ}F$) until they were placed in the $100^{\circ}F$ temperature chamber. The test was conducted at atmospheric pressure.

3.5.1 Temperature

Iron-constantan thermocouples were mounted on one specimen on each of the six breadboards (Figure 7). A thermocouple was also used to control the chamber air temperature to $100^{\circ} \pm 3^{\circ}F$. The chamber temperature was held to $100^{\circ} \pm 3^{\circ}F$ for the entire period of testing and irradiation.

3.5.2 Nuclear

All semiconductor specimens were subjected to a simulated RIFT vehicle

nuclear environment. Nuclear irradiation took place in two phases; the first phase was conducted behind a 20" water shield which served as a neutron attenuator and the second phase was conducted with no shielding. The neutron/gamma ratio behind the shield was about 10^6 nvt/r as compared to about 10^8 nvt/r without the shield. The neutron/gamma ratio predicted for the instrumentation unit of the RIFT vehicle is about 2×10^5 nvt/r. During the irradiation, both neutron and gamma radiation were monitored and recorded for each breadboard. Isoline radiation flux plots were made for the test panel to aid in data reduction.

3.5.2.1 Gamma Dose Measurements

Lockheed Model 505 ionization chambers were used to monitor the gamma dose rate. The Model 505 is a graphite-walled CO_2-filled chamber with a sensitive volume of 4 cubic centimeters. To insure accuracy of the gamma measurements, each chamber was calibrated prior to the irradiation test in a known Co^{60} source field.

The gamma dose rate was the independent variable for the first phase of the irradiation. Gamma dose was monitored by (12) Model 505 ion chambers and the radiation rate level set by utilizing data obtained from those located near the test panel center. The ion chamber locations were as shown in Figure 8.

3.5.2.2

Neutron activation foils and a GNL Thorium (Th^{232}) plate fission

counter were used to measure the neutron flux for the fast and thermal energy regions. The fission chamber permitted flux monitoring during irradiation and was used as a reference check on the reactor power setting and activation foil data.

Thirty nickel (Ni^{58}) activation foils were mounted on the breadboards prior to irradiation (Figure 8). Immediately after the first irradiation phase, all foils were removed and counted to determine the integrated neutron flux. Fresh foils were positioned prior to the second irradiation phase and were removed for measurement immediately after cessation of the test. Foil activation was measured following the first and second phases of irradiation, with integrated flux data calculated from the reactor power history and fission chamber data.

A foil packet was located near the test panel center to determine the neutron energy spectrum both with and without the water shield (see Figures 1 and 8). The foil packet materials and their respective reactions are tabulated below:

Foil Material & Reaction	Effective Threshold Cross Section* (Barns)	Effective Threshold Energy* (Mev)
Th^{232} (n, f) F. P.	0.15	1.75
S^{32} (n, p) P^{32}	0.30	2.9
Ni^{58} (n, p) C^{58}	1.23	5.0
Mg^{24} (n, p) Na^{24}	0.048	6.3
Al^{27} (n, a) Na^{24}	0.11	8.1
Co^{59} (n, γ) Co^{60}**	36.3***	Thermal
Na^{23} (n, γ) Na^{24}**	0.536***	Thermal
Mn^{55} (n, γ) Mn^{56}**	13.3***	Thermal

*Effective threshold cross sections and the corresponding effective threshold energies are calculated on the basis of a fission spectrum (Figures 9 and 10).

**These foils are cadmium covered. An additional Co^{59} foil was bare.

***2200 m/s reaction cross section.

4.0 METHOD OF DATA ANALYSIS

Standard statistical techniques were used in the reduction and analysis of the data obtained during the test. The parameters which were measured, or derived from the measured data, were assumed to be normally distributed. Normalization of a parameter was accomplished in the usual manner, i.e., by dividing each measured value by its corresponding pre-irradiation value.

Standard deviations were computed from an accepted formula for small groups when the population mean is unknown. This formula is:

$$S = \sqrt{\frac{\Sigma(X^2) - (\Sigma X)^2/n}{n-1}}$$

Group means were computed in the normal manner.

In those cases where specimens of the same type had different histories (some were new, some had been temperature cycled, etc.), those specimens with the same history were grouped, and means and standard deviations were computed for each group. In order to determine whether or not significant differences existed between the groups, the means were compared using the 'students'-t' test and the variances were compared using the 'variance-ratio' test. The 95% confidence level was used for both tests. For the 2N722 transistors no significant difference between the means of the groups was indicated. However, significant difference between the groups' variances was indicated. Consequently, the data have been presented separately for each group (Figures 25 through 30). Data for the three groups of the 2N1016 transistor have likewise been presented separately because the tests indicated significant differences between group means and variances.

With respect to certain parameters some specimens appeared to behave quite differently from the majority of their respective groups. The data from these non-conforming specimens have been presented in separate figures and were not included in the calculation of group means and standard deviations.

Radiation environmental data shown on the figures' abscissae were obtained by integrating with respect to time the applicable gamma dose rates and heutron flux rates.

Most of the figures which present the test data show a smooth curve through the means and two other smooth curves through the loci of the points which fall plus and minus one standard deviation from the curve through the means. The two outer curves delineate a zone which theoretically contains about 68% of the population. A zone twice as wide as the one shown and centered on the mean theoretically contains 95% of the population; a similar zone three times as wide as the one shown theoretically contains 99.7% of the population.

5.0 TEST DATA AND DISCUSSION OF RESULTS

The test data has been presented herein in graphical form. The radiation exposure, plotted on the abscissa, is in all cases, a combination of neutrons and gammas. The graphs, however, are drawn considering only one of these parameters at a time. Two separate plots are therefore included for each test value. It should be noted, however, that, even though the graph considers only one type of radiation the other was also inherent in the irradiation.

5.1 SILICON CONTROL RECTIFIERS TYPE 2N1774

Fifteen SCR type 2N1774 were subjected to the radiation environment. On 10 of the specimens the following parameters were monitored during the irradiation: gate firing voltage, V_{gf}, gate firing current, I_{gf}, and holding current, I_h. Reverse current, I_r, and breakover voltage, V_{bo}, were monitored on the other five specimens. All of the test specimens survived the radiation exposure experienced behind the water shield without significant degradation of their parameters. A factor of two increase in the holding current was noted at an integrated flux of about 2×10^{12} n/cm^2 (Figure 15). The specimens started to suffer complete failure at about 5×10^{12} n/cm^2. All parameters of the SCR's exhibited increased parameter spreads as a function of radiation. Erratic operation of some test specimens which was noted at low radiation levels, appeared to be more erratic as the radiation level increased.

The most significant parameter change was the holding current, I_h. V_{gf} and I_{gf} increased by factors of about two just before complete

failure, where circuit design safety factors are normally on the order of three or four times. The complete failure mentioned here means the SCR would not support current flow; i.e., would not fire.

Figures 11 and 12 present the mean and standard deviation of the gate firing voltage as a function of integrated neutron flux and gamma dose respectively. An increase in the spread of the gate firing voltage over the ten test specimens is seen as the radiation level increases. The increased spread points to a possible decrease in the reliability of these devices when operated to radiation levels of this order. A small discontinuity is noted when the water shield is removed. This discontinuity is similar to those seen in other SCR parameters and in the transistor specimens. The dip in the curve noted at 2×10^{12} n/cm^2 is apparently a characteristic of the SCR's, since all test specimens exhibited this phenomena. Figure 12 is presented primarily for reference. On Figure 11 note that the tangential slope of the mean curve is very nearly equal before and after the water shield was removed. It may be concluded then that the degradation suffered by the SCR's is contributed almost entirely by the neutrons.

Figures 13 and 14 present the gate firing current as a function of integrated neutron flux and gamma dose respectively. As is probably to be expected, these curves are very similar to the gate firing voltage curves just presented. A gradual increase in gate firing current with the radiation level is seen and a slight discontinuity is again noted at the point where the water shield was removed. The data point at about 2.4×10^{11} appears to be erroneous.

Figures 15 through 21 show the holding current measured for the test specimens. Figure 15 shows the holding current of five specimens vs. integrated flux. Figures 17 through 21 show the holding current of the remaining five specimens. The specimens shown in these last five figures exhibited erratic behavior during the irradiation. The means of the holding current of the five consistent specimens (Figure 15) show the large increases in holding current before failure of the test specimens. This increase in holding current is significant to the design engineer.

Specimens 2, 6, 7, 8, and 9 all show a tendency to operate in two different holding current modes. Both modes offer data points which describe parallel loci. All specimens except specimen #6 exhibit this behavior starting after an integrated neutron flux of about 10^{10} n/cm^2. The current difference between the two modes of operation varied from 10 ma to 20 ma. Specimen #6 exhibited its first shift, increasing its holding current to 22 ma, at 1.09×10^8 n/cm^2.

The mean reverse current measured through Specimens 11, 13, 14 and 15 is shown in Figure 22. The mean of the specimens and the standard deviations have been presented. No significant changes in the reverse current are noted up to a radiation level of 2×10^{12} n/cm^2. The variations seen in the figure are most likely due to variations in the instrumentation. At higher radiation exposures a definite decrease in the I_r parameter is seen. The effect appears to be due to the total radiation exposure and no radiation rate effects are noted. Specimen #12 exhibited considerably different reverse current characteristics and was plotted separately in Figure 23. A negative current of 80 μa was

measured through this specimen which increased to a current of about $-30\,\mu a$ at 10^{12} n/cm^2. Considerable apparent annealing during the time that the water shield was removed is also noted. The reason the specimen exhibited much different characteristics from the other reverse current specimens is not known. The reverse current for Specimens 11, 13, 14 and 15 is shown in Figure 24 plotted as a function of gamma dose.

The radiation did not cause the breakover voltage, V_{bo}, to become greater than the test voltage, 480 v dc.

5.2 TRANSISTORS TYPE 2N722 (PNP)

Twenty-seven (27) type 2N722 (PNP) transistors were tested. Of the twenty-seven, fifteen were new (Group N), six had been subjected to temperature cycling (Group T), and six had been subjected to vibrations and accelerations (Group V) prior to irradiation.

The data obtained from the specimens were grouped into three groups according to the specimens' histories. The reduced data were then subjected to certain statistical tests as explained in Section 4. The parameters measured during the test were current gain h_{FE}, or β, and the leakage current, I_{cbo}.

Figures 25, 27, and 29 present the normalized beta parameter of the three groups versus integrated neutron flux. Figures 26, 28, and 30 show the same data versus gamma dose. Both plots are presented because, it is believed that both types of radiation appear to contribute to parameter degradation. From the figures it can be seen that h_{FE} for all three groups experienced degradation at almost the same rate as radiation exposure increased. The h_{FE} parameter had decreased to 70% of its pre-irradiation value after a combined exposure of

1.4×10^{12} n/cm^2 and 5.4×10^5 r (Figures 25 and 26). Other degradation percentages, as desired, can be determined from the figures.

Groups V (previously vibrated and accelerated specimens) had the largest variations in beta.

Maximum instrumentation sensitivity for the leakage current measurement was 1.0×10^{-7} amps. Only a limited number of specimens exhibited leakage currents large enough to measure both prior to, and during irradiation. The limited amount of data obtained appears to indicate that the leakage current decreases as radiation exposure increases. The data obtained was too limited for statistical treatment. It is summarized below for Groups N, T and V.

GROUP N (15 SPECIMENS)

Radiation Level n/cm^2	Radiation Level r	No. of Specimens With $I_{cbo} \geq 0.1 \mu a$	Range of I_{cbo} (μa)
0	0	6	.138 - .237
2.03×10^9	1.70×10^3	3	.129 - .138
2.19×10^{10}	1.84×10^4	3	.100 - .129
4.72×10^{10}	3.97×10^4	4	.100 - .129
7.25×10^{10}	6.09×10^4	4	.100 - .119
1.00×10^{11}	8.40×10^4	3	.100 - .109
1.23×10^{11}	1.03×10^5	2	.100 - .109
1.49×10^{11}	1.25×10^5	3	.100 - .109
1.82×10^{11}	1.53×10^5	2	.100
2.18×10^{11}	1.83×10^5	2	.100
2.67×10^{11}	2.24×10^5	1	.100
3.09×10^{11}	2.60×10^5	1	.100
		None until reactor shutdown for removal of water shield; then:	
6.47×10^{11}	5.43×10^5	3	.100 - .109
6.47×10^{11}	5.43×10^5	4	.100 - .326
		None after reactor startup	

GROUP T (6 SPECIMENS)

Radiation Level n/cm^2	Radiation Level r	No. of Specimens With $I_{cbo} \geq 0.1\mu a$	Range of $I_{cbo}(\mu a)$
0	0	1	.178
2.00×10^9	1.68×10^3	1	.178
2.16×10^{10}	1.82×10^4	1	.198
		This same specimen (No. 51) continued to show I_{cbo} varying between .188 and .198 μa until reactor shutdown for water shield removal; then:	
6.39×10^{11}	5.37×10^5	2	.129 - .168
6.39×10^{11}	5.37×10^5	2	.109 - .178
6.39×10^{11}	5.37×10^5	3	.100 - .178
		After reactor start-up specimen No. 51 continued to show I_{cbo} throughout the test varying between .168 - .208	

GROUP V (6 SPECIMENS)

Radiation Level n/cm^2	Radiation Level r	No. of Specimens With $I_{cbo} \geq 0.1\mu a$	Range of $I_{cbo}(\mu a)$
0	0	4	.119 - .702
1.99×10^9	1.67×10^3	3	.129 - .148
2.15×10^{10}	1.81×10^4	0	-
4.64×10^{10}	3.90×10^4	2	.119 - .237
7.14×10^{10}	5.99×10^4	0	-
1.21×10^{11}	1.02×10^5	1	.109
1.46×10^{11}	1.23×10^5	0	-
		No change until reactor shutdown for water shield removal; then:	
6.36×10^{11}	5.34×10^5	1	.138
6.36×10^{11}	5.34×10^5	4	.100 - .336
6.36×10^{11}	5.34×10^5	2	.100 - .227
		None after reactor start up	

5.3 TRANSISTORS TYPE 2N657A (NPN)

Since all 15 specimens of this type had the same history, the data for all was grouped and treated as explained in Section 4. The parameters measured during the test were the current gain h_{FE}, or β, and the leakage current, I_{cbo}.

Figure 31 shows the normalized h_{FE} parameter versus neutrons/cm^2. Figure 32 shows the same data versus gamma dose. From the figures it can be seen that the h_{FE} had decreased to 70% of its original value after exposure to 4.8×10^{10} n/cm^2 (Figure 31) plus 4×10^4 r (Figure 32). The beta parameter continued to decrease as radiation exposure increased.

This type transistor appears to be considerably less radiation resistant with regard to h_{FE} than the type 2N722 transistor discussed above. (Note, also, that the variation of mean beta was much larger than was that of the 2N722.)

Figure 33 shows leakage current for the 2N657A transistor versus integrated flux. Figure 34 shows the same data versus gamma dose. From the figures it can be seen that leakage current increased as integrated flux and gamma dose increased. It is also readily seen from the discontinuities and the varying slopes that there is a pronounced radiation rate effect on this parameter. Also, from the data obtained after reactor shutdown for water shield removal and upon completion of irradiation, it appears that this parameter shows some annealing.

5.4 TRANSISTORS TYPE 2N697 (NPN)

The data for all fifteen specimens were grouped and treated as described in Section 4.0.

Figure 35 shows the normalized h_{FE} plotted against integrated neutron flux, while Figure 36 shows the same data plotted against gamma dose. A discontinuity occurs in the curve at the point where the water shield was removed. As radiation exposure increased, h_{FE} decreased reaching 70% of its initial value at about 2.2×10^{12} n/cm^2 and 7.0×10^5 r. This performance was slightly better than that of the 2N722 transistor and considerably better than that of the 2N657A transistor. Variations in the h_{FE} value were about equal to those of the 2N657A Group V (previously vibrated and accelerated) specimens.

Leakage current for all specimens was initially less than 0.1 μa, and remained so until an accumulated exposure of 4.57×10^{13} n/cm^2 and 1.07×10^6 r had been received. At this point leakage currents varied from .138 to .208 μa. However, at the same point, the beta parameter was less than 20% of its initial value so the data on leakage current at the high exposure level are only of an academic interest.

5.5 TRANSISTORS TYPE 2N1016 (NPN)

The data from the fifteen specimens of this transistor were grouped as follows:

5 specimens (used) of 2N1016C
5 specimens (new) of S2N1016D
5 specimens (used) of 2N1016D

Figures 37, 39, and 41 present the normalized h_{FE} parameter for the three groups versus integrated flux. Figures 38, 40 and 42 present the same data versus gamma dose. All three groups experienced decreasing h_{FE} with increasing flux and dose levels. The used specimens of the 2N1016C group (Figure 37) exhibited a slightly slower rate of decrease than the other two groups (Figures 39 and 41). However, the variation in h_{FE} were larger for this group (2N1016C) than for either of the other two groups. From Figures 37 through 42 the accumulated radiation levels for 70% of initial h_{FE} are:

Group	Accumulated Radiation Level
2N1016 (used)	1.05×10^{11} n/cm^2 + 9.00×10^4 r
S2N1016D (new)	6.50×10^{10} n/cm^2 + 5.40×10^4 r
2N1016D (used)	4.50×10^{10} n/cm^2 + 3.80×10^4 r

Other percentages, as desired, may be determined from the figures in similar fashion. Figures 43 through 48 show the normalized leakage current (I_{cbo}) versus integrated flux and versus gamma dose. Some of the curves have been drawn with discontinuities at points of rate change. These discontinuities are suggested by the data obtained and have been confirmed by experience gained in other radiation tests. Whether or not similar discontinuities exist in the curves for the 2N1016D group (Figures 47 and 48) at rate change points cannot be determined from the data obtained.

Leakage current data for groups 2N1016C (used) and S2N1016D (new) Figures 43 through 46 show similar characteristics; i.e. an increase in

leakage current with increasing radiation at constant rate, and a "jump" in leakage current at the point of a radiation rate change. Group S2N1016D (new) showed the largest overall increase (Figures 45 and 46). Both groups showed a definite annealing effect when the reactor was shut down for removal of the water shield.

The leakage current data for Group 2N1016D (used) showed a decrease in leakage current as radiation exposure increased (Figures 47 and 48). This was in direct contrast with the other two groups. The mean leakage current for this group was significantly higher than the mean for the other groups prior to irradiation. This could mean that the first series of environmental tests deteriorated this parameter and the radiation caused annealing of the deterioration. This group also exhibited annealing when the reactor was shut down for water shield removal.

TABLE I - CONDITIONING OF TEST SPECIMENS

Semi-conductor Type	Specimen Numbers	Previous Specimen Tests			
		New Specimens	Used Specimens*	Temperature Cycled	Vibration & Acceleration
2N722	31 - 45	x			
2N722	46 - 51			x	
2N722	52 - 57				x
2N657A	1 - 15	x			
2N697	16 - 30	x			
2N1016C	11 - 15		x		
S2N1016D	1 - 5	x			
2N1016D	21 - 25		x		
2N1774	1 - 15	x			

* Previous environmental conditions unknown

TABLE 2 - MANUFACTURER'S SPECIFICATION FOR TRANSISTOR SPECIMENS

Transistor Type	Manufacturer	Description	Case Type	h_{FE}	I_{cbo}	f_{hfb}
2N657A	General Electric	NPN low power silicon mesa transistor ft · 15 mcs	TO-5	V_{ce} = 10 v 30-90, I_c = 200 ma	V_{cb} = 30 v 250 ma, T_j = 150°C	
2N697	General Electric	NPN low power silicon planar passivated transistor ft · 130 mcs	TO-5	V_{ce} = 10 v 40-120, I_c = 150 ma	V_{cb} = 30 v 100 ma, T_j = 150°C	80 mcs
2N722	Texas Instruments	PNP low power silicon transistor	TO-18	30	V_{cb} = 10 v 1 μa, T_j = 25°C	96 mcs
2N1016C	Westinghouse	NPN high power fused silicon transistor	MT-1	10-18	V_{cb} = 4 v 10 ma, T_j = 25°C	30 kcs
2N1016D	Westinghouse	NPN high power fused silicon transistor	MT-1	10-18	V_{cb} = 4 v 10 ma, T_j = 25°C	30 kcs
S2N1016D	"	NPN transistor	MT-1	-	-	-

TABLE 3 - MANUFACTURER'S SPECIFICATION FOR SCR SPECIMENS

SCR Type	Manufacturer	V_{gf}	I_{gf}	I_H	I_r	V_{bo}	G. E. Case Outline Drawing
2N1774	General Electric	10.0 v (peak value)	2.0 amps (peak value)	4.0 ma	3.0 ma	200 v min	C11B

TABLE 4 - TRANSISTOR TEST BIAS CONDITIONS

Transistor Type	Measured Parameter		Bias Conditions			
	I_{cbo}	h_{FE}	V_{cb}	I_e	V_{ce}	I_c
2N657A	x		30 volts dc	0	-	-
2N657A		x	-	-	10 volts dc	50 ma
2N697	x		30 volts dc	0	-	-
2N697		x	-	-	10 volts dc	25 ma
2N722	x		-40 volts dc	0	-	-
2N722		x	-	-	-10 volts dc	5 ma
2N1016C	x		30 volts dc	0	-	-
2N1016C		x	-	-	30 volts dc	500 ma
2N1016D	x		30 volts dc	0	-	-
2N1016D		x	-	-	30 volts dc	500 ma
S2N1016D	x		30 volts dc	0	-	-
S2N1016D		x	-	-	30 volts dc	500 ma

TABLE 5 - SCR TEST BIAS CONDITIONS

SCR Type	Measured Parameter			Test Conditions		
	V_{gf}, I_{gf}, I_H	I_r	V_{bo}*	I_f	V_{gf}	P_{rv}
2N1774	x			1.0 amps	-	-
2N1774		x		-	0.0 volts	200 volts dc
2N1774			x	-	0.0 volts	

* Maximum test Vbo was limited to 480 v dc.

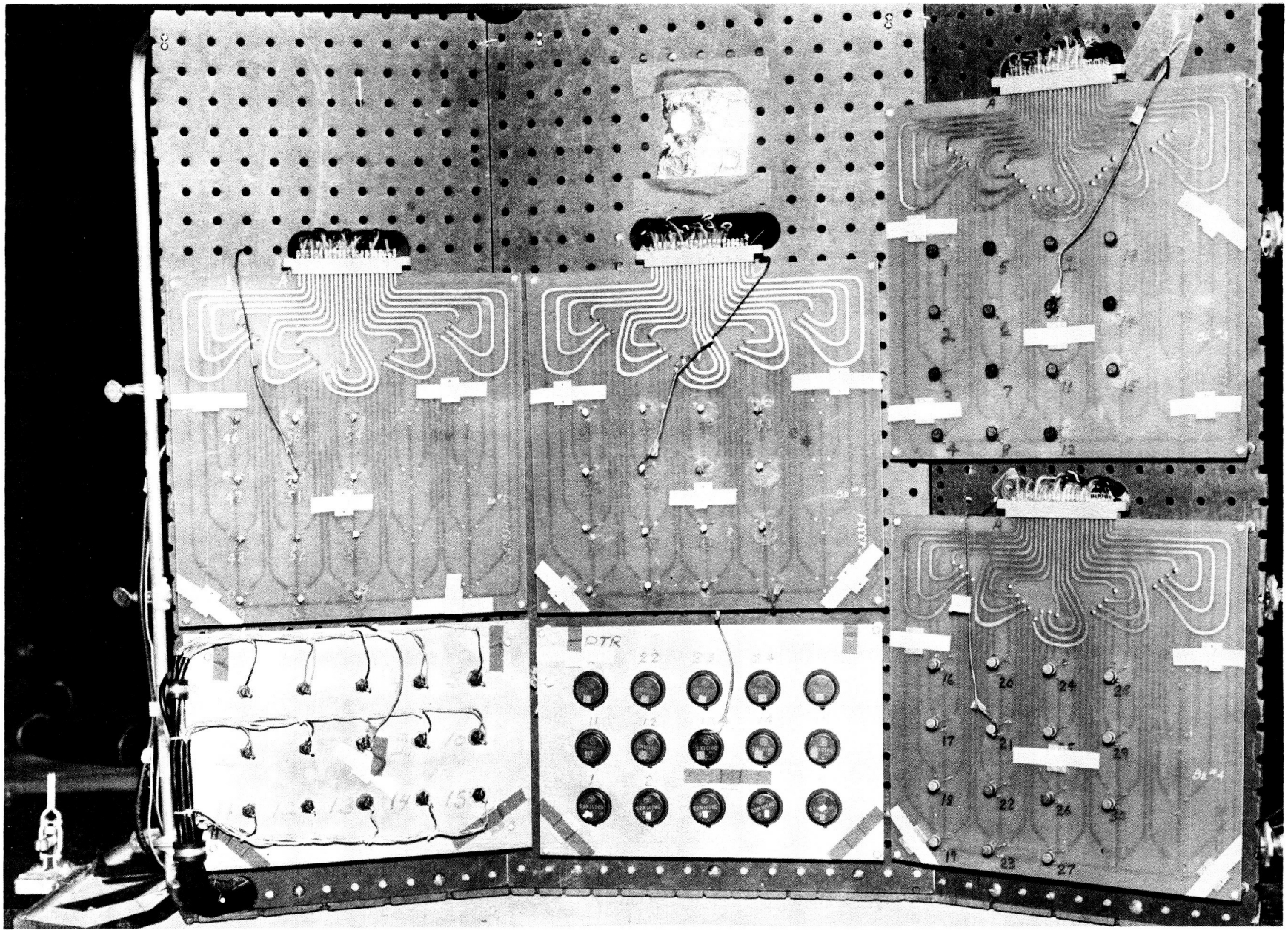

FIGURE 1 SPECIMENS MOUNTED ON TEST PANEL

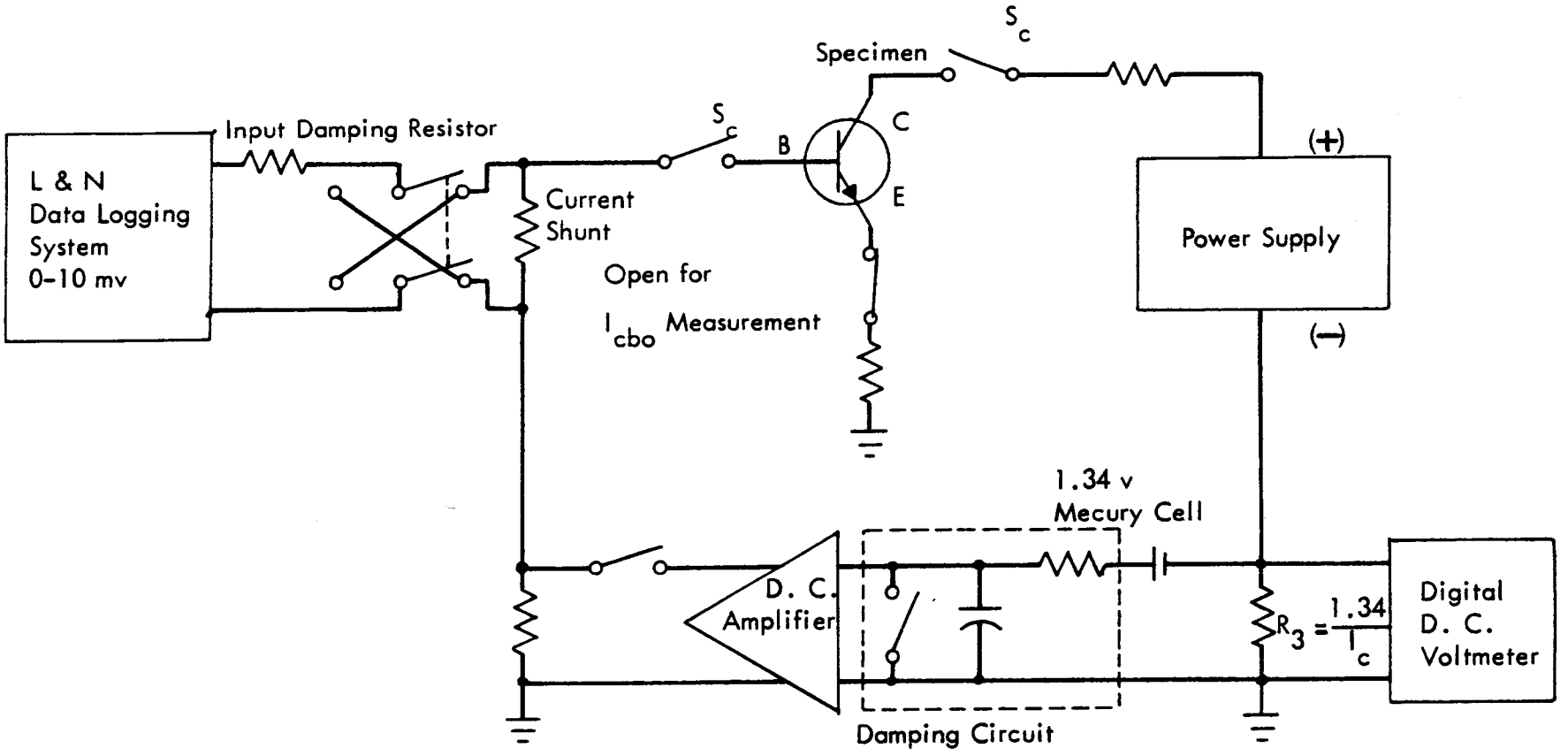

(1) All switches are shown in the h_{FE} measurement configuration.
(2) Sources and Data Logging System polarities are reversed for a PNP type transistor.
(3) Commutator switches are denoted by S_c.

FIGURE 2 TRANSISTOR MEASUREMENT CIRCUIT

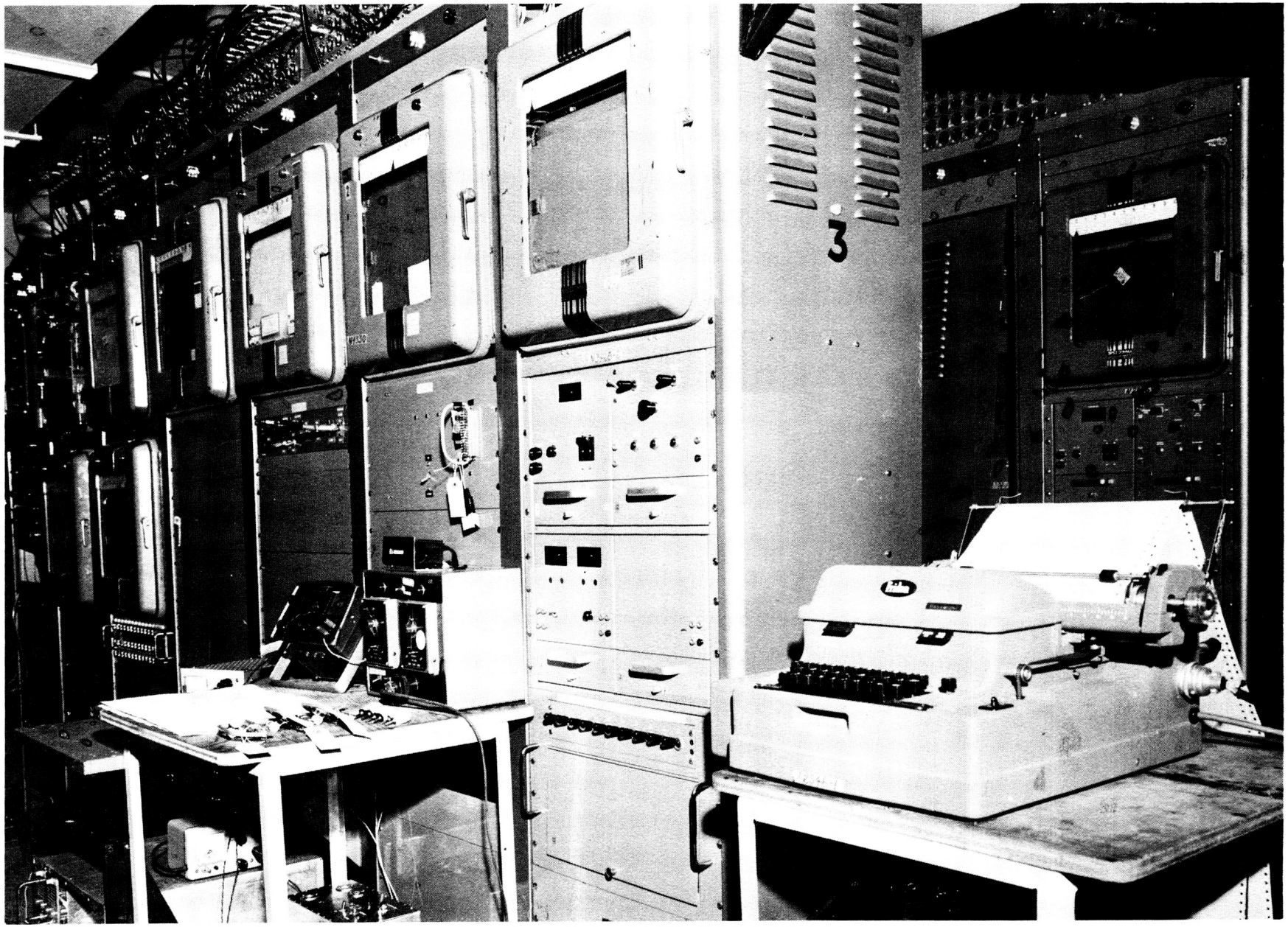

FIGURE 3 TRANSISTOR INSTRUMENTATION

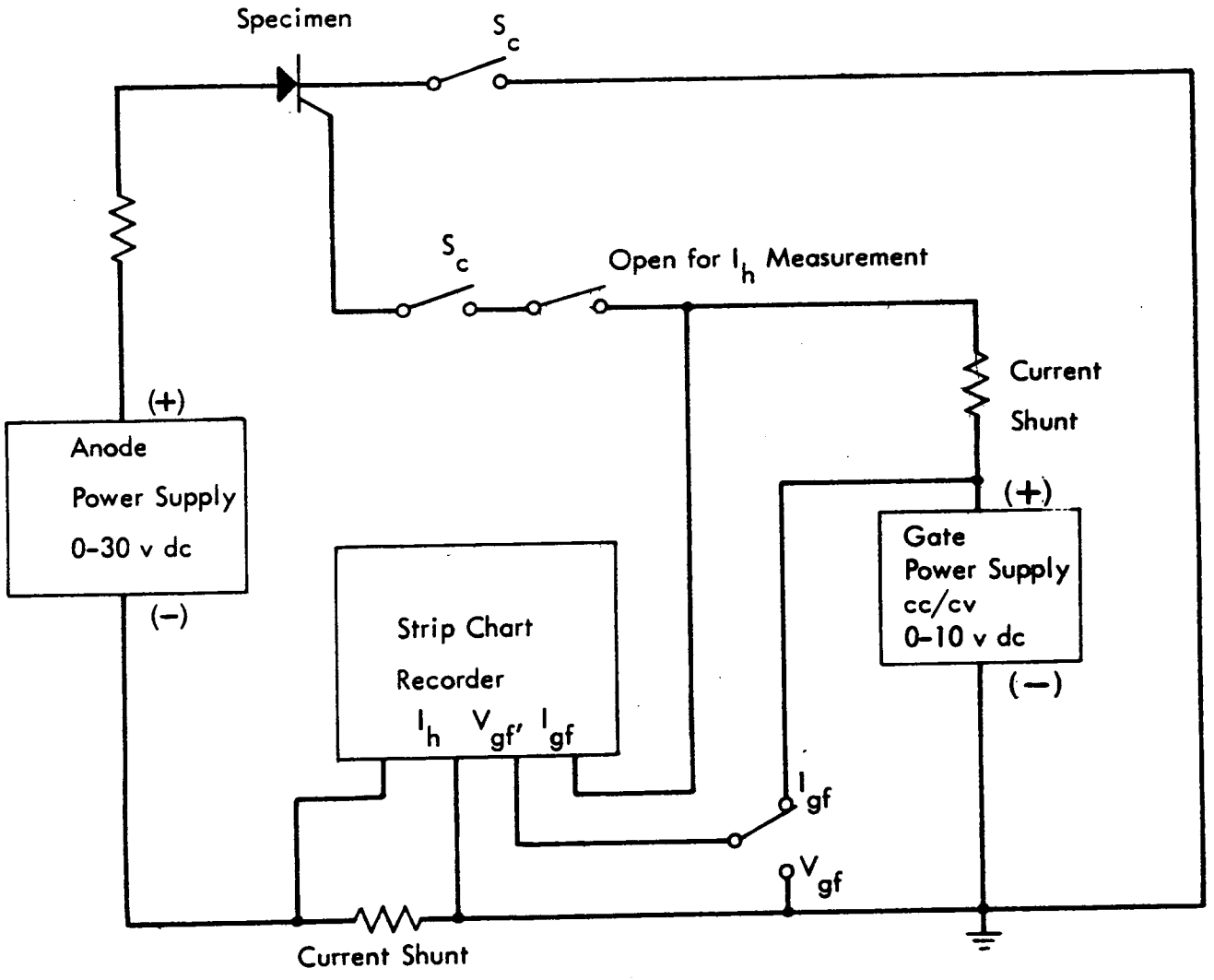

Commutator switches denoted by S_c.

FIGURE 4 SCR MEASUREMENT CIRCUIT FOR V_{GF}, I_{GF}, AND I_H

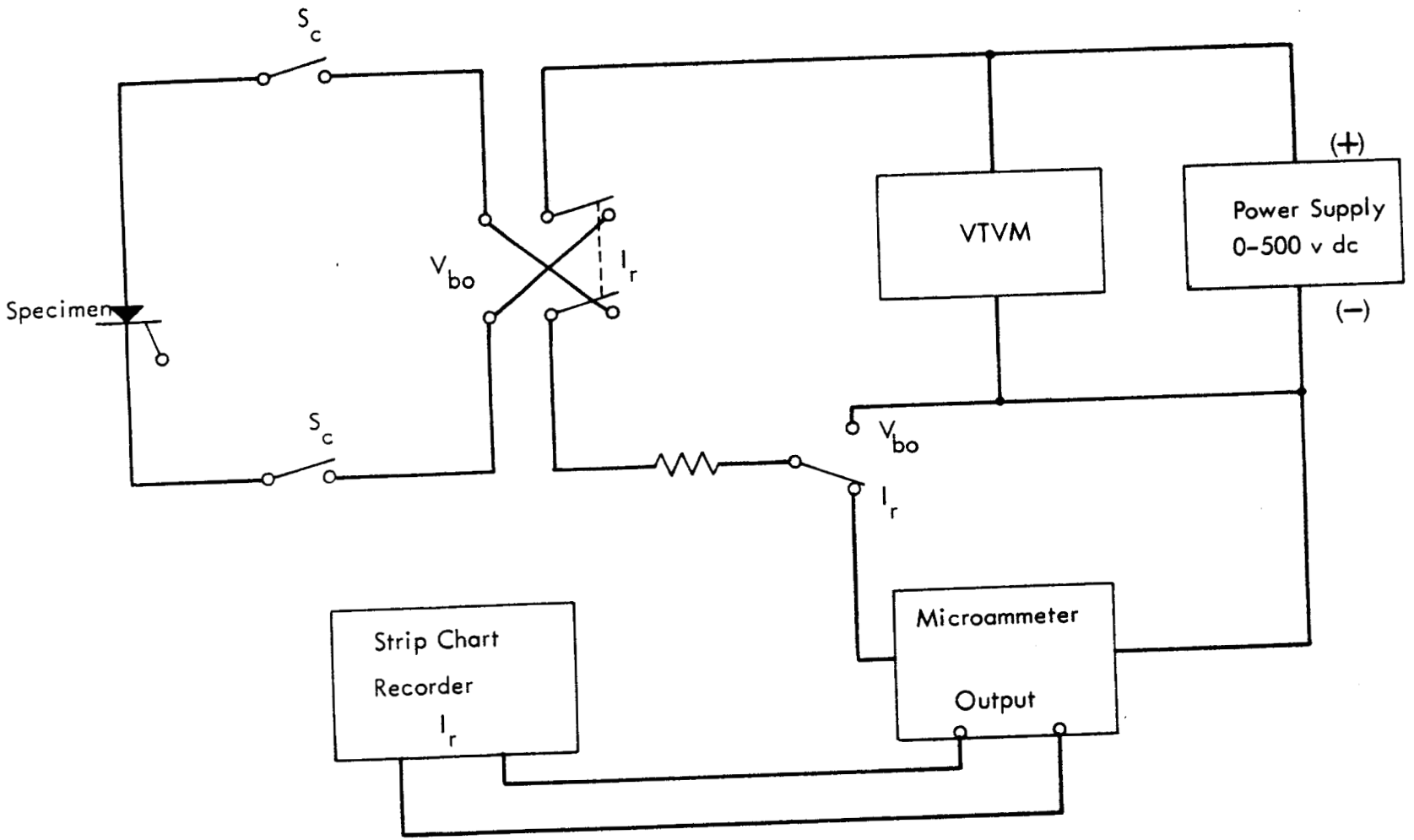

Commutator switches denoted by S_c.

FIGURE 5 SCR MEASUREMENT CIRCUIT FOR V_{BO}, I_R

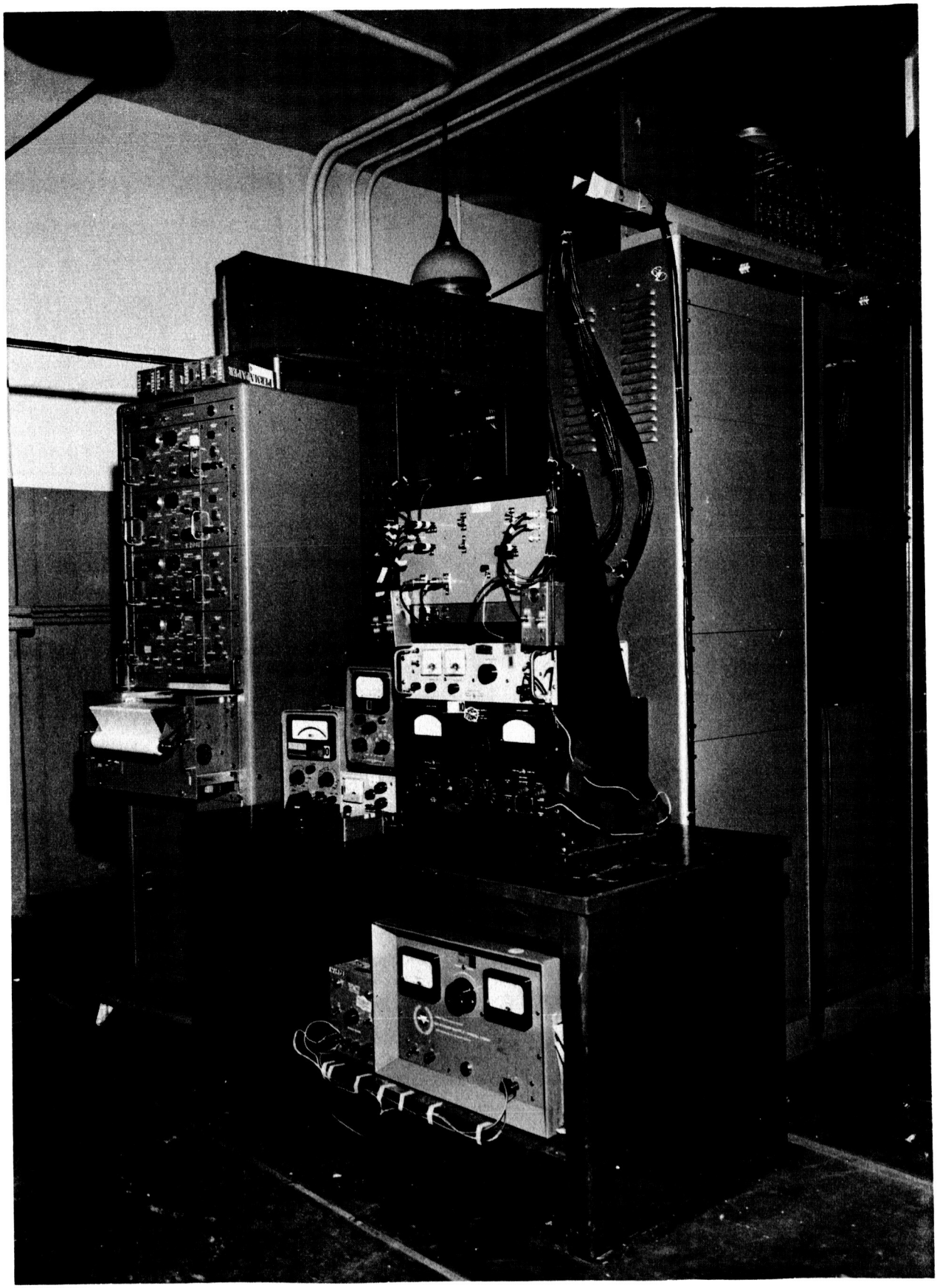

FIGURE 6 SCR INSTRUMENTATION

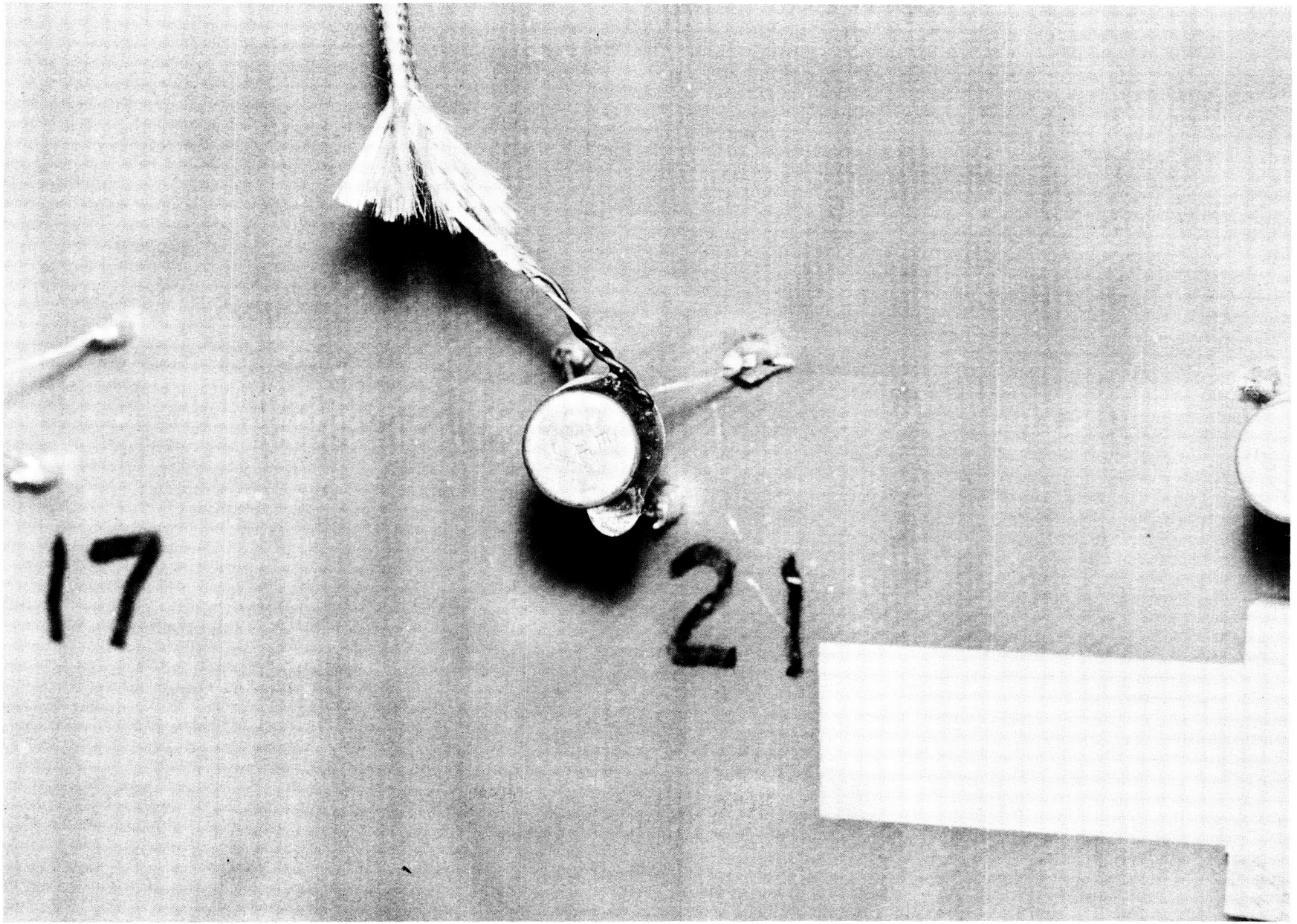

FIGURE 7 TEMPERATURE MEASUREMENT OF TRANSISTOR SPECIMEN

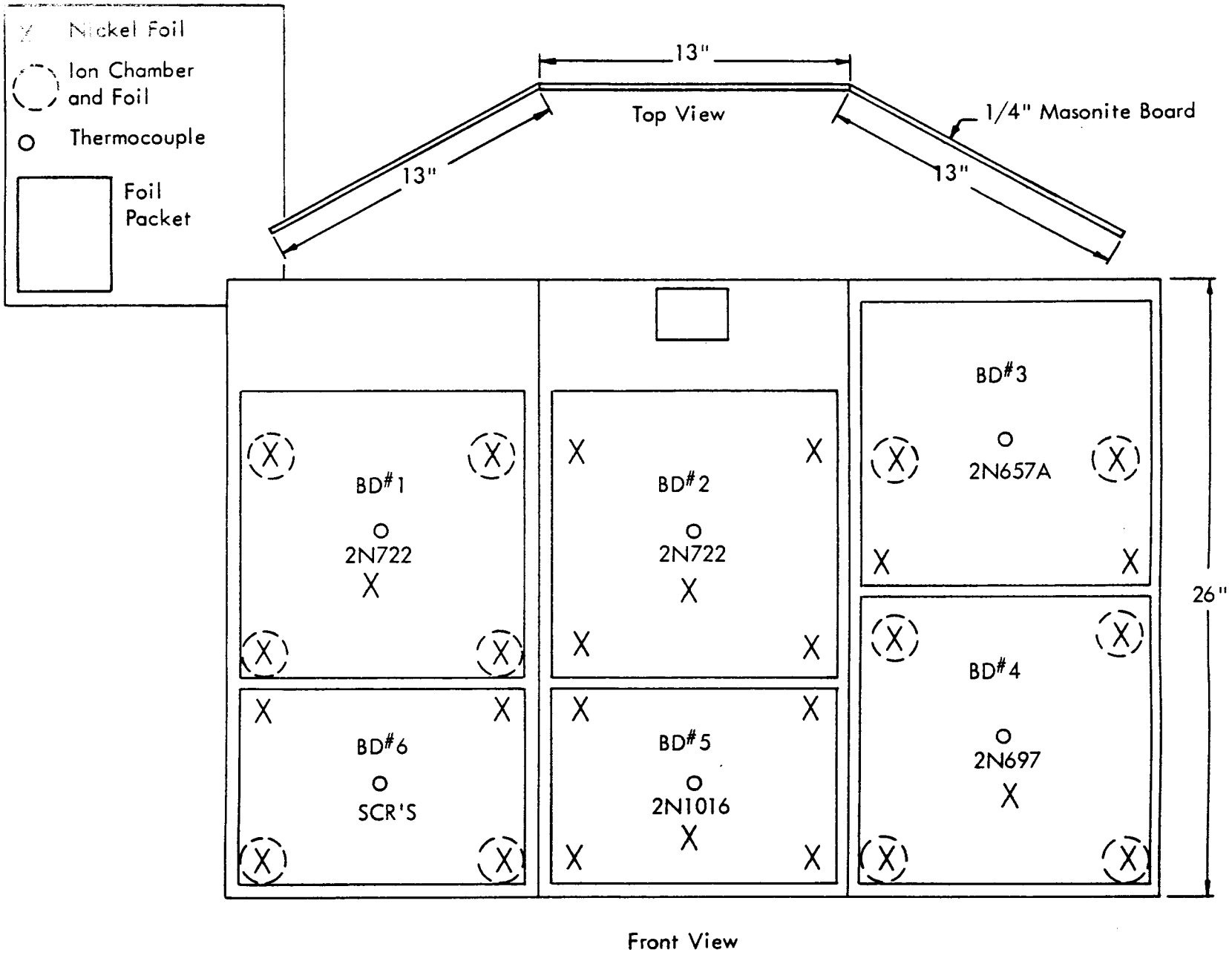

FIGURE 8 IRRADIATION TEST PANEL

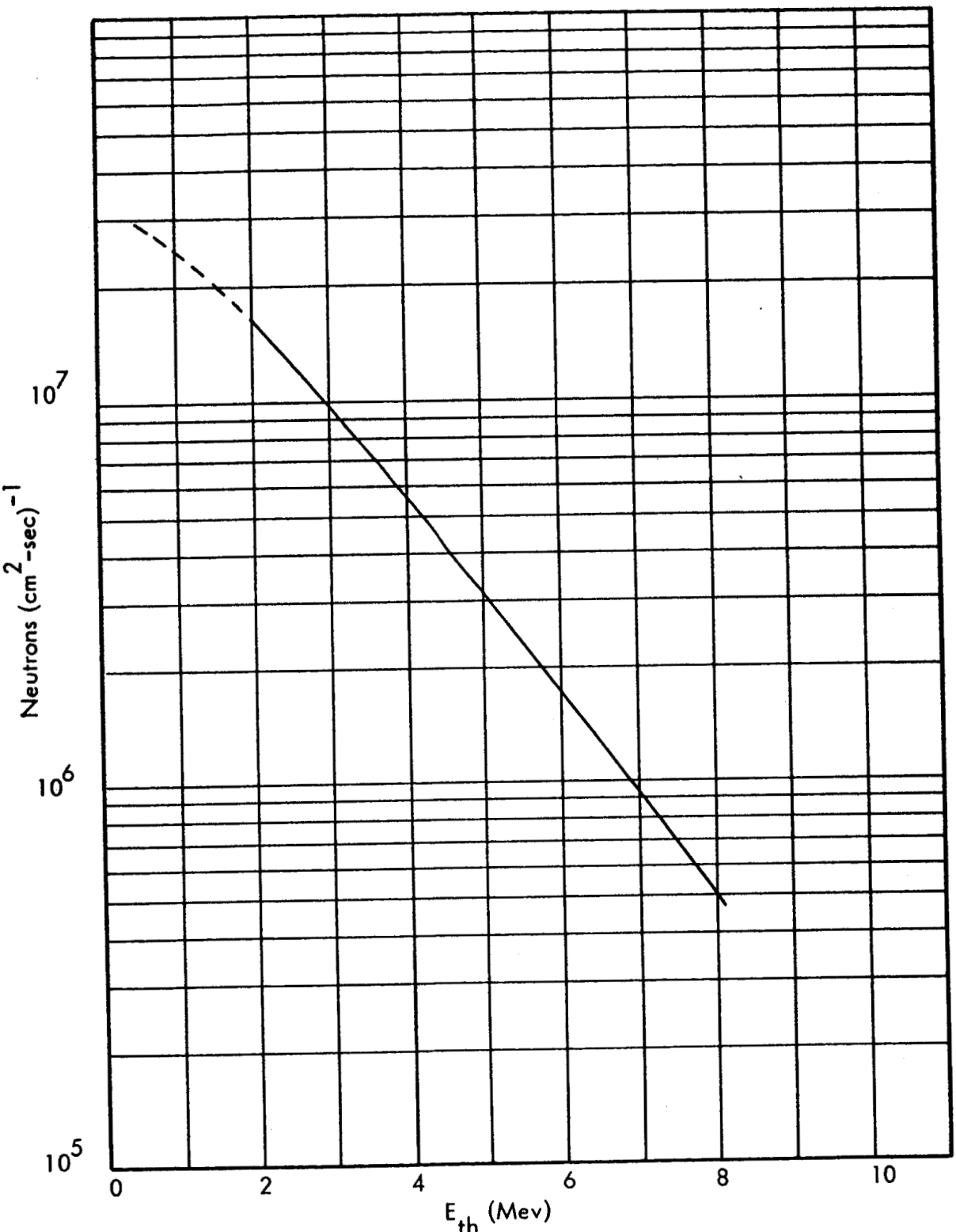

FIGURE 9 FAST NEUTRON SPECTRUM WITH WATER SHIELD

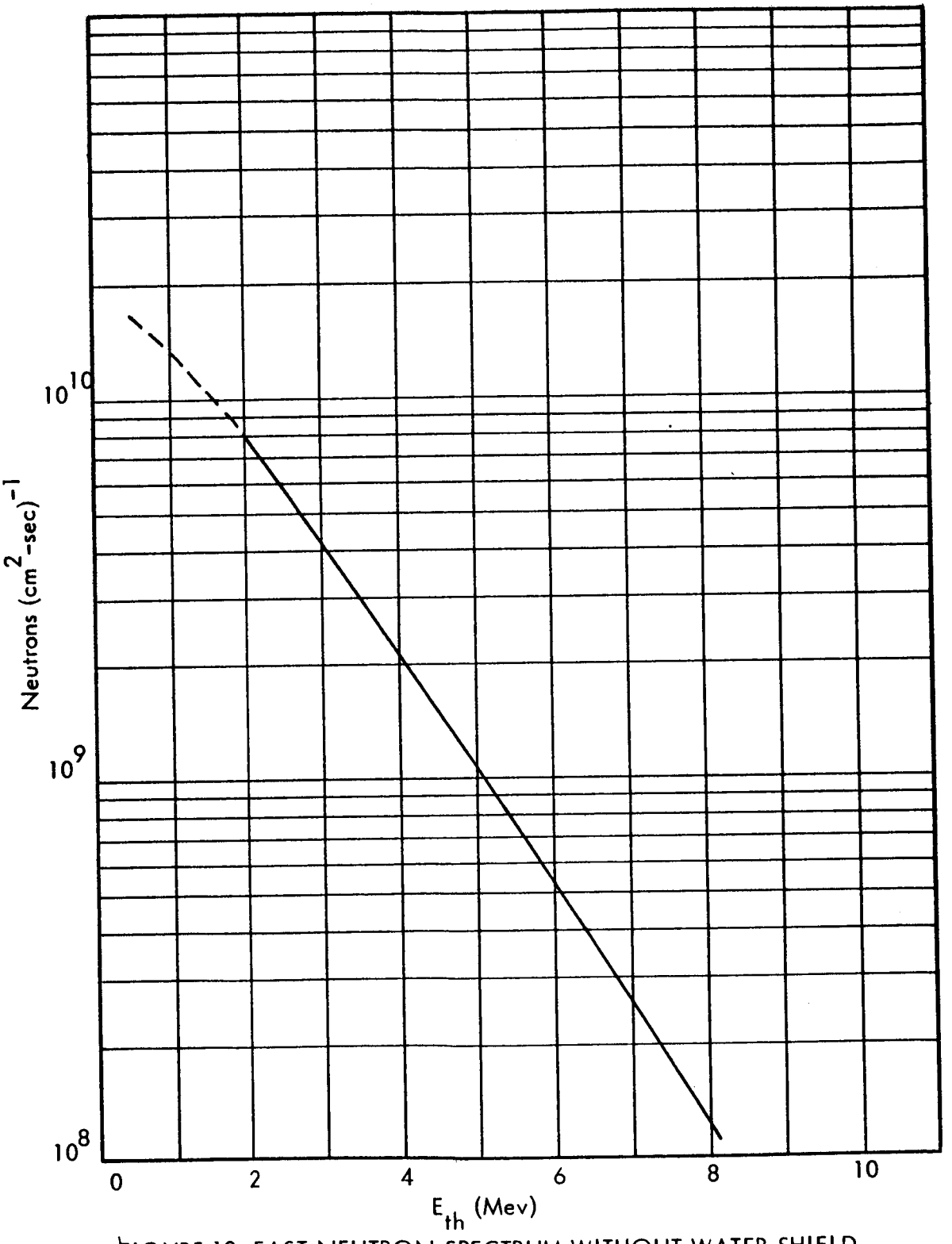

FIGURE 10 FAST NEUTRON SPECTRUM WITHOUT WATER SHIELD

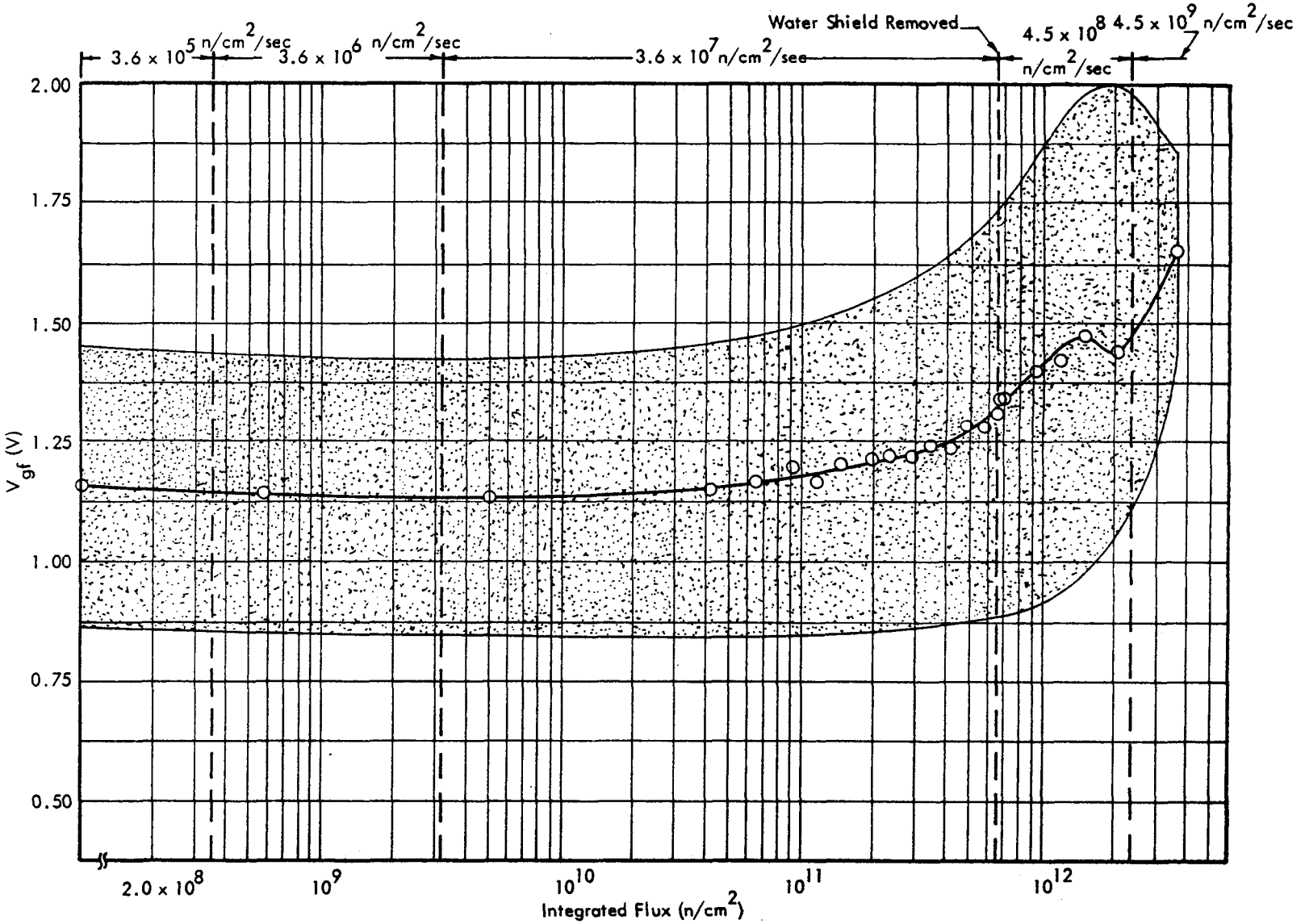

FIGURE 11 SCR 2N1774 - MEAN GATE FIRING VOLTAGE VERSUS INTEGRATED FLUX

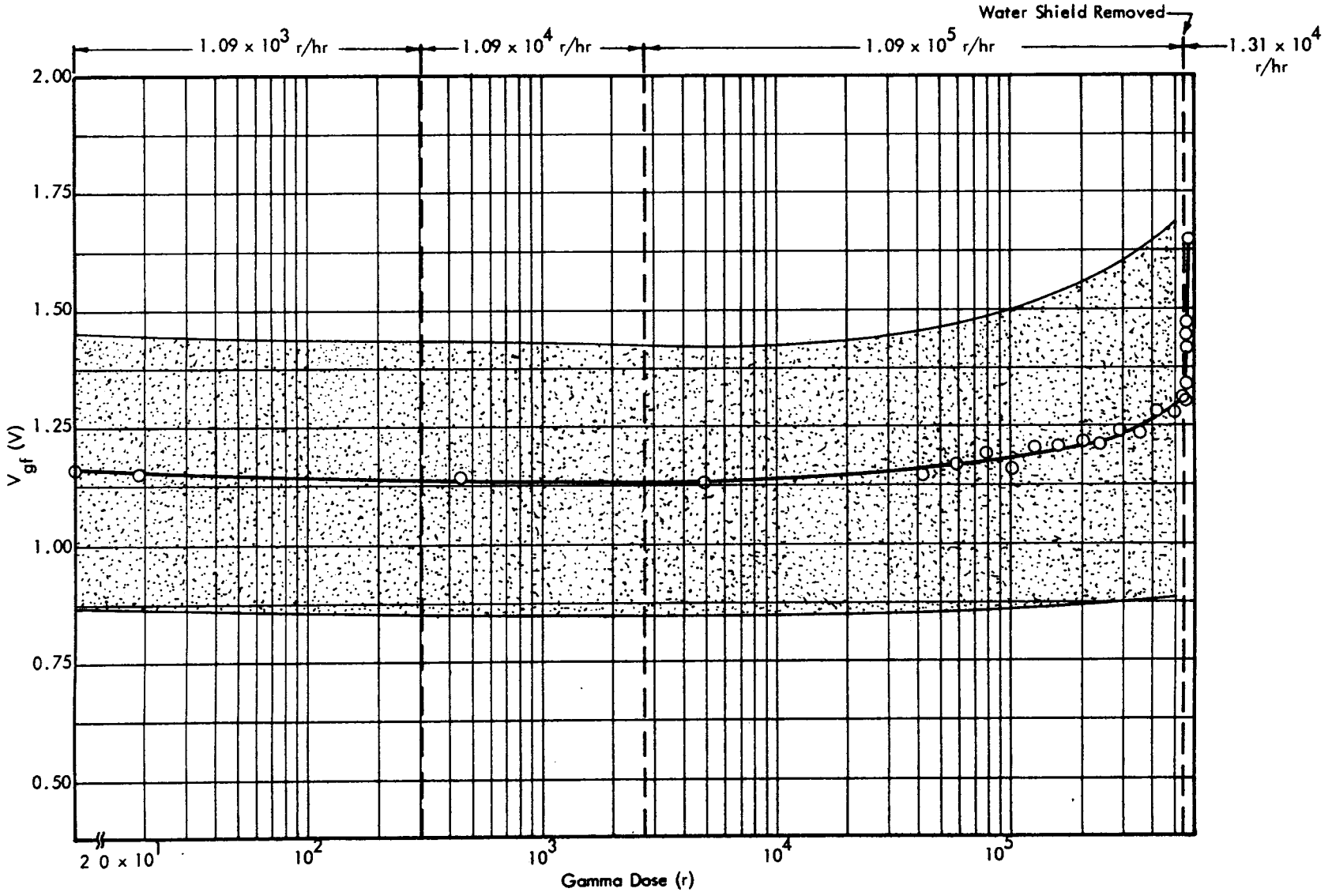

FIGURE 12 SCR 2N1774 - MEAN GATE FIRING VOLTAGE VERSUS GAMMA DOSE

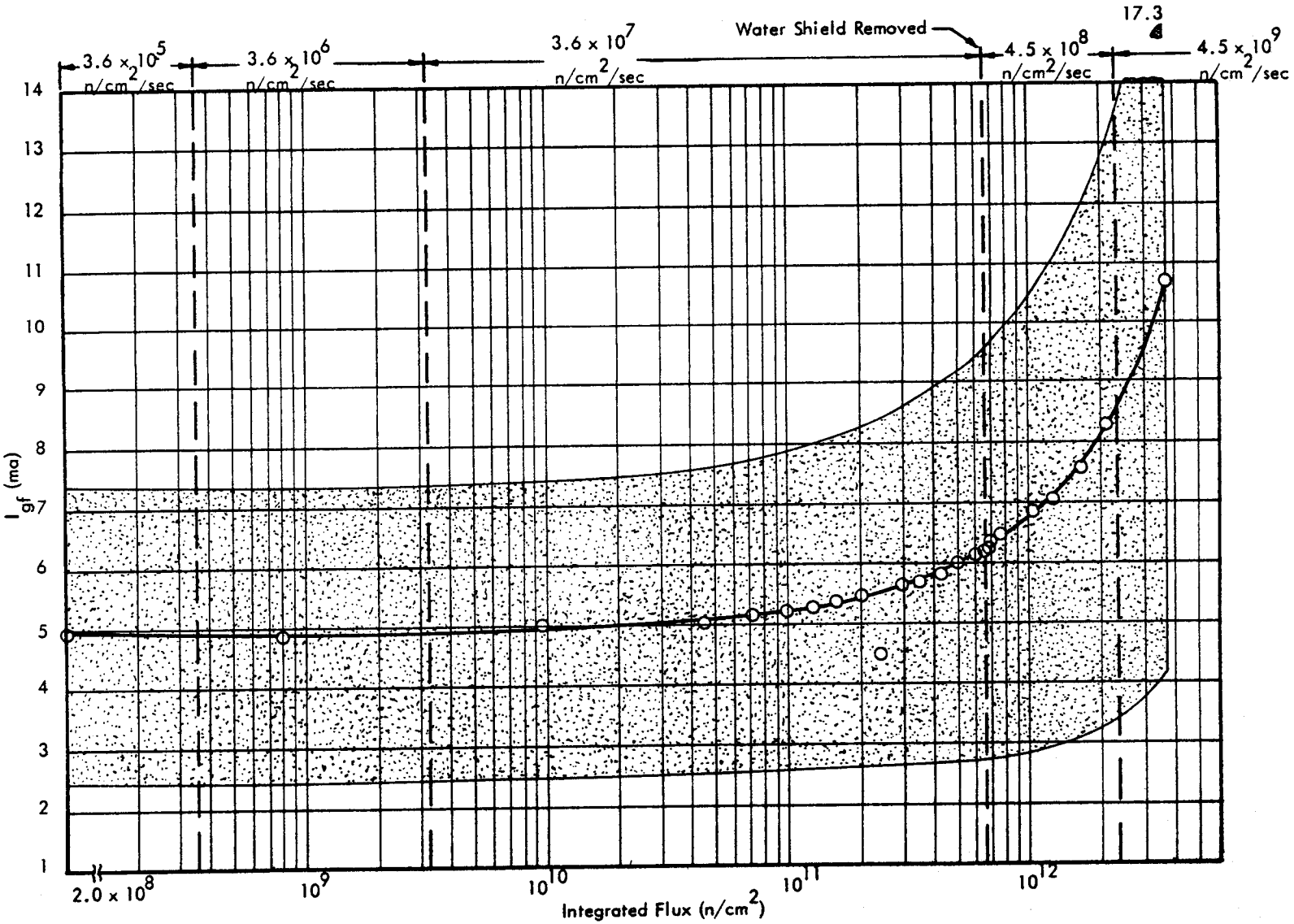

FIGURE 13 SCR 2N1774 - MEAN GATE FIRING CURRENT VERSUS INTEGRATED NEUTRON FLUX

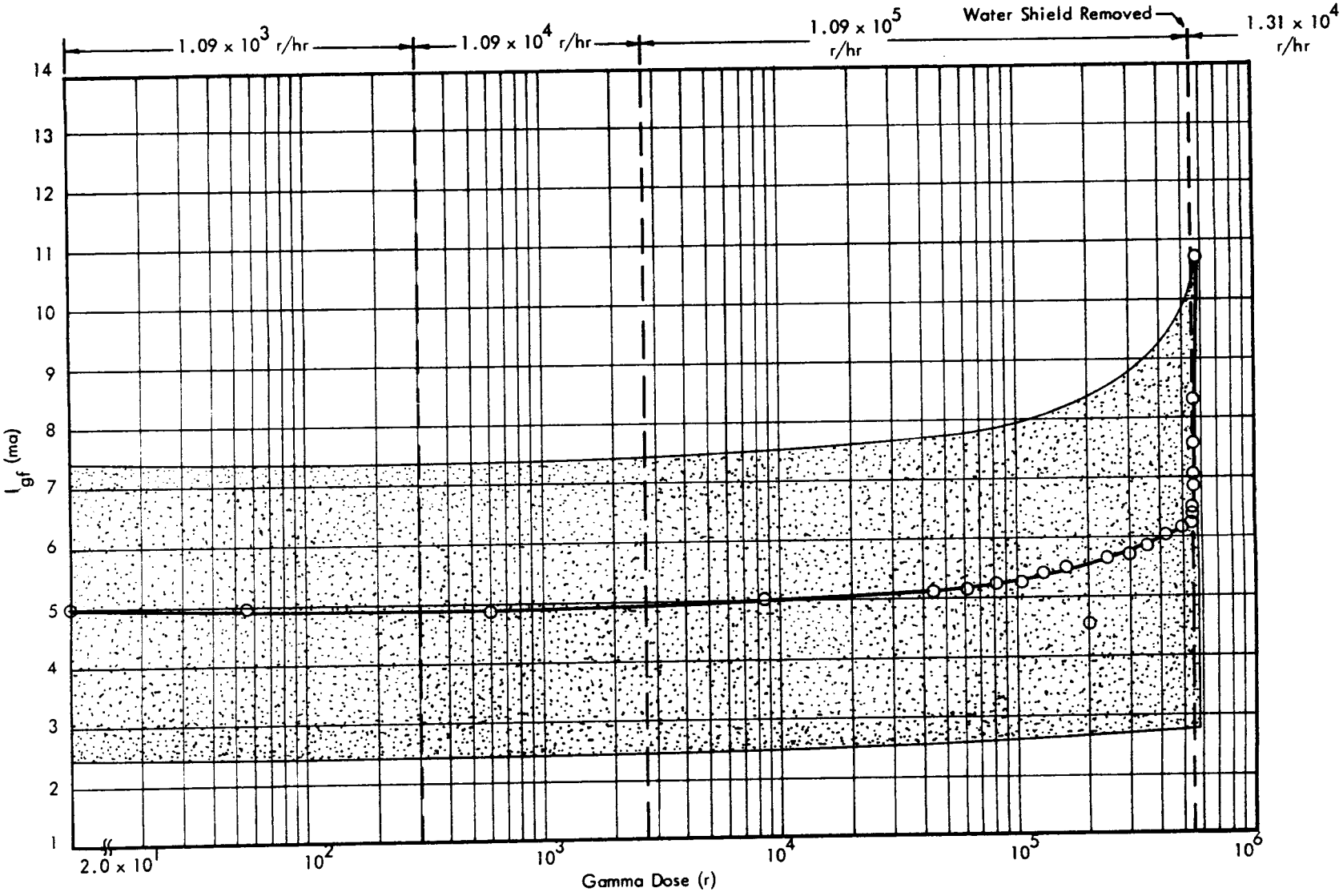

FIGURE 14 SCR 2N1774 - MEAN GATE FIRING CURRENT VERSUS GAMMA DOSE

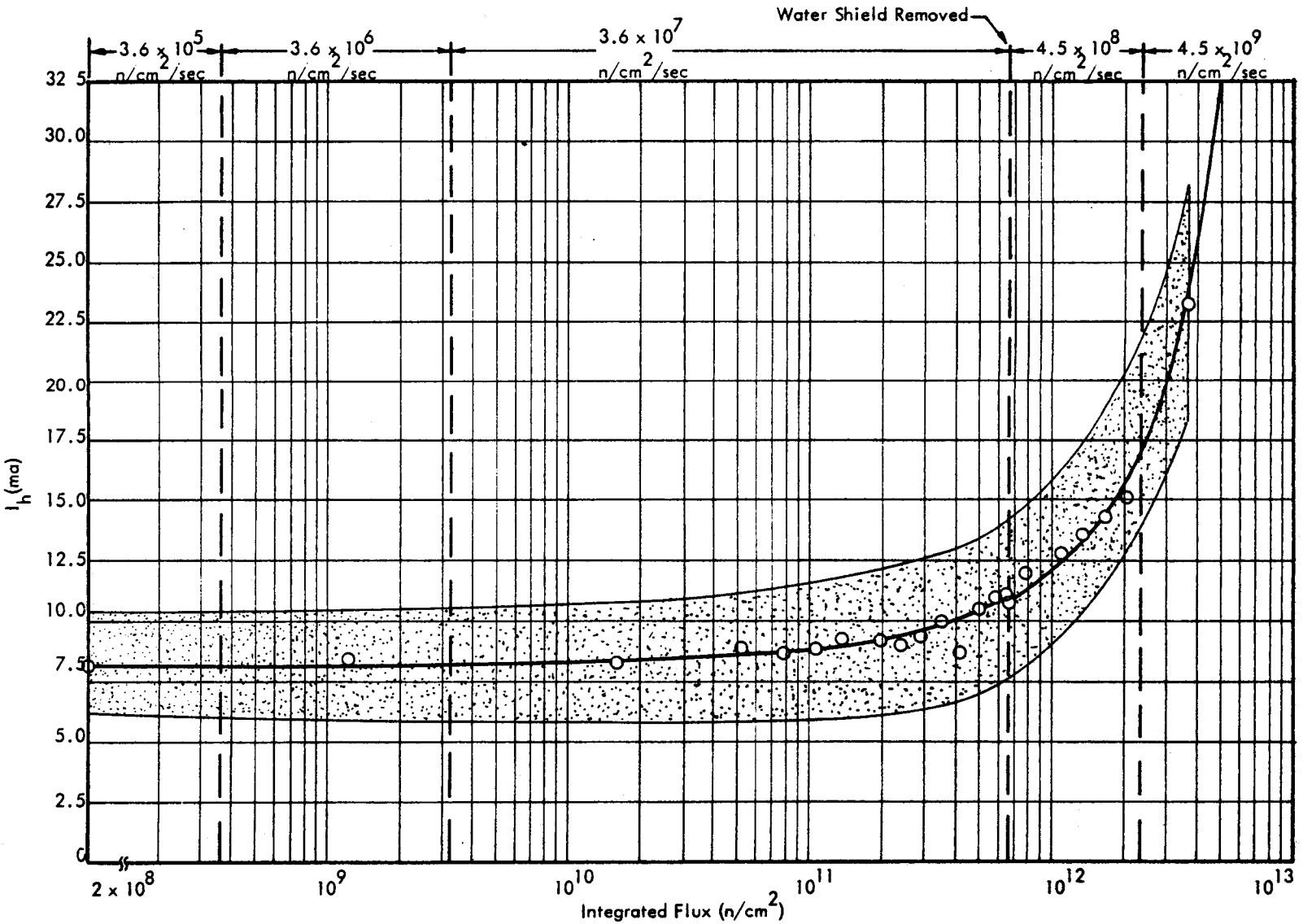

FIGURE 15 SCR 2N1774 - HOLDING CURRENT (SPECIMENS #1, 3, 4, 5, & 10) VS. INTEGRATED FLUX

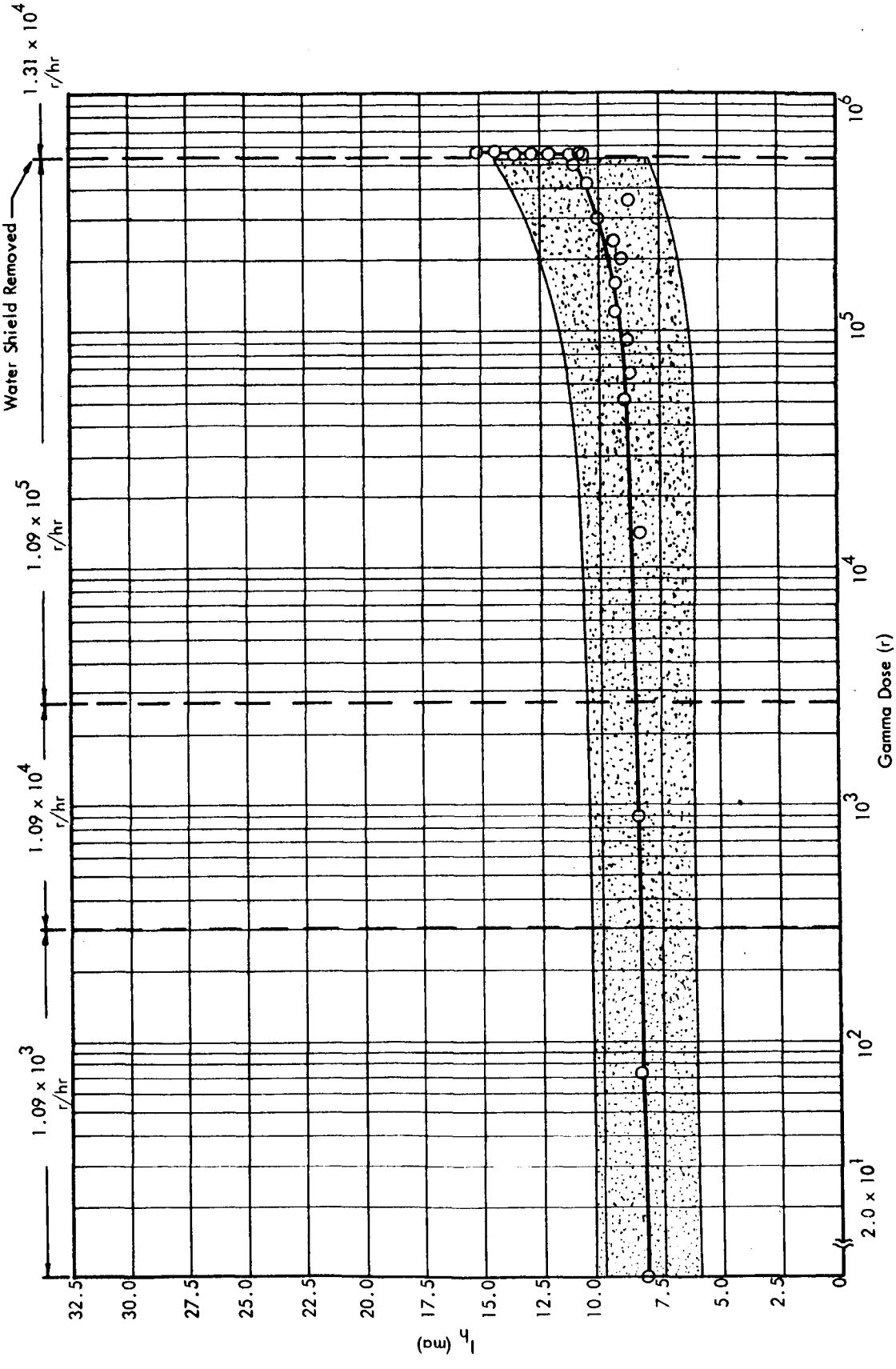

FIGURE 16 SCR 2N1774 - HOLDING CURRENT (SPECIMENS #1, 3, 4, 5 & 10) VS. GAMMA DOSE

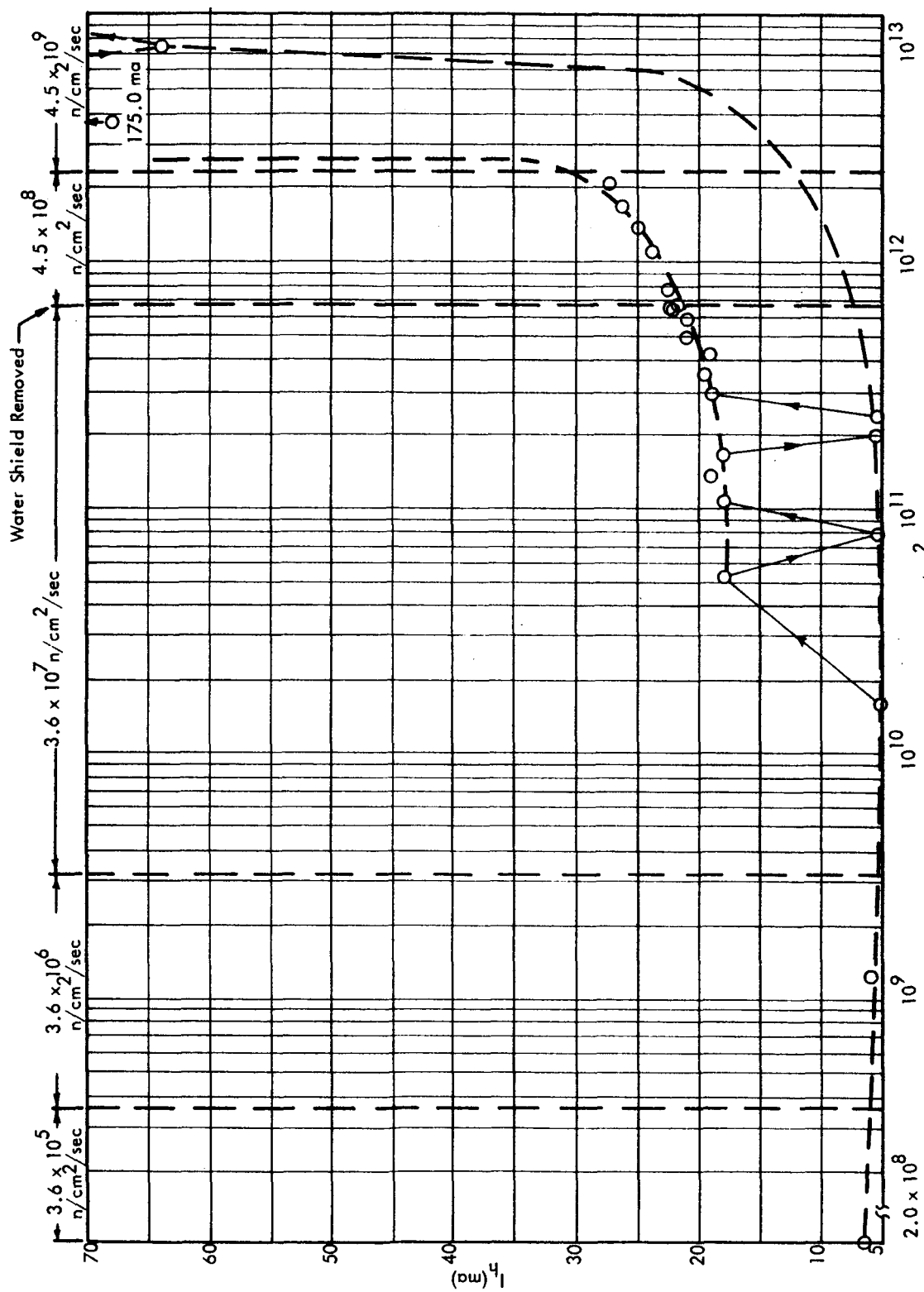

FIGURE 17 SCR 2N1774 - HOLDING CURRENT VS. INTEGRATED NEUTRON FLUX - SPECIMEN #2

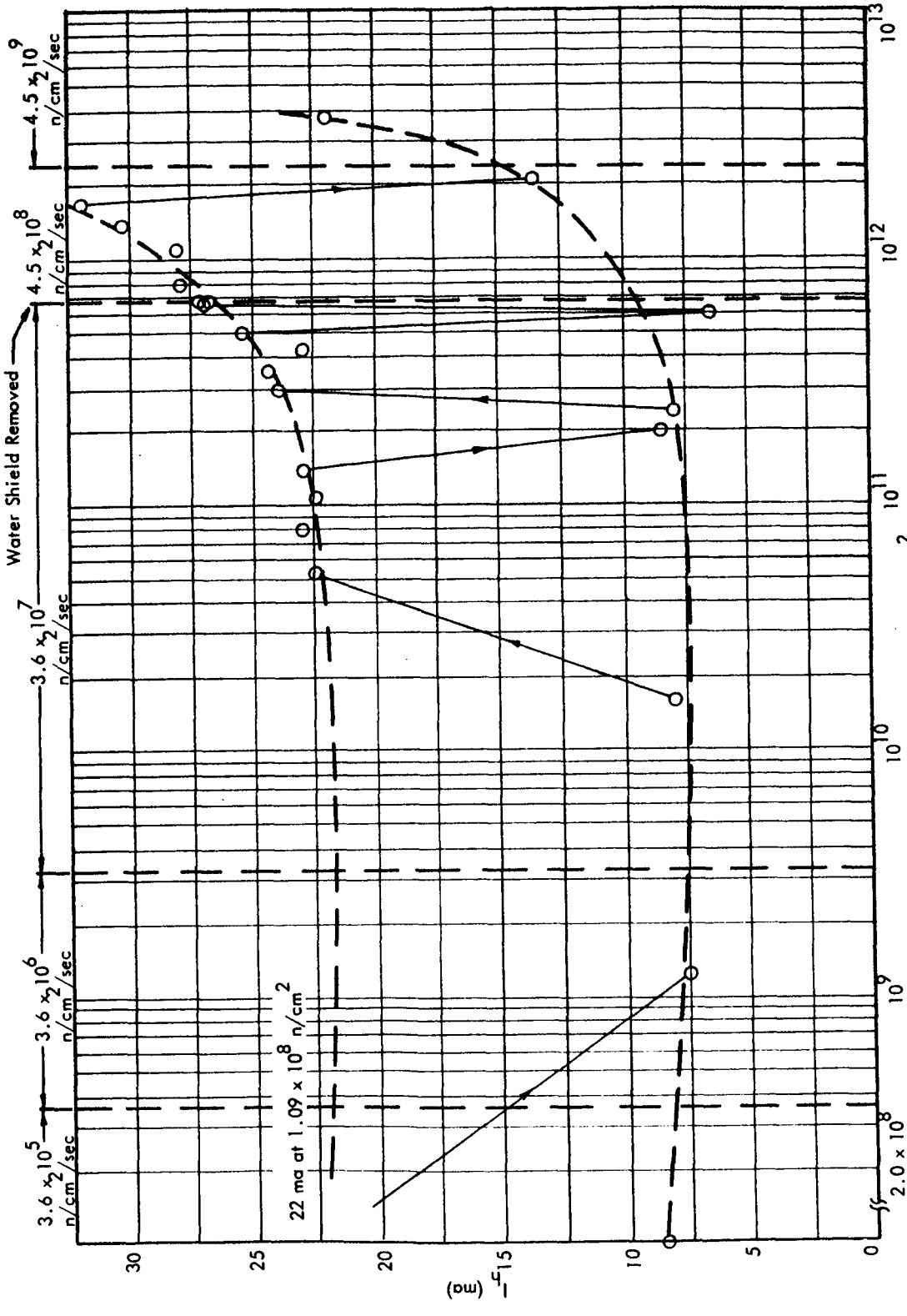

FIGURE 18 SCR 2N1774 - HOLDING CURRENT VS. INTEGRATED NEUTRON FLUX - SPECIMEN #6

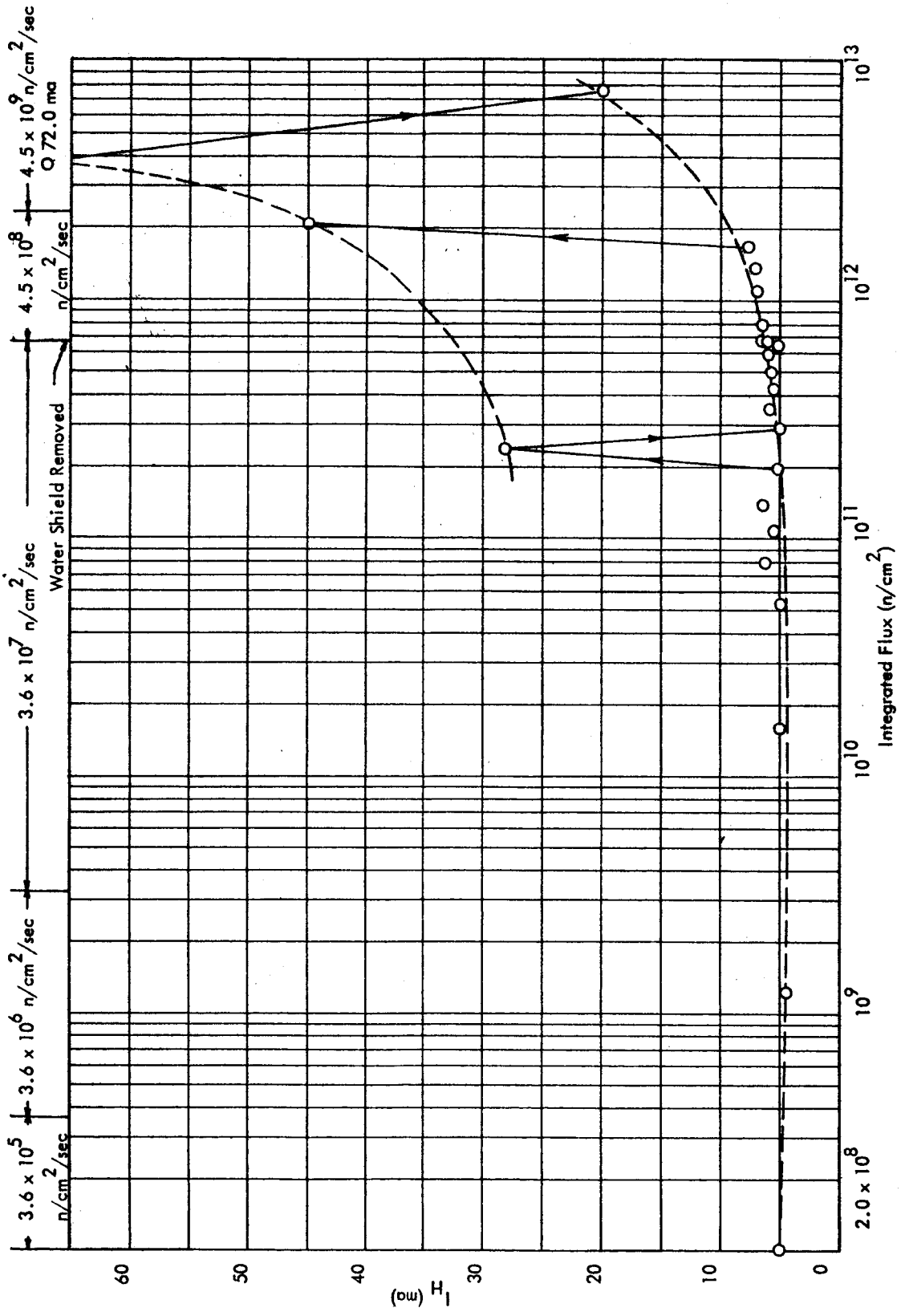

FIGURE 19 SCR 2N1774 - HOLDING CURRENT VERSUS INTEGRATED NEUTRON FLUX (SPECIMEN NO. 7)

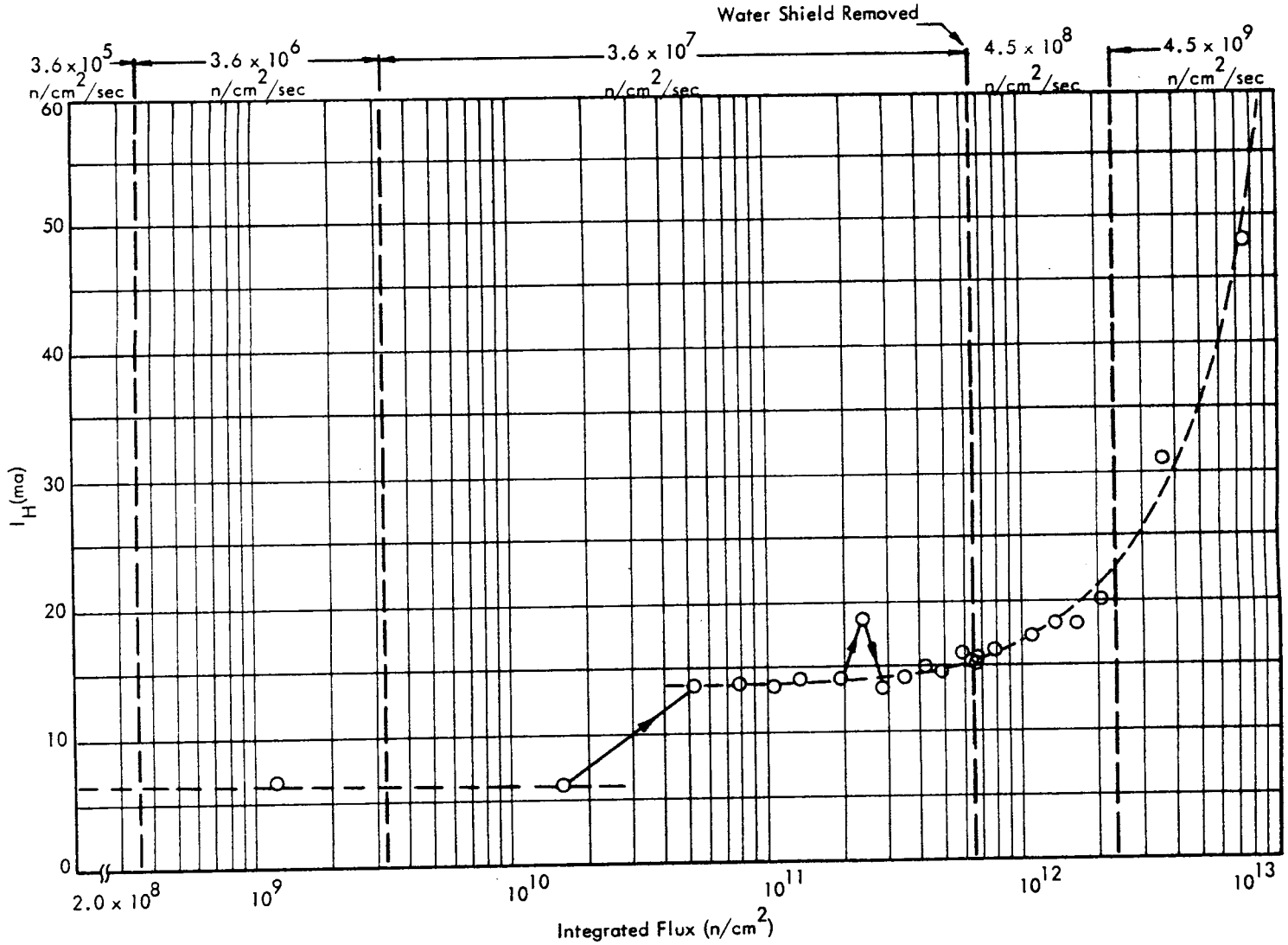

FIGURE 20 SCR 2N1774-HOLDING CURRENT VS. INTEGRATED NEUTRON FLUX (SPECIMEN #8)

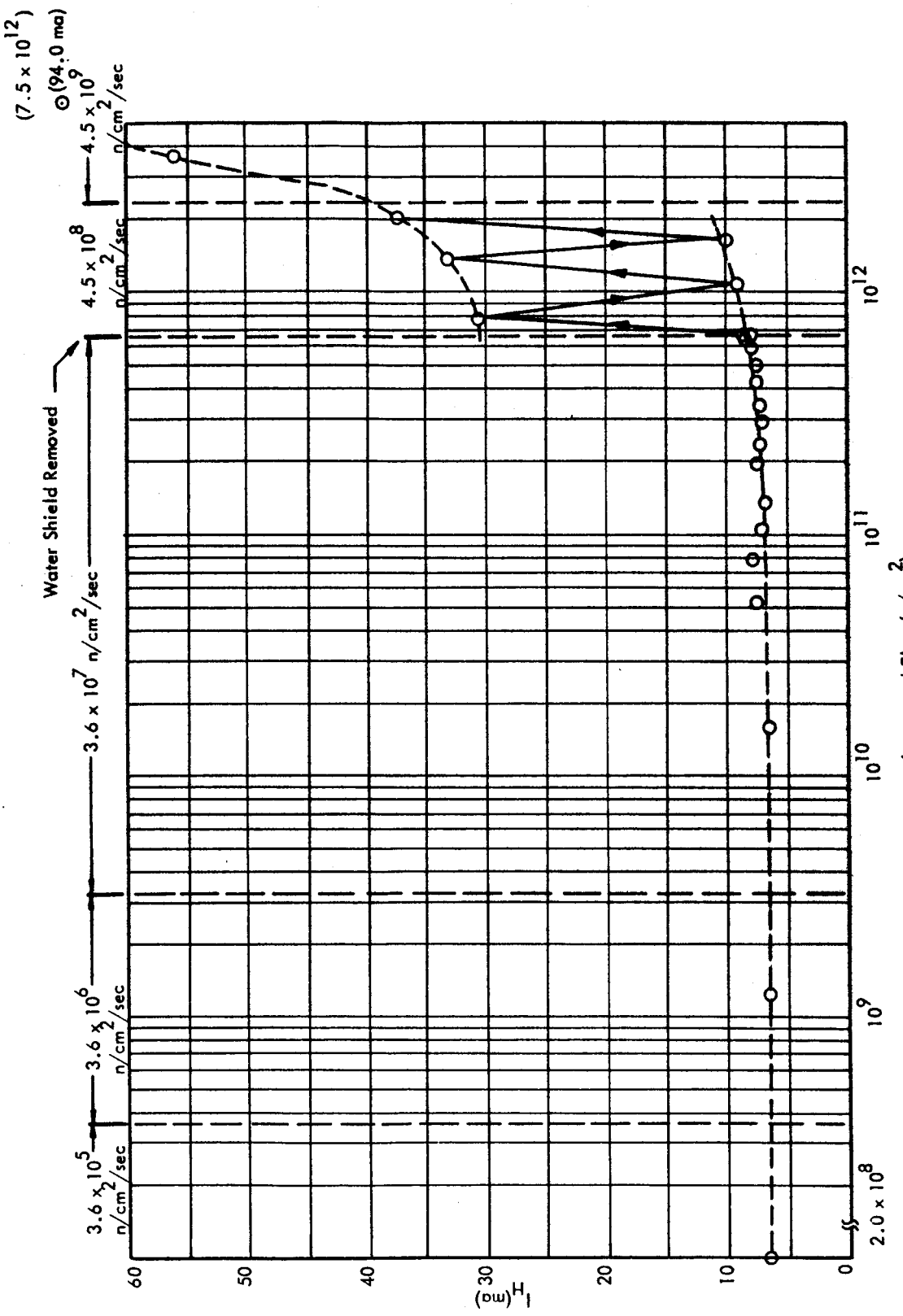

FIGURE 21 SCR 2N1774 HOLDING CURRENT VS. INTEGRATED NEUTRON FLUX (SPECIMEN #9)

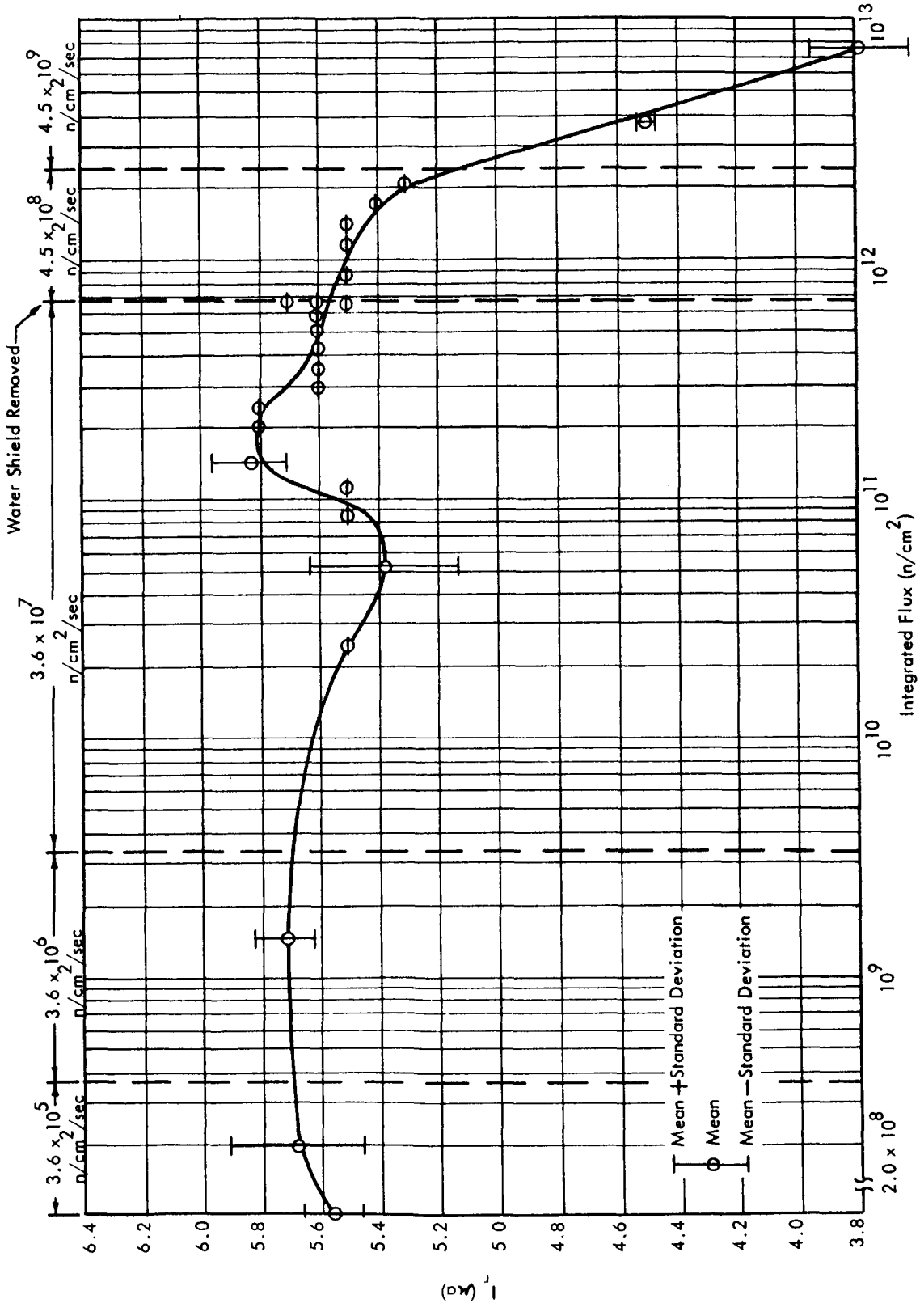

FIGURE 22 SCR 2N1774 - REVERSE CURRENT (SPECIMENS #11, 13, 14 & 15) VS. INTEGRATED FLUX

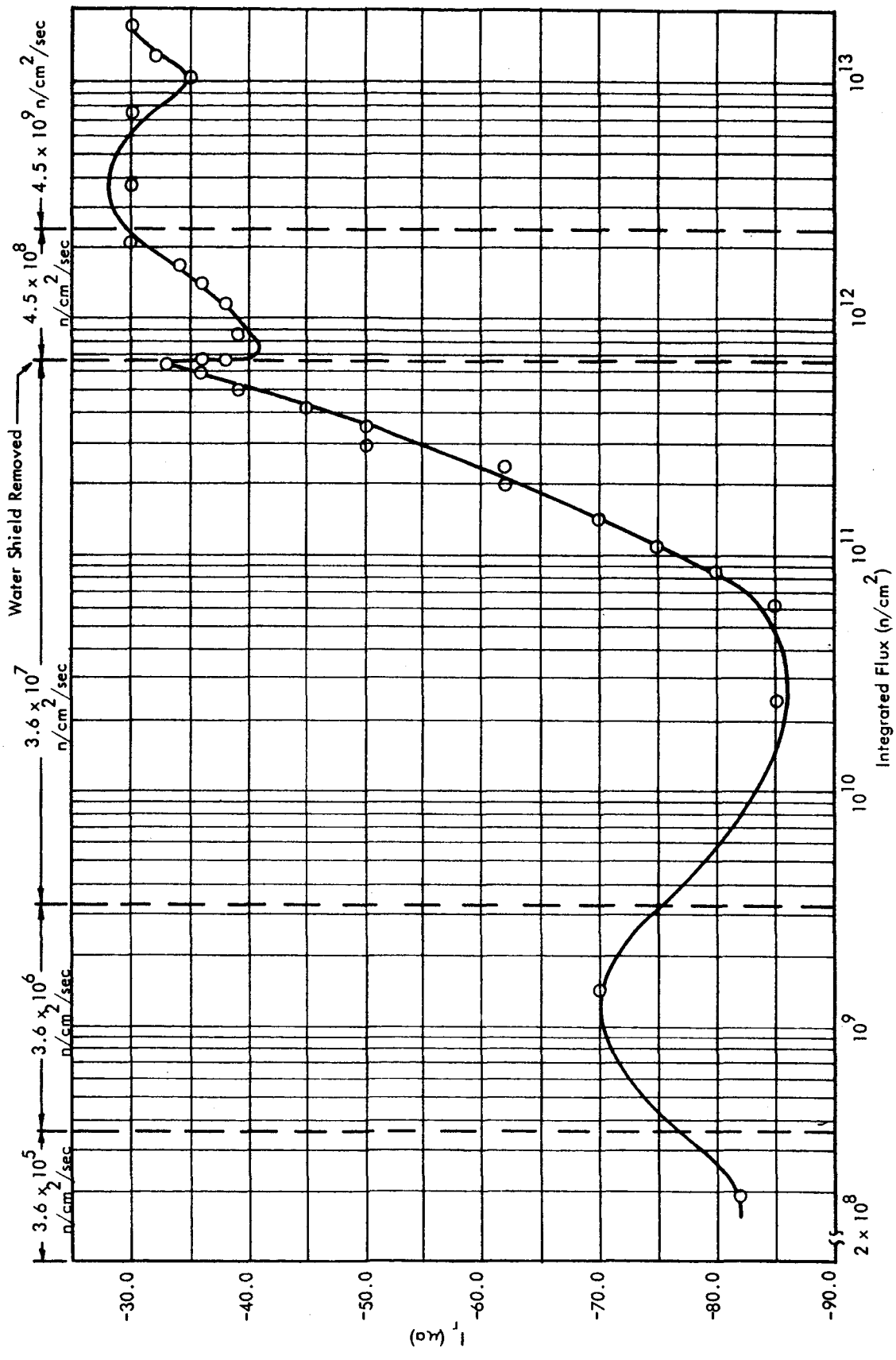

FIGURE 23 SCR 2N1774 - SPECIMEN #12 - REVERSE CURRENT VS. INTEGRATED FLUX

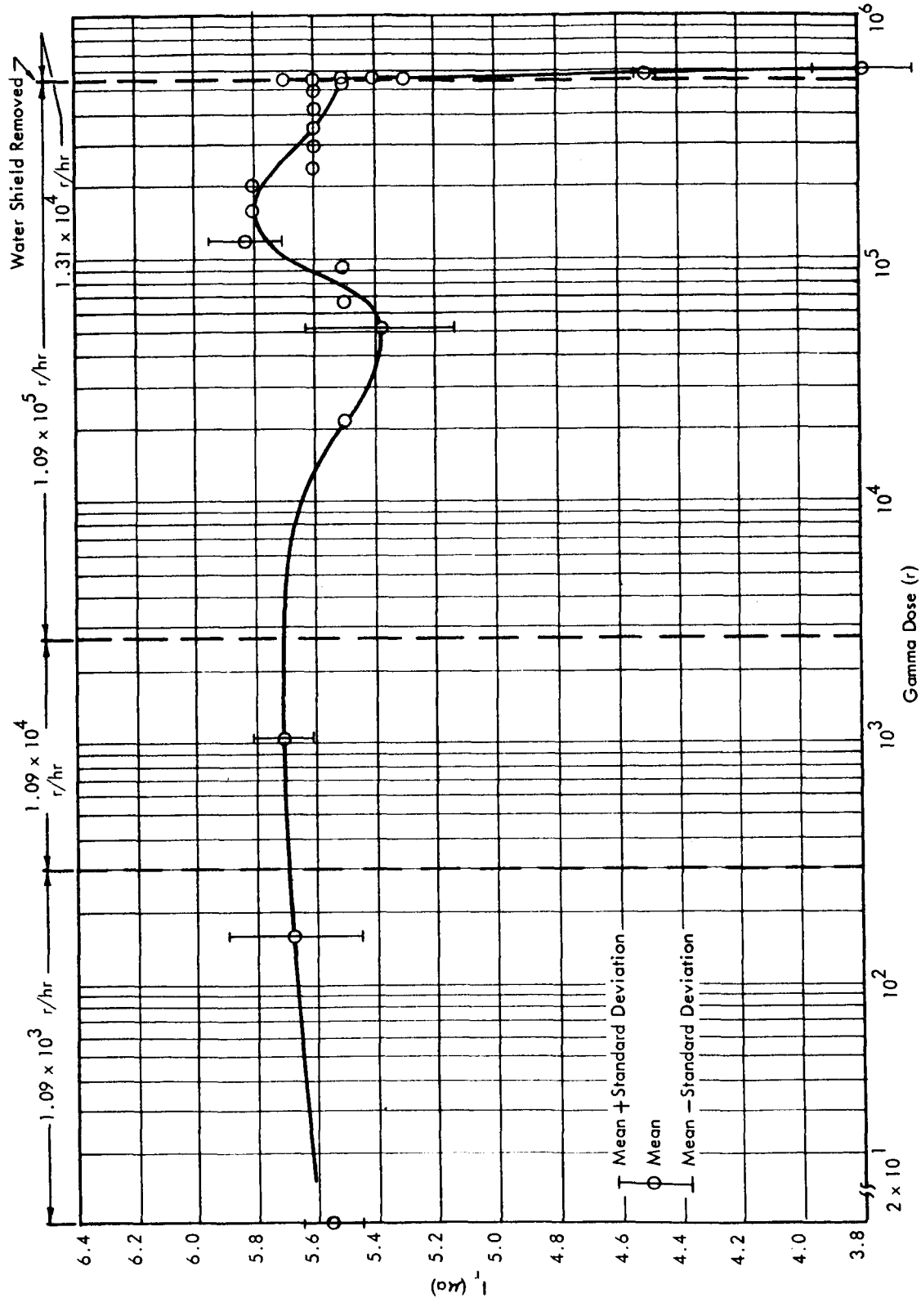

FIGURE 24 SCR 2N1774 - REVERSE CURRENT (SPECIMENS #11, 13, 14 & 15) VS. GAMMA DOSE

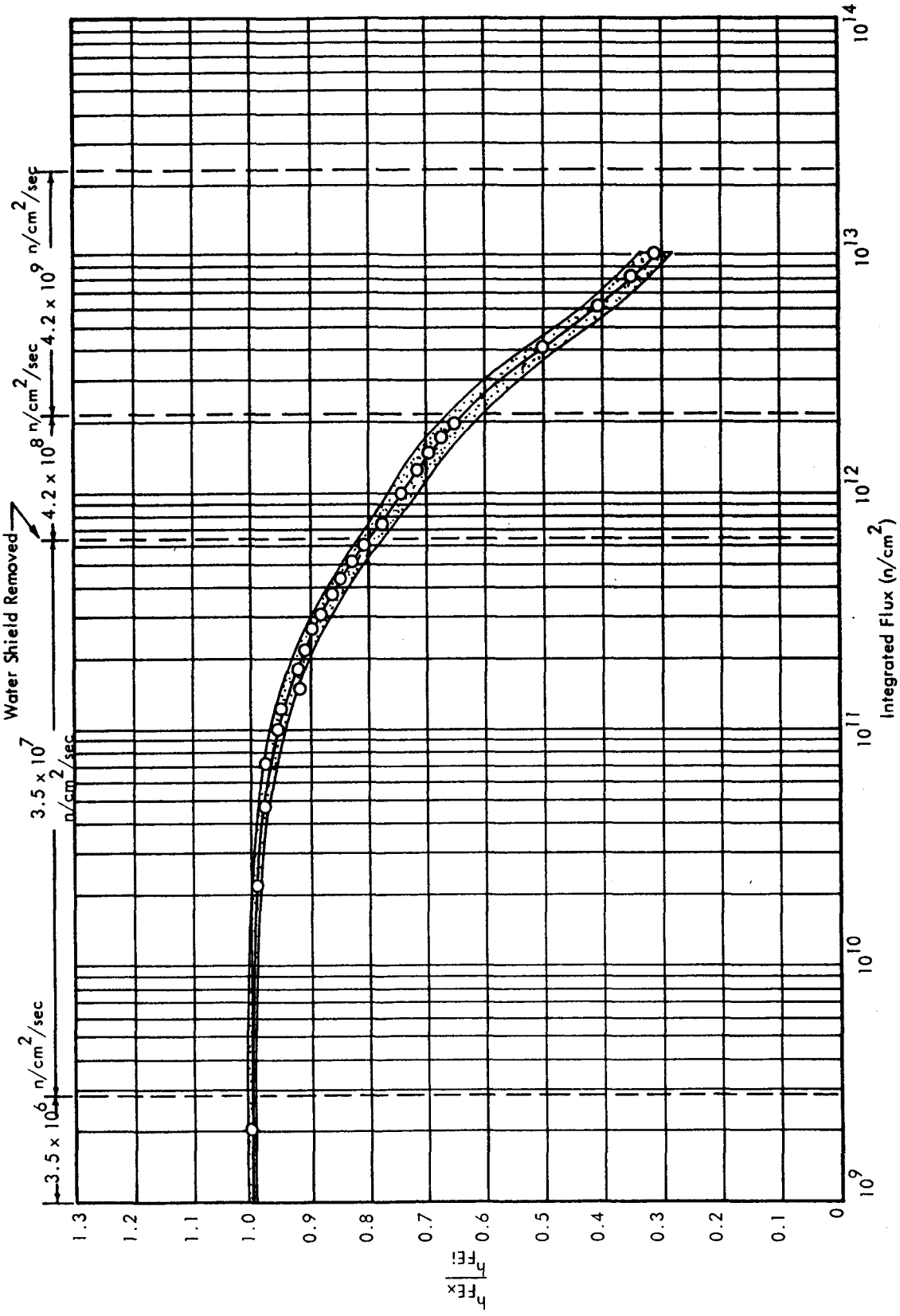

FIGURE 25 2N722 - GROUP N (NEW) - NORMALIZED BETA VS. INTEGRATED FLUX

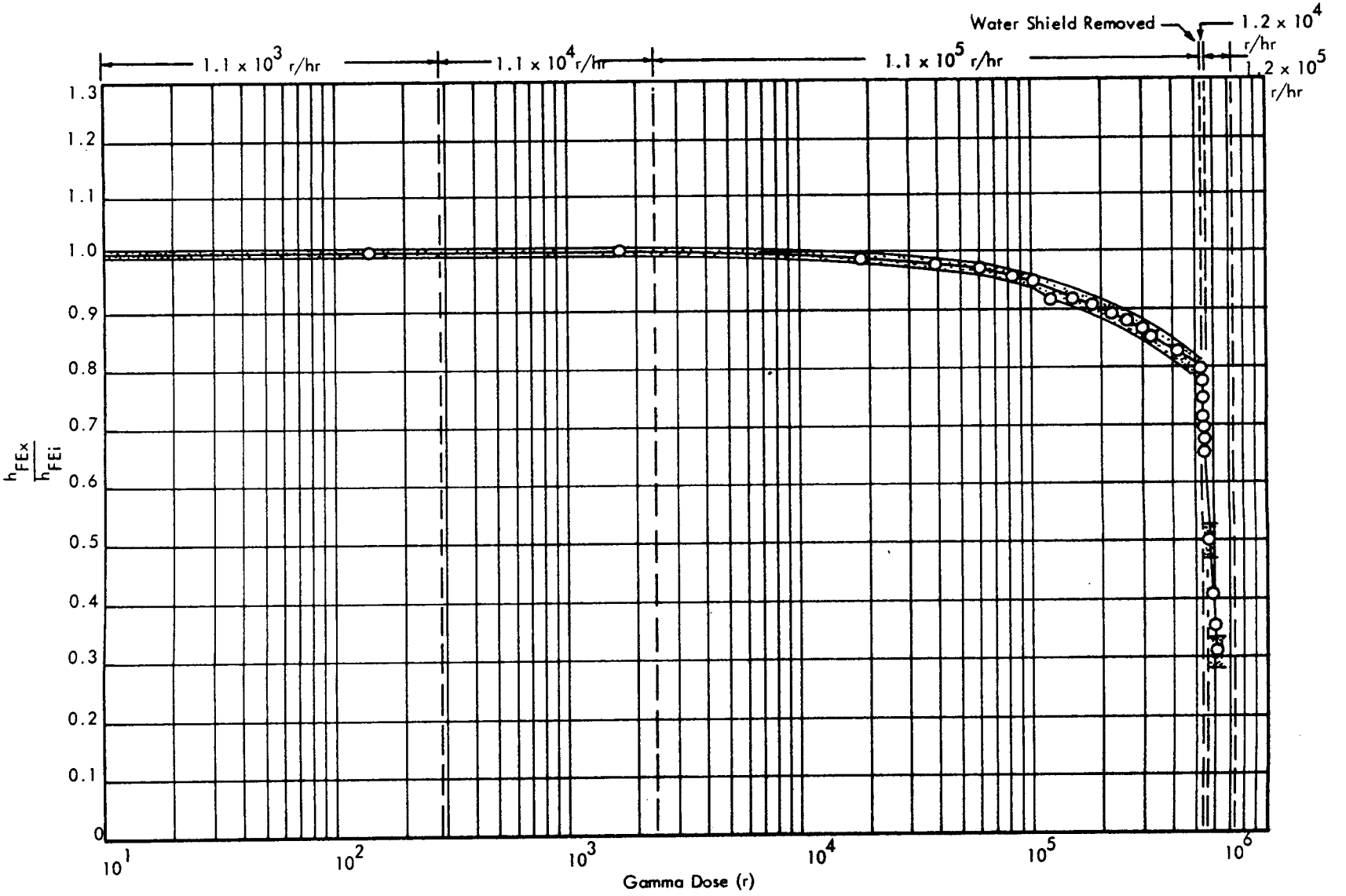

FIGURE 26 2N722 - GROUP N (NEW) - NORMALIZED BETA VERSUS GAMMA DOSE

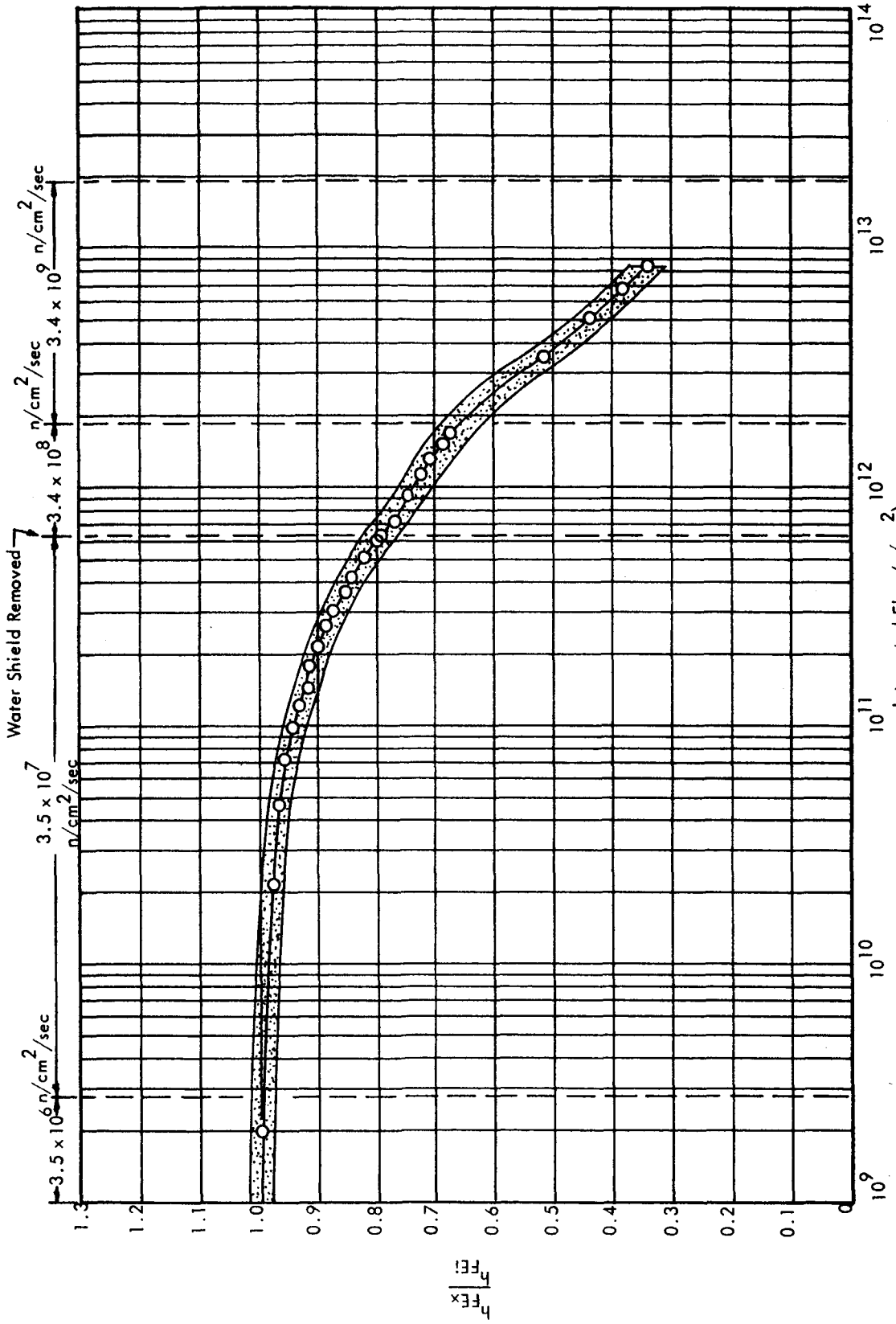

FIGURE 27 2N722 - GROUP T (TEMPERATURE CYCLED) - NORMALIZED BETA VS. INTEGRATED FLUX

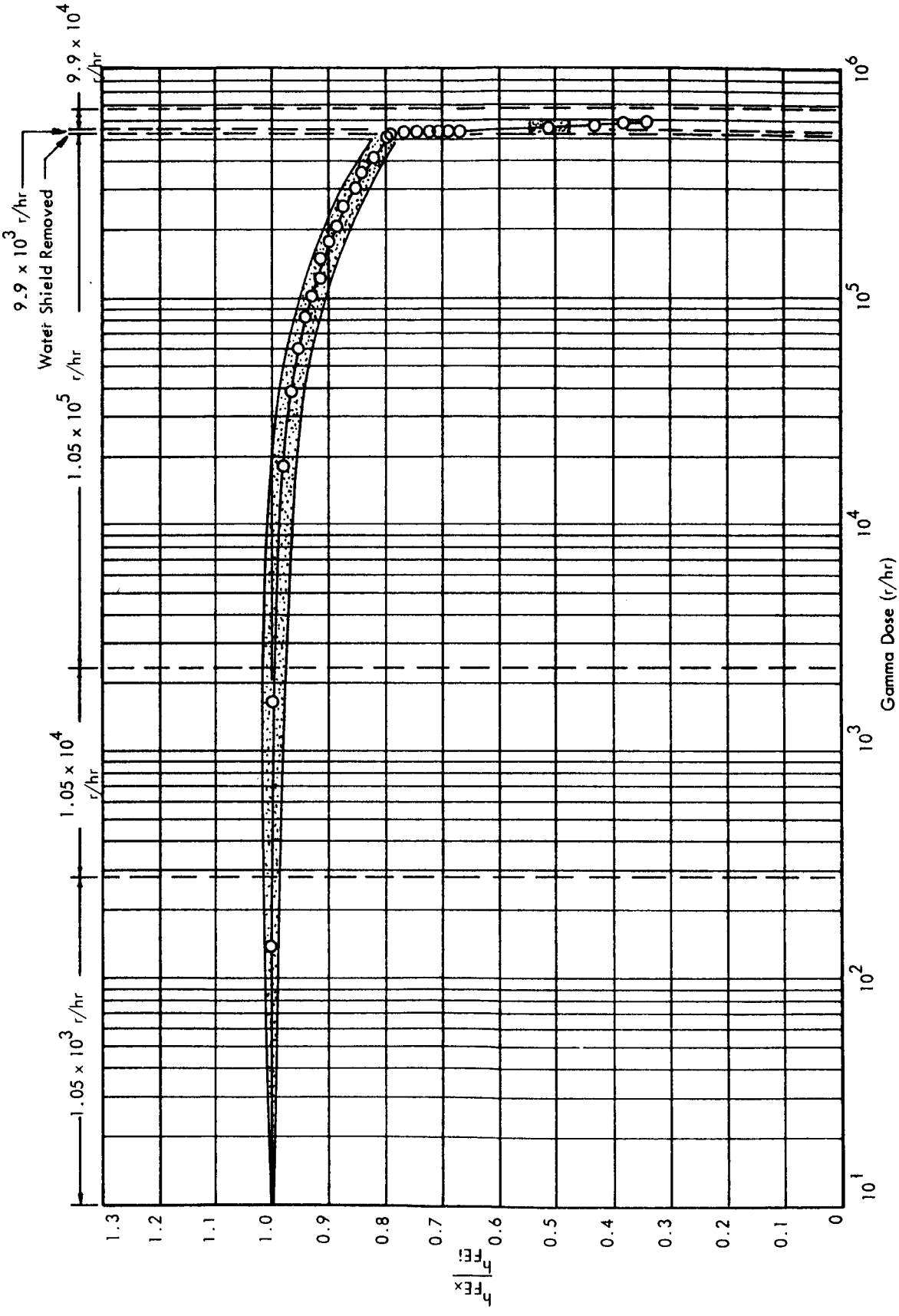

FIGURE 28 2N722 - GROUP T (TEMPERATURE CYCLED) - NORMALIZED BETA VS. GAMMA DOSE

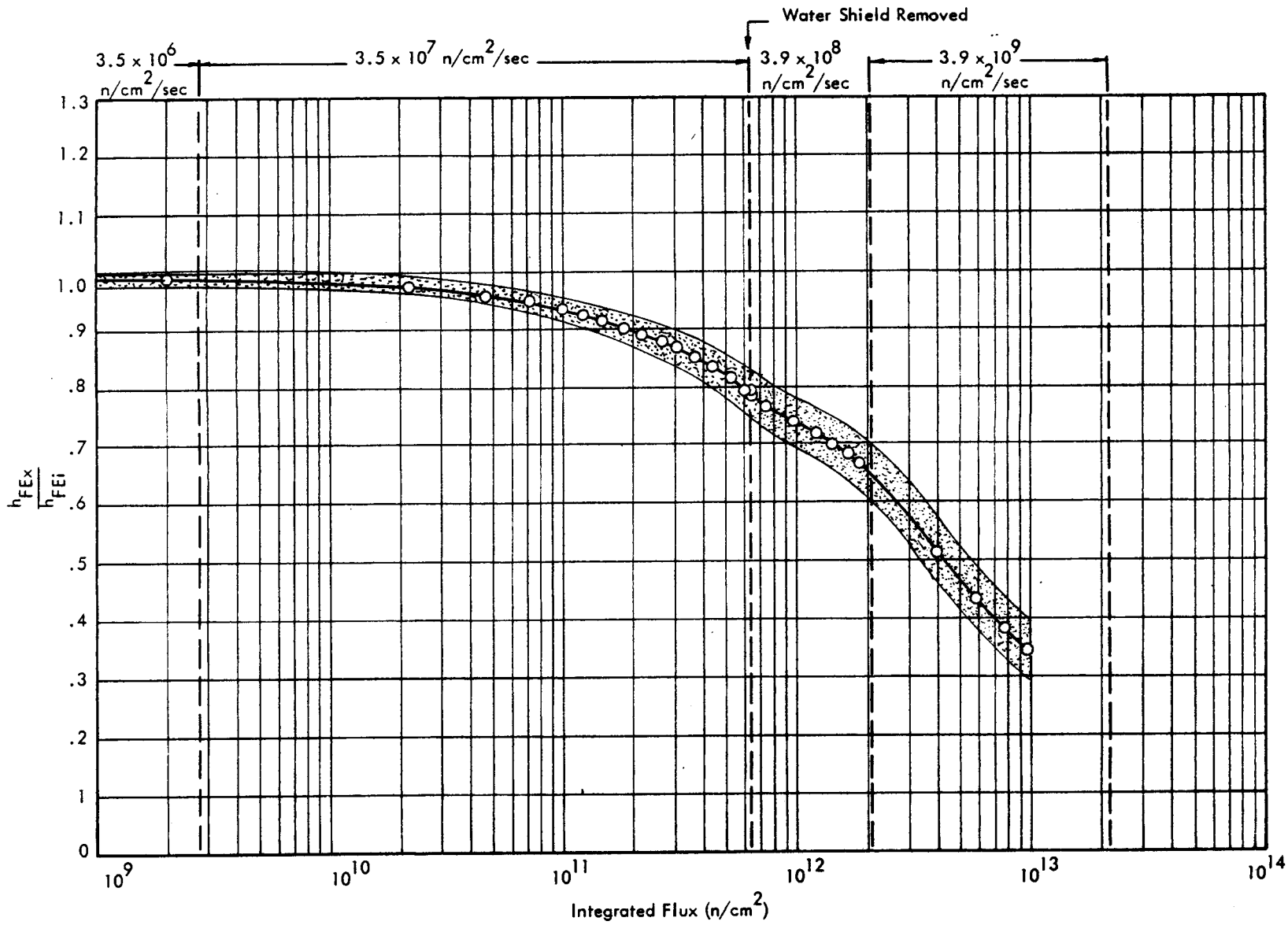

FIGURE 29 2N722-GROUP V (VIBRATED AND ACCELERATED)

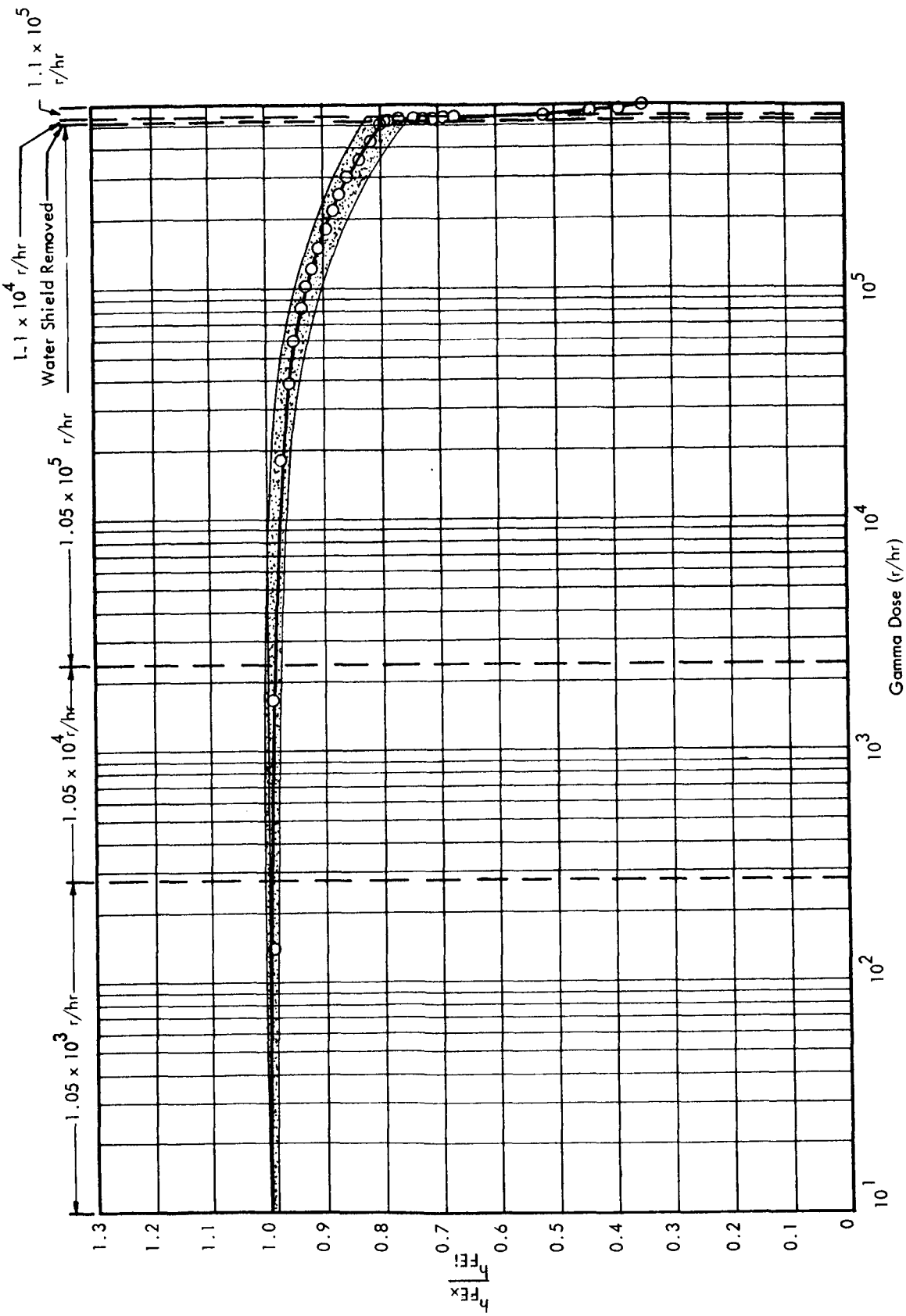

FIGURE 30 2N722 - GROUP V (VIBRATED AND ACCELERATED) NORMALIZED BETA VS. GAMMA DOSE

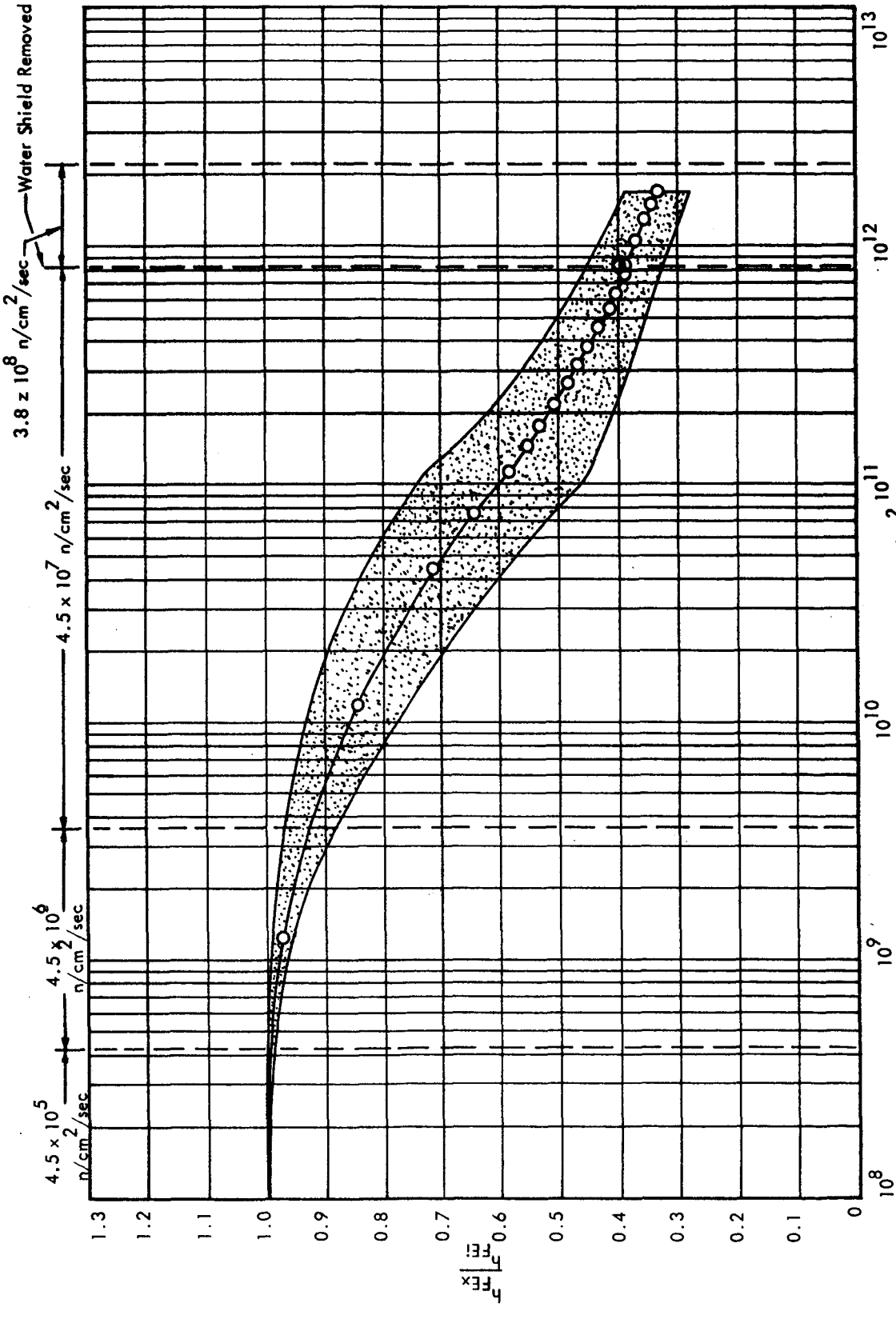

FIGURE 31 2N657A - NORMALIZED BETA VS. INTEGRATED FLUX

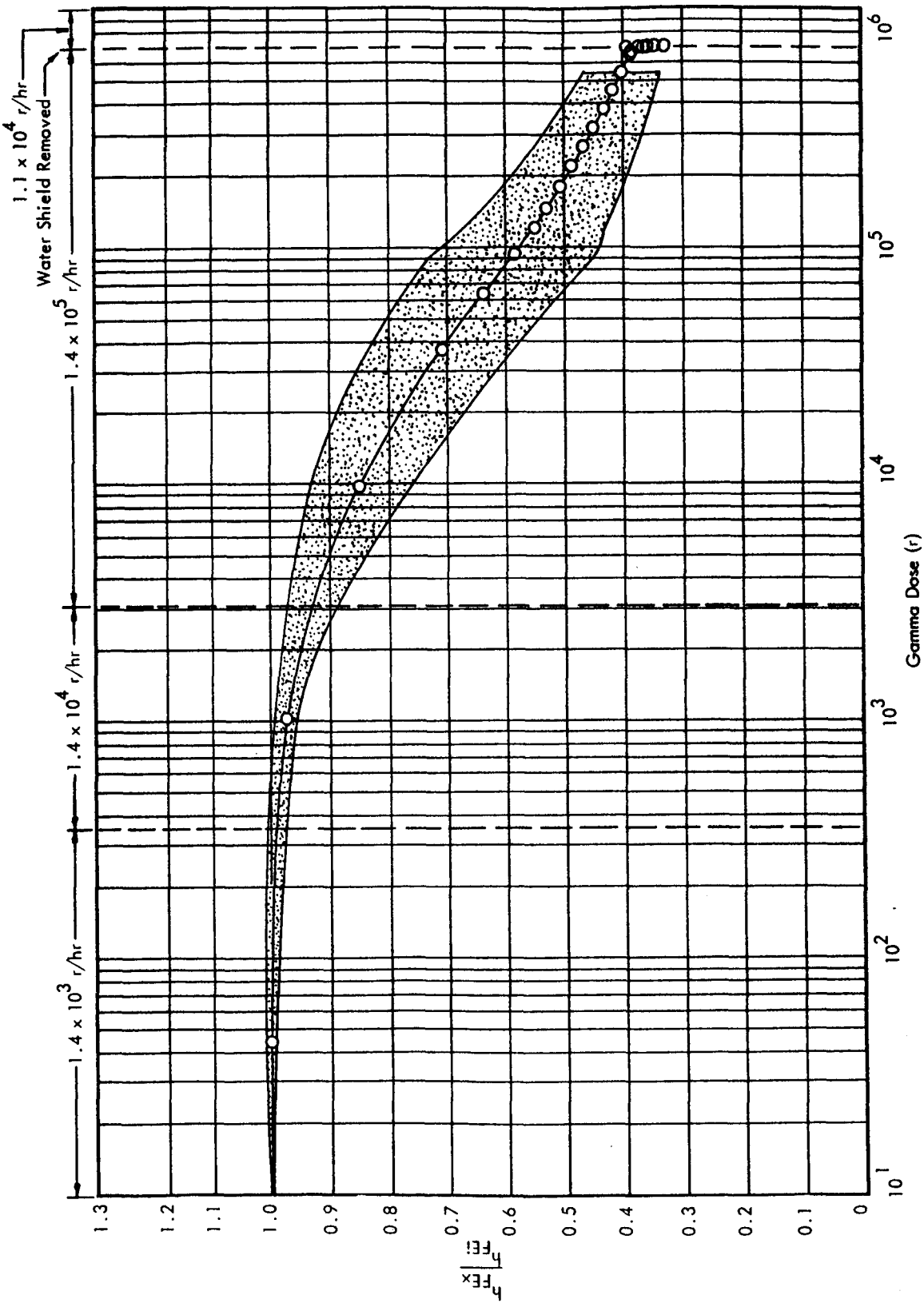

FIGURE 32 2N657A - NORMALIZED BETA VS. GAMMA DOSE

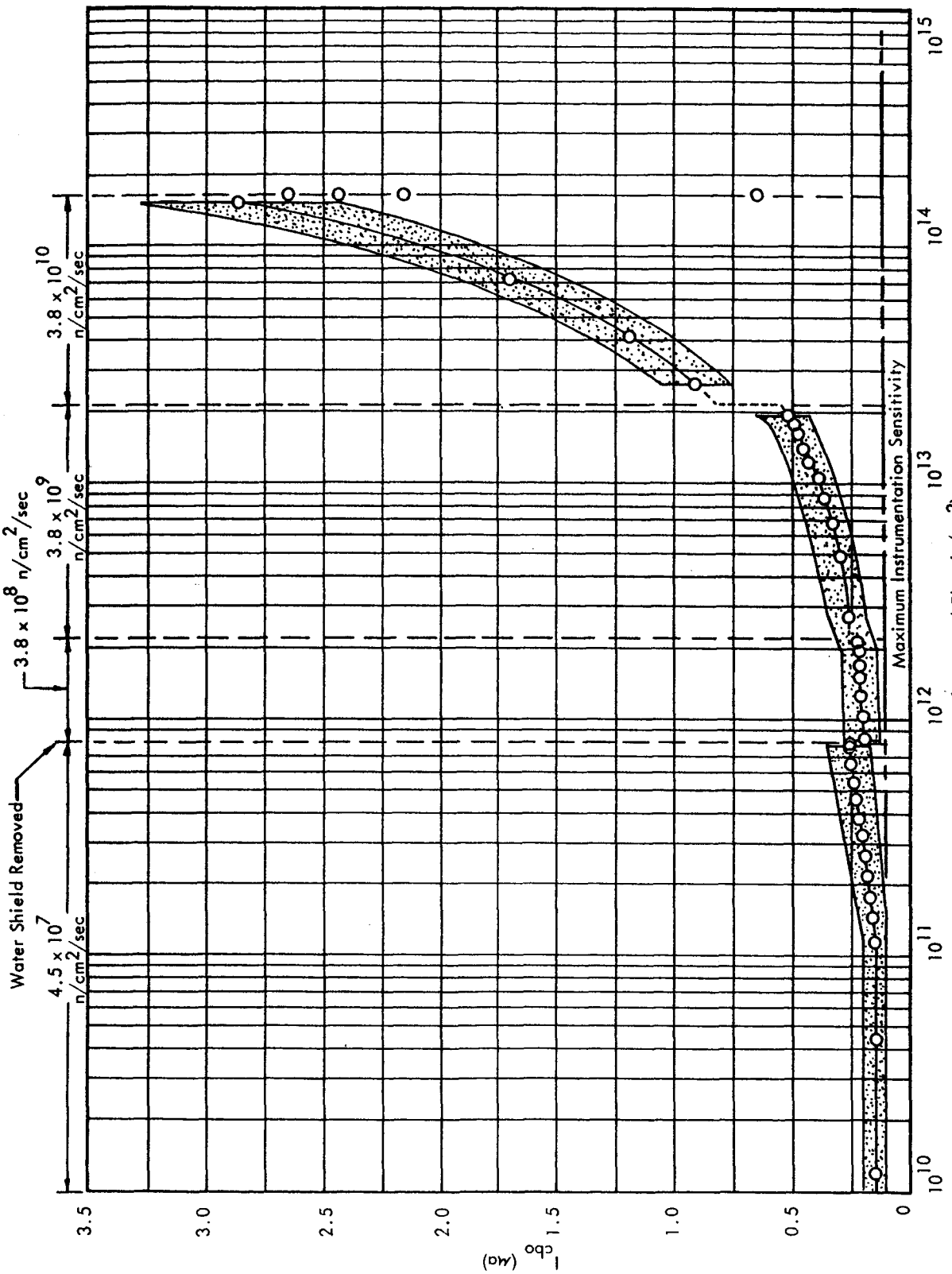

FIGURE 33 2N657A - LEAKAGE CURRENT (COLLECTOR TO BASE) VS. INTEGRATED FLUX

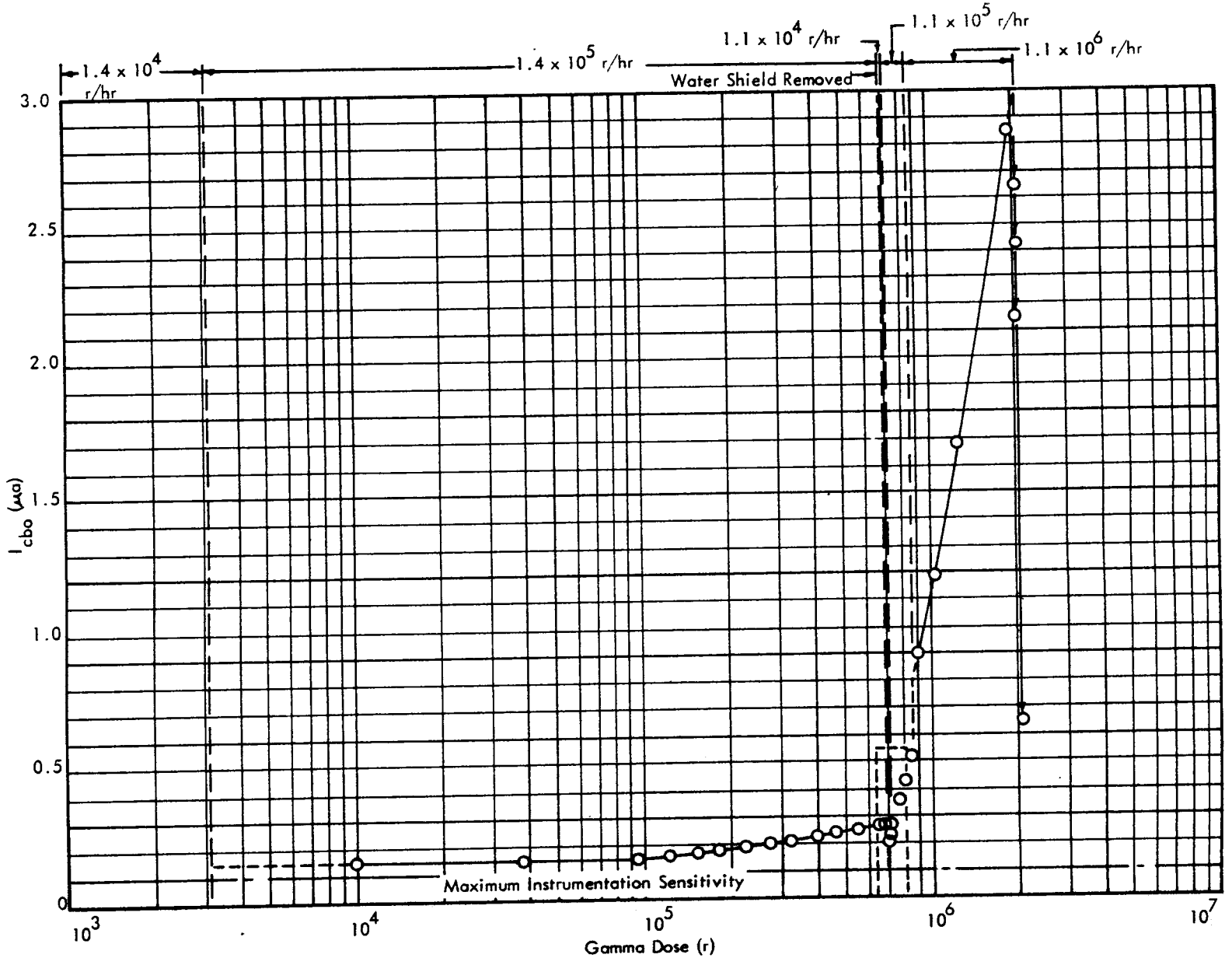

FIGURE 34 2N657A - LEAKAGE CURRENT (COLLECTOR TO BASE) VS. GAMMA DOSE

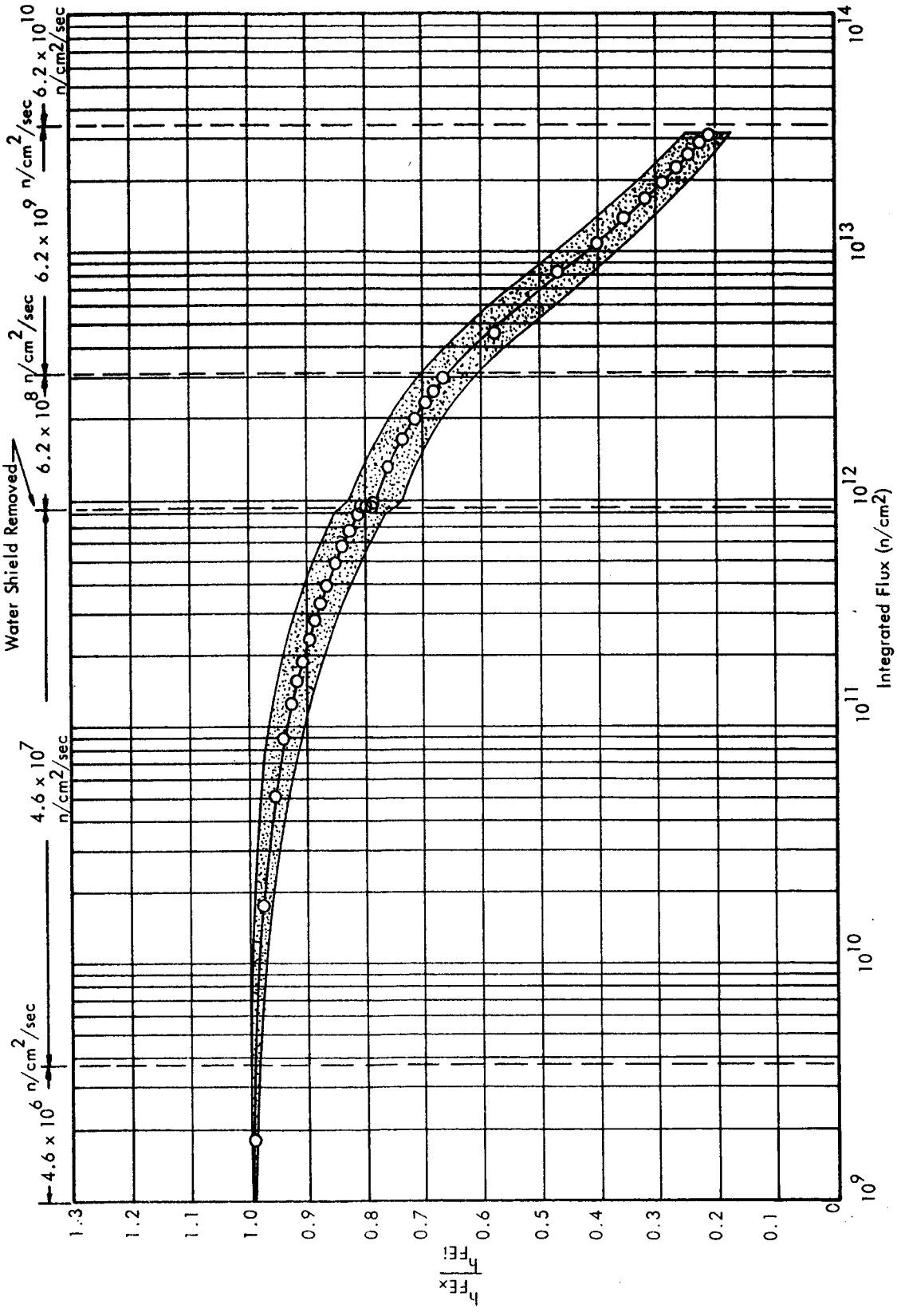

FIGURE 35 2N697 - NORMALIZED BETA VS. INTEGRATED FLUX

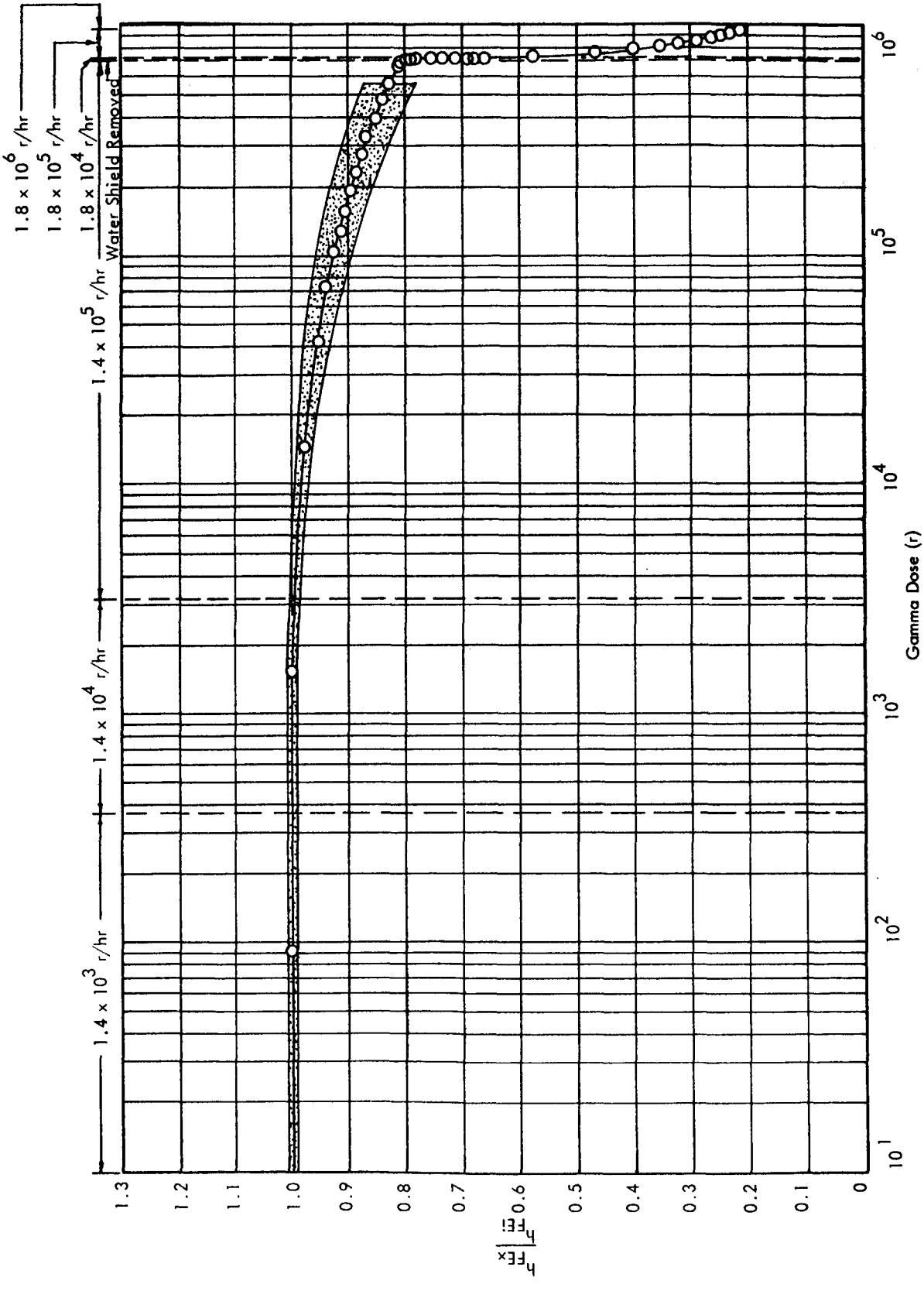

FIGURE 36 2N697 - NORMALIZED BETA VS. GAMMA DOSE

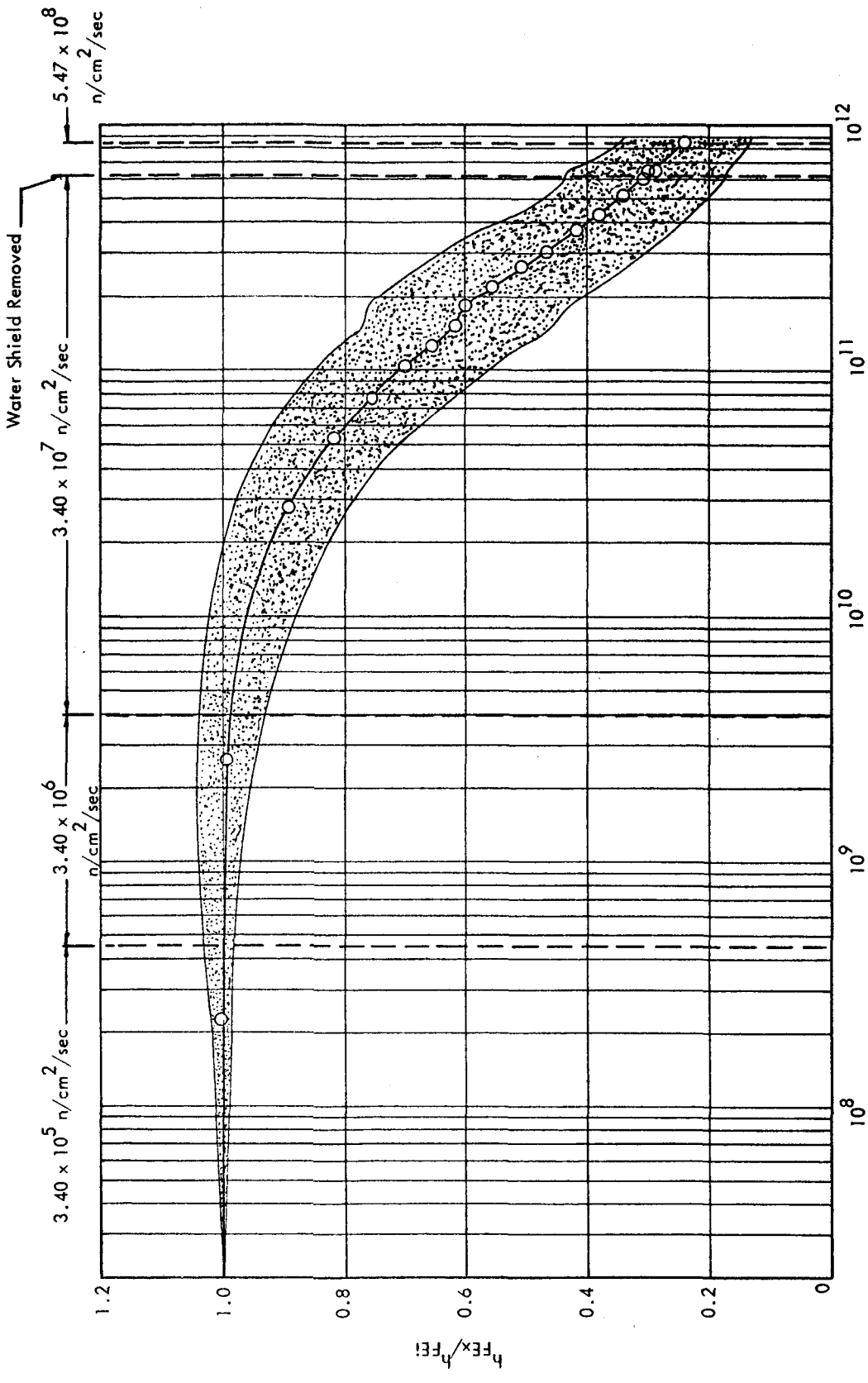

FIGURE 37 2N1016C (USED)-NORMALIZED h_{FE} VS. INTEGRATED FLUX

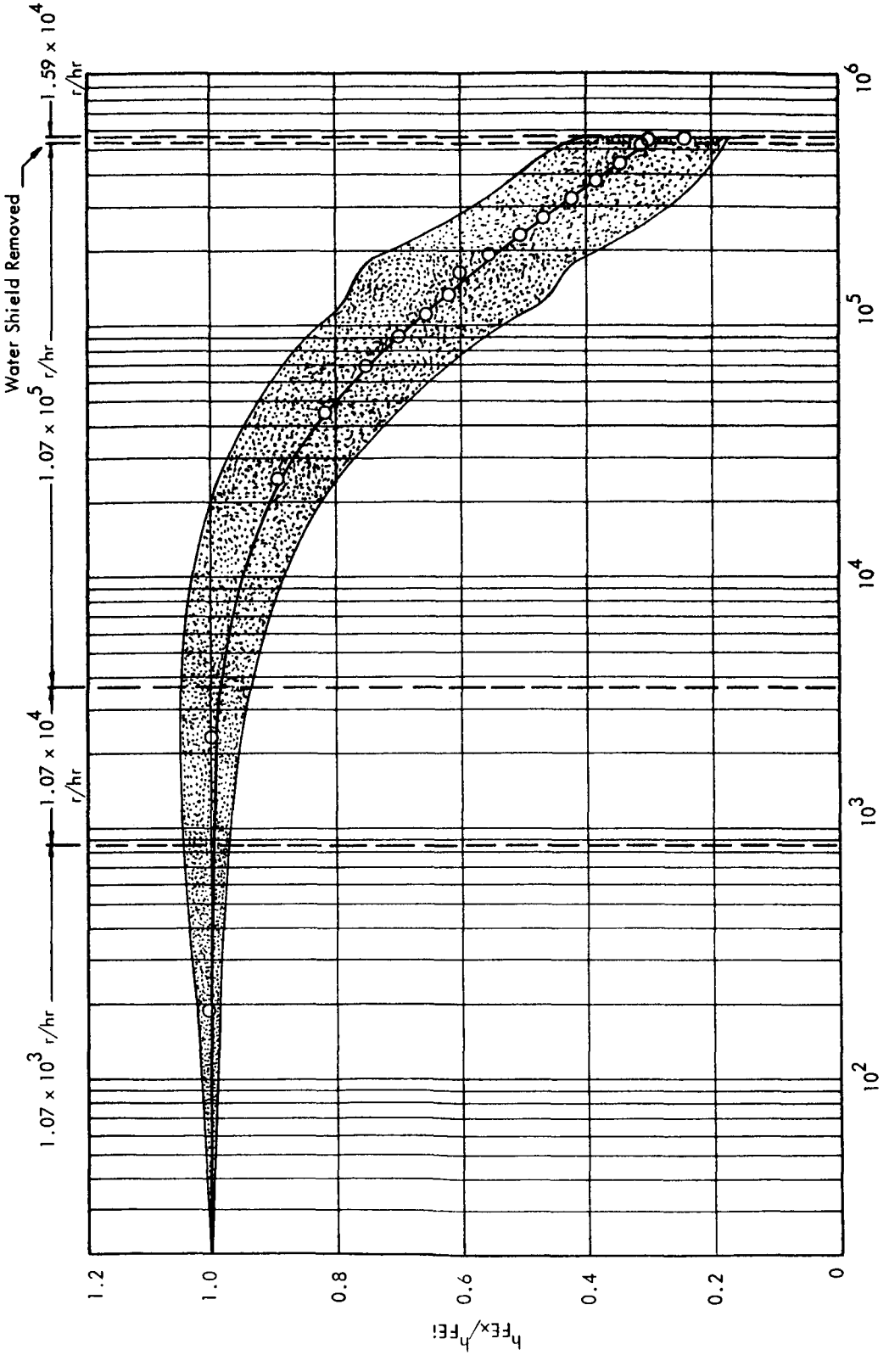

FIGURE 38 2N1016C (USED)–NORMALIZED h_{FE} VS. GAMMA DOSE

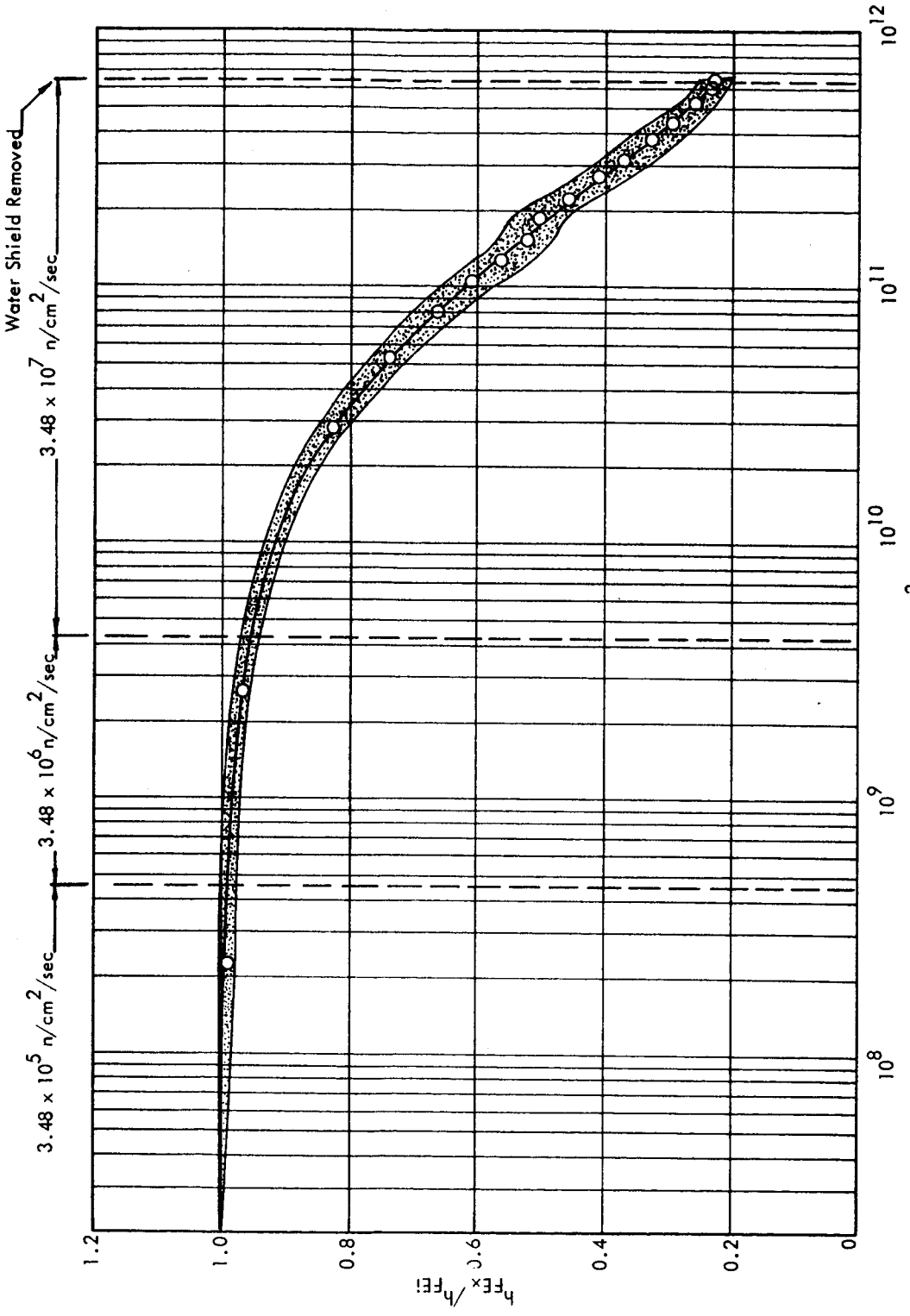

FIGURE 39 S2N1016D (NEW) NORMALIZED h_{FE} VS. INTEGRATED FLUX

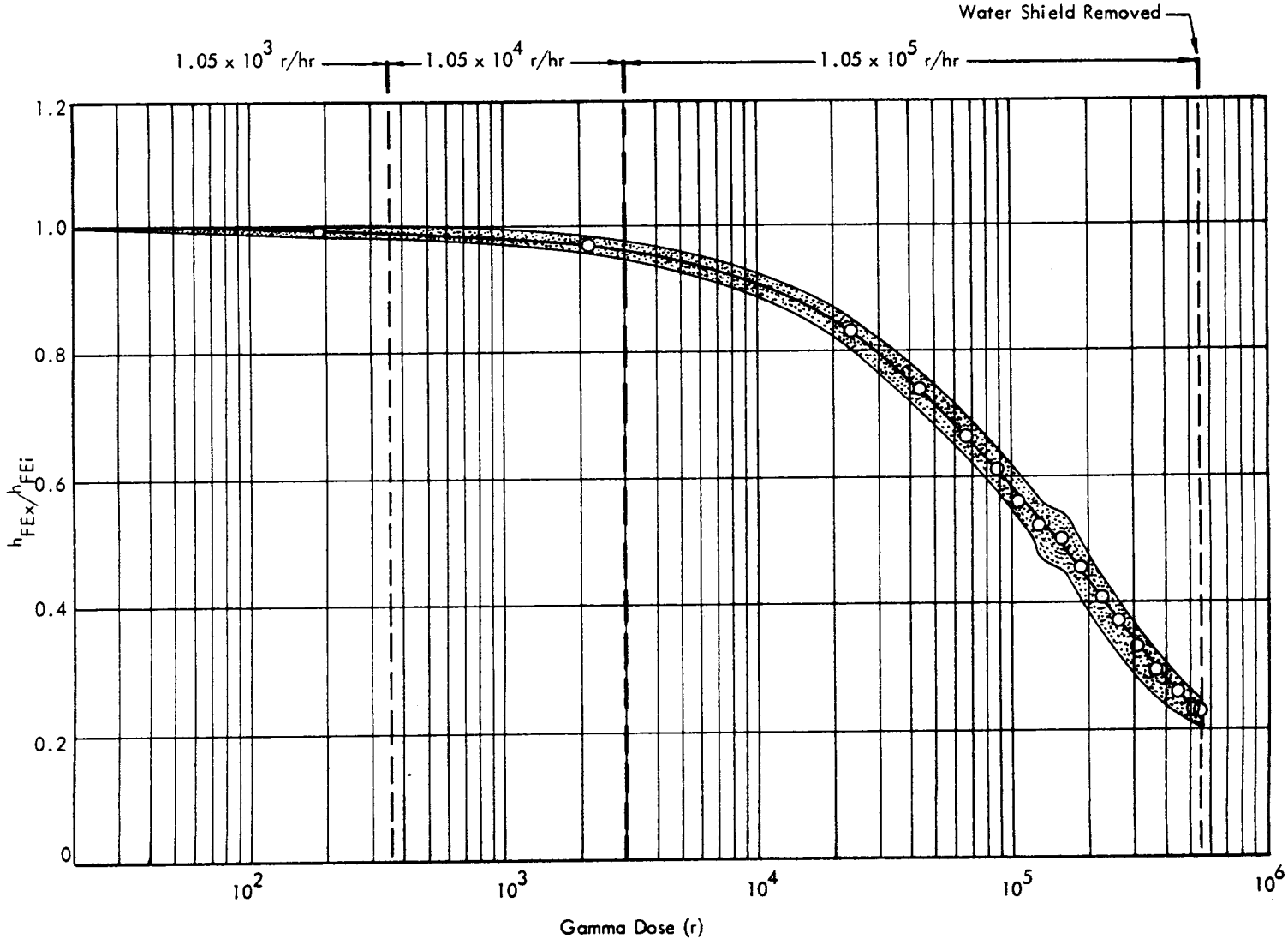

FIGURE 40 S2N1016D (NEW)-NORMALIZED h_{FE} VS. GAMMA DOSE

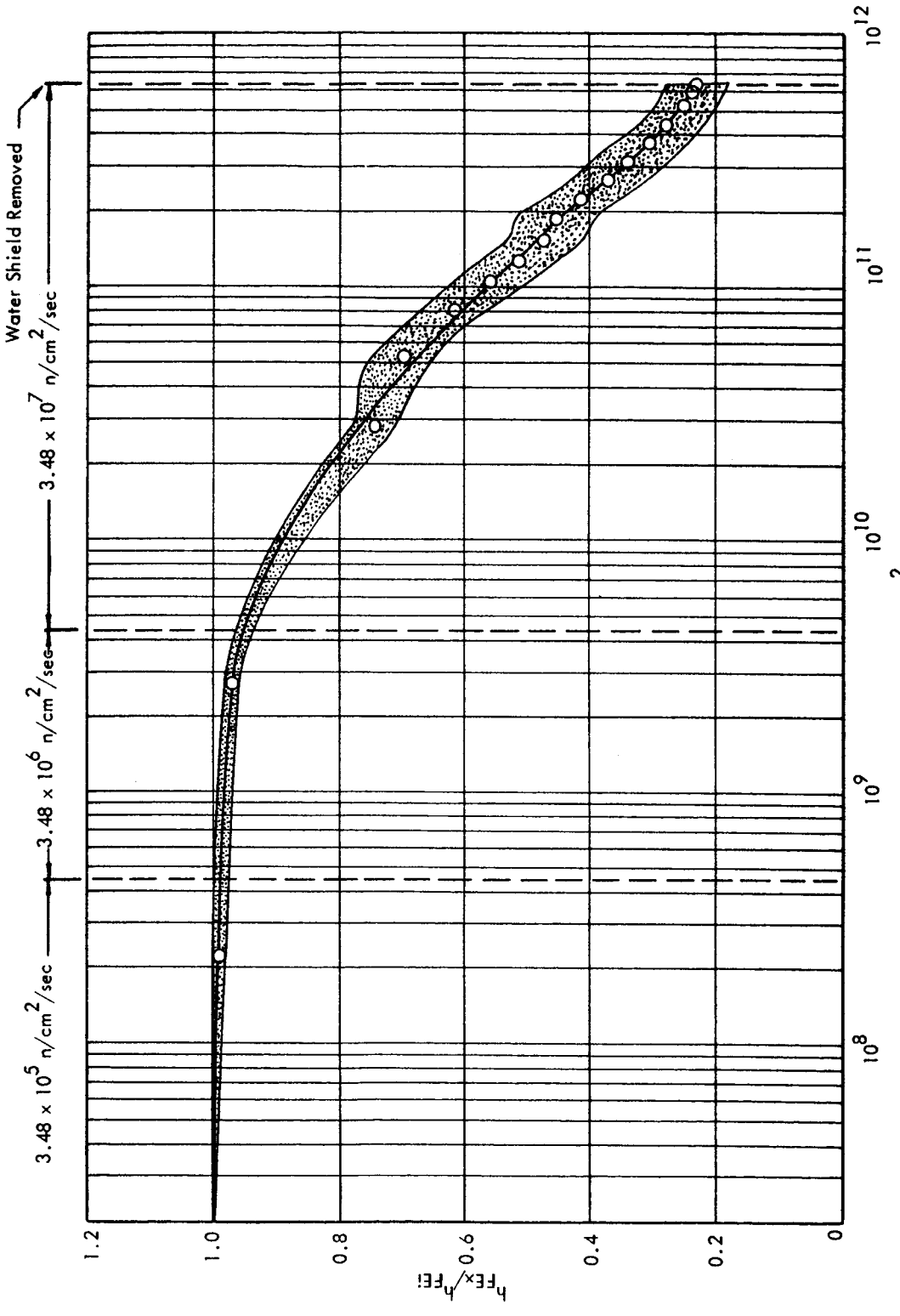

FIGURE 41 2N1016D (USED)-NORMALIZED h_{FE} VS. INTEGRATED FLUX

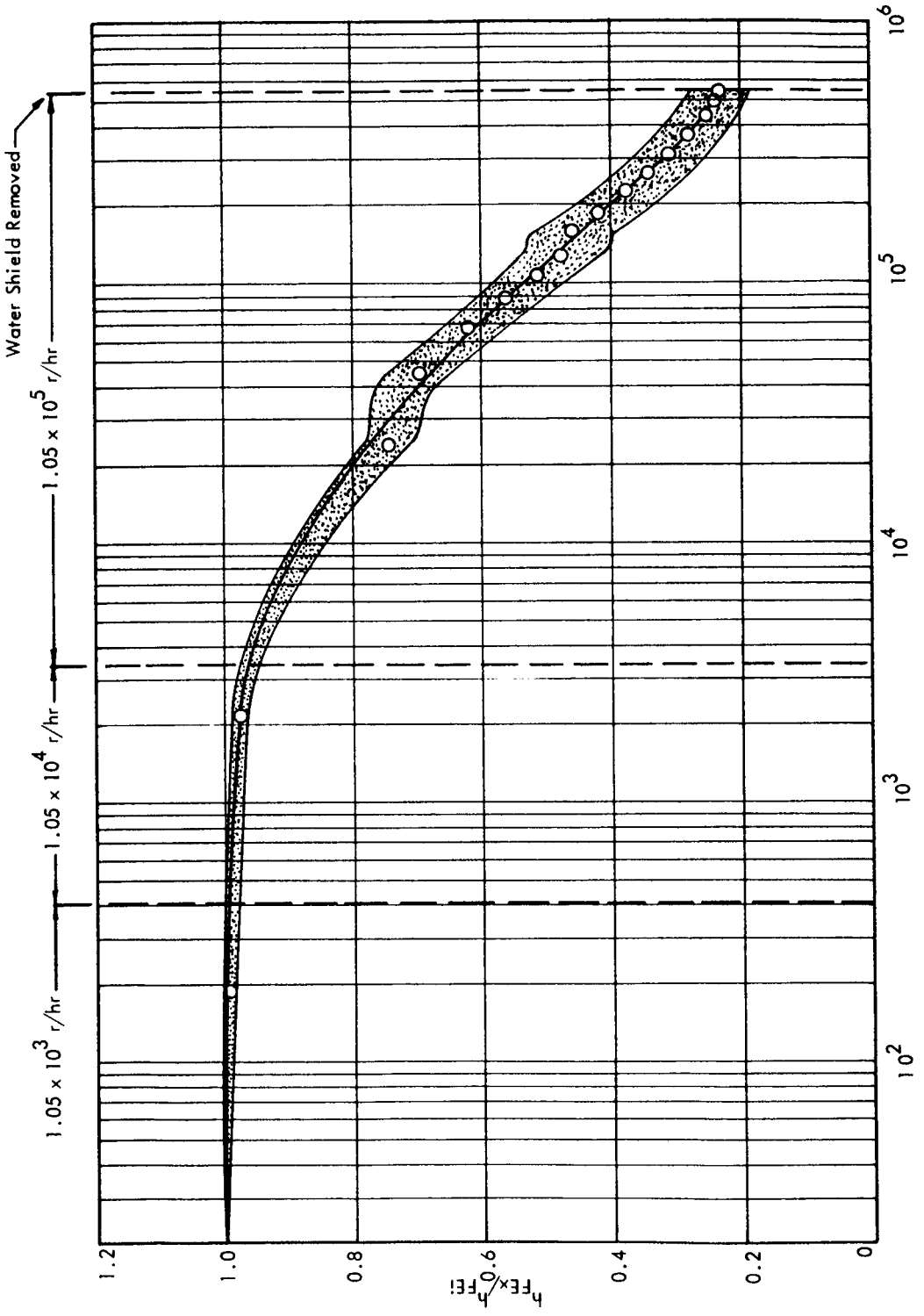

FIGURE 42 2N1016D (USED)-NORMALIZED h_{FE} VS. GAMMA DOSE

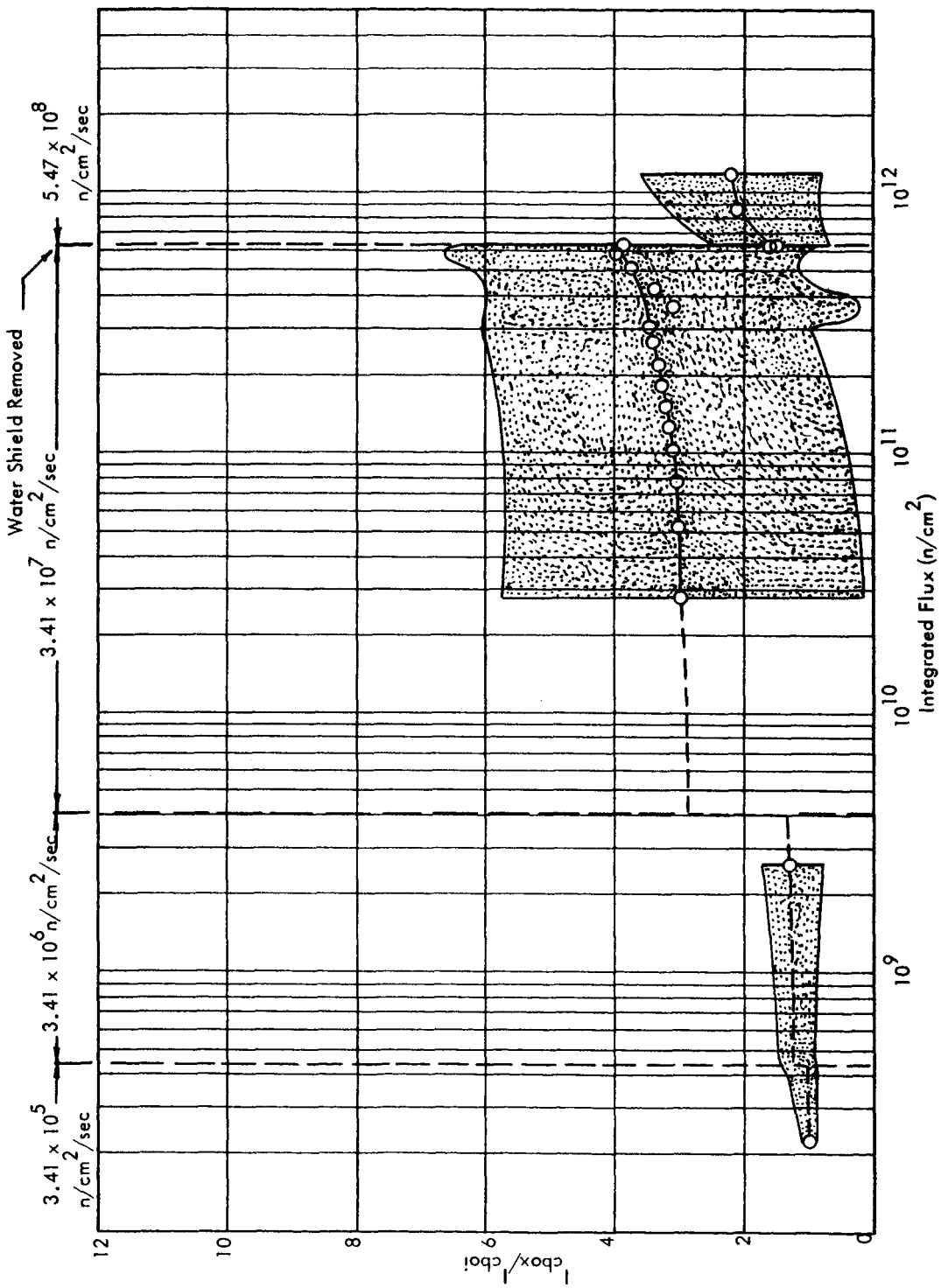

FIGURE 43 2N1016C (USED)-NORMALIZED LEAKAGE CURRENT (COLLECTOR TO BASE) VS. INTEGRATED FLUX

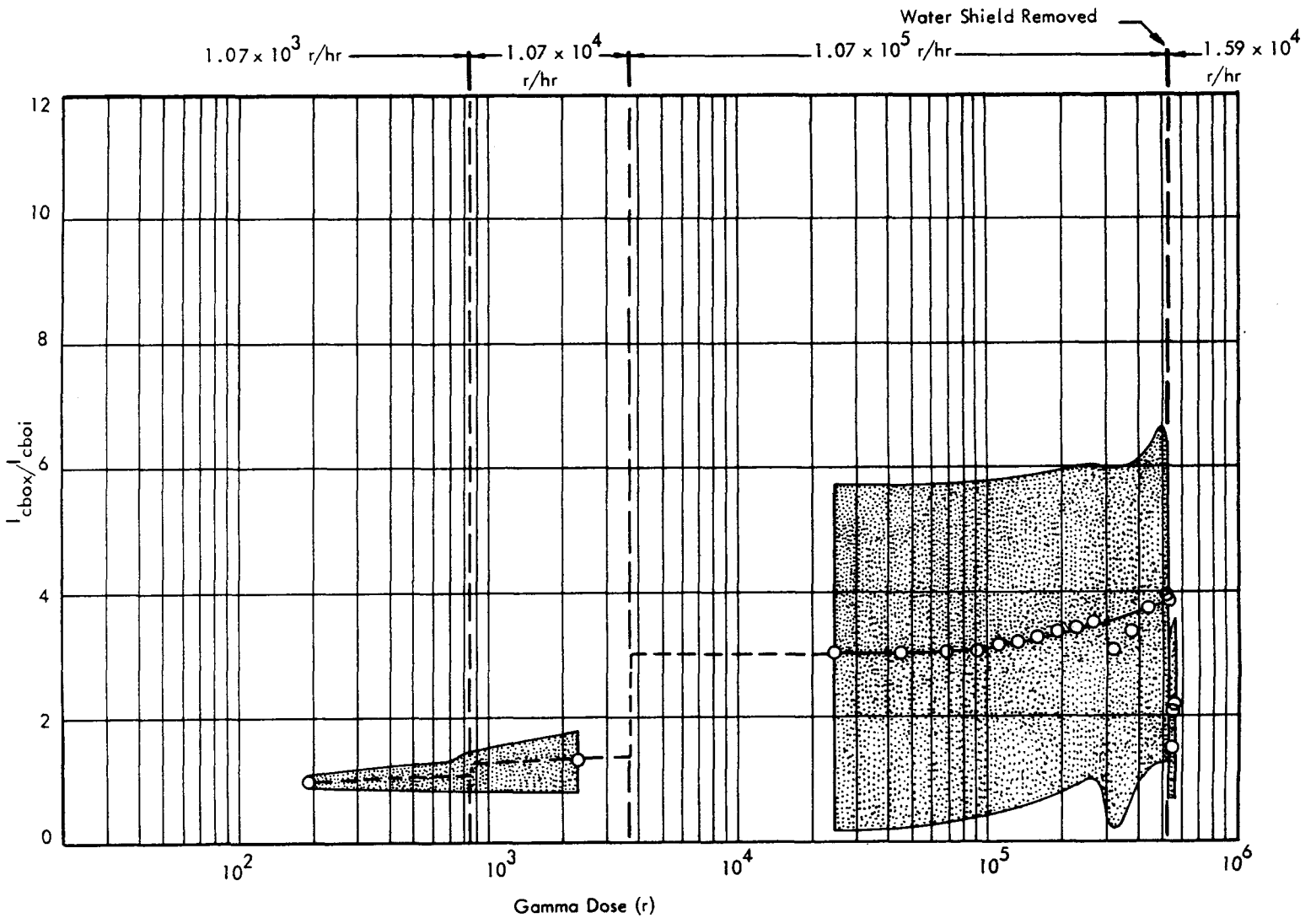

FIGURE 44 2N1016C (USED)-NORMALIZED LEAKAGE CURRENT (COLLECTOR TO BASE) VS. INTEGRATED FLUX

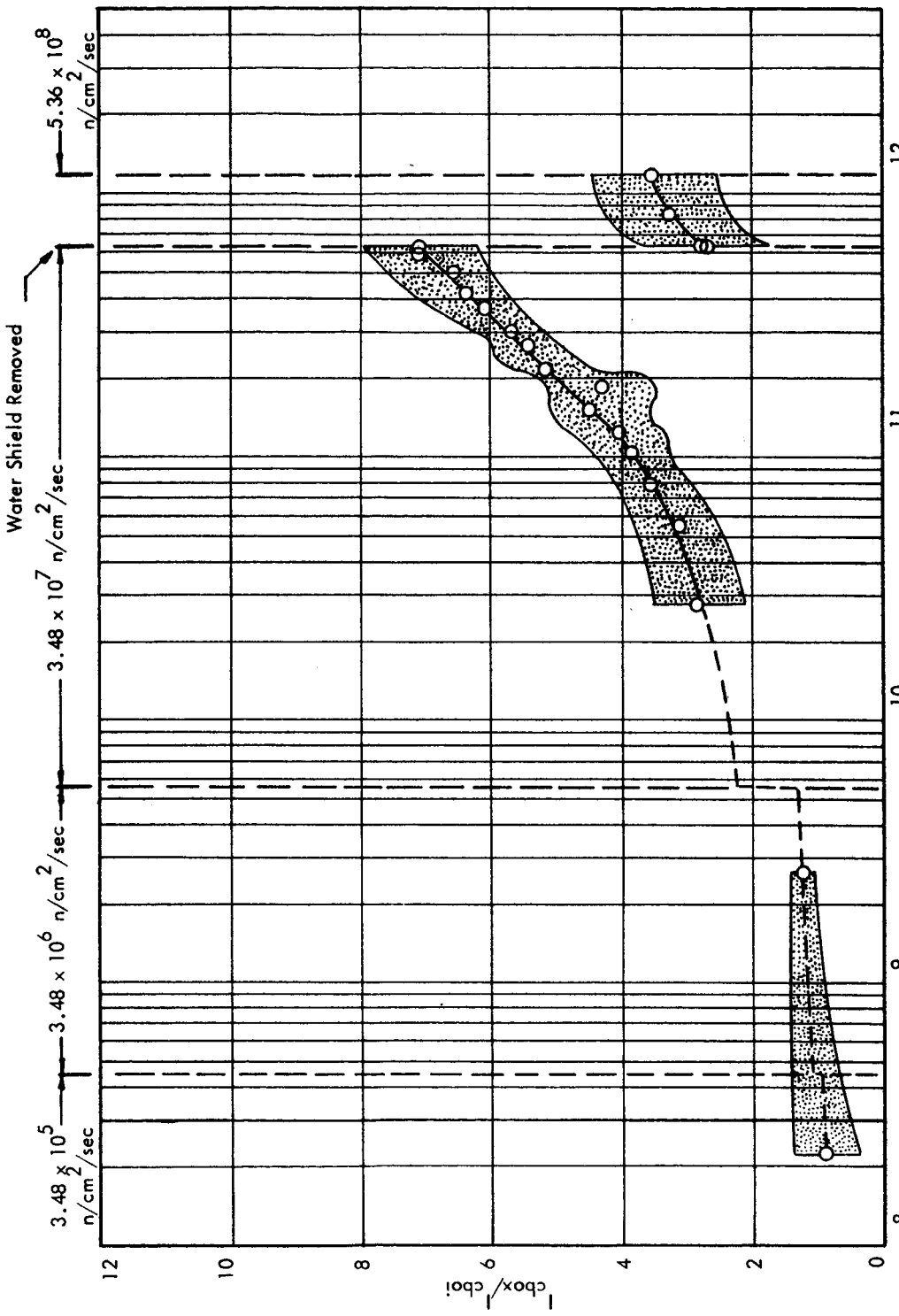

FIGURE 45 S2N1016D (NEW)-NORMALIZED LEAKAGE CURRENT (COLLECTOR TO BASE) VS. INTEGRATED FLUX

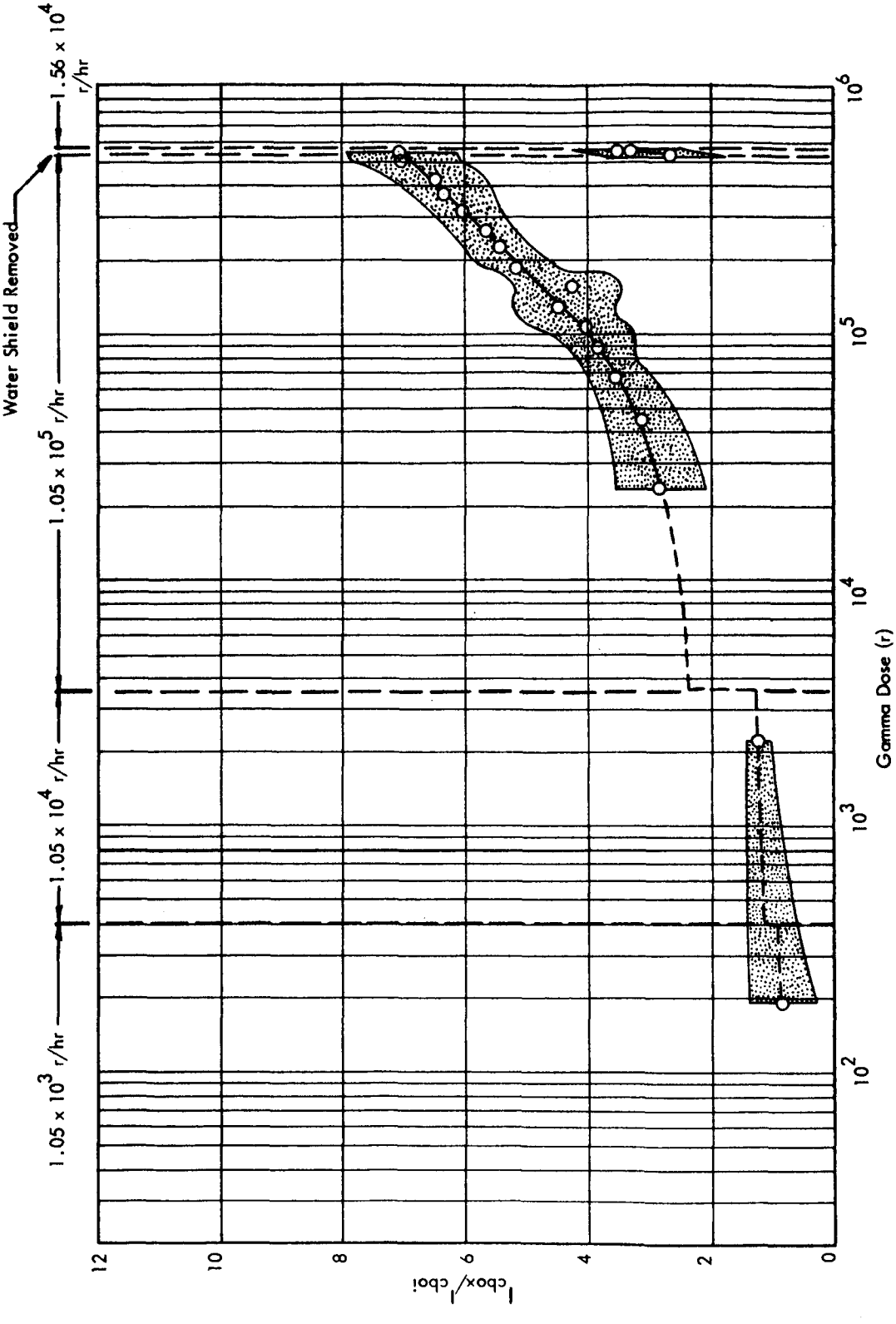

FIGURE 46 S2N1016D (NEW) NORMALIZED LEAKAGE CURRENT (COLLECTOR TO BASE) VS. GAMMA DOSE

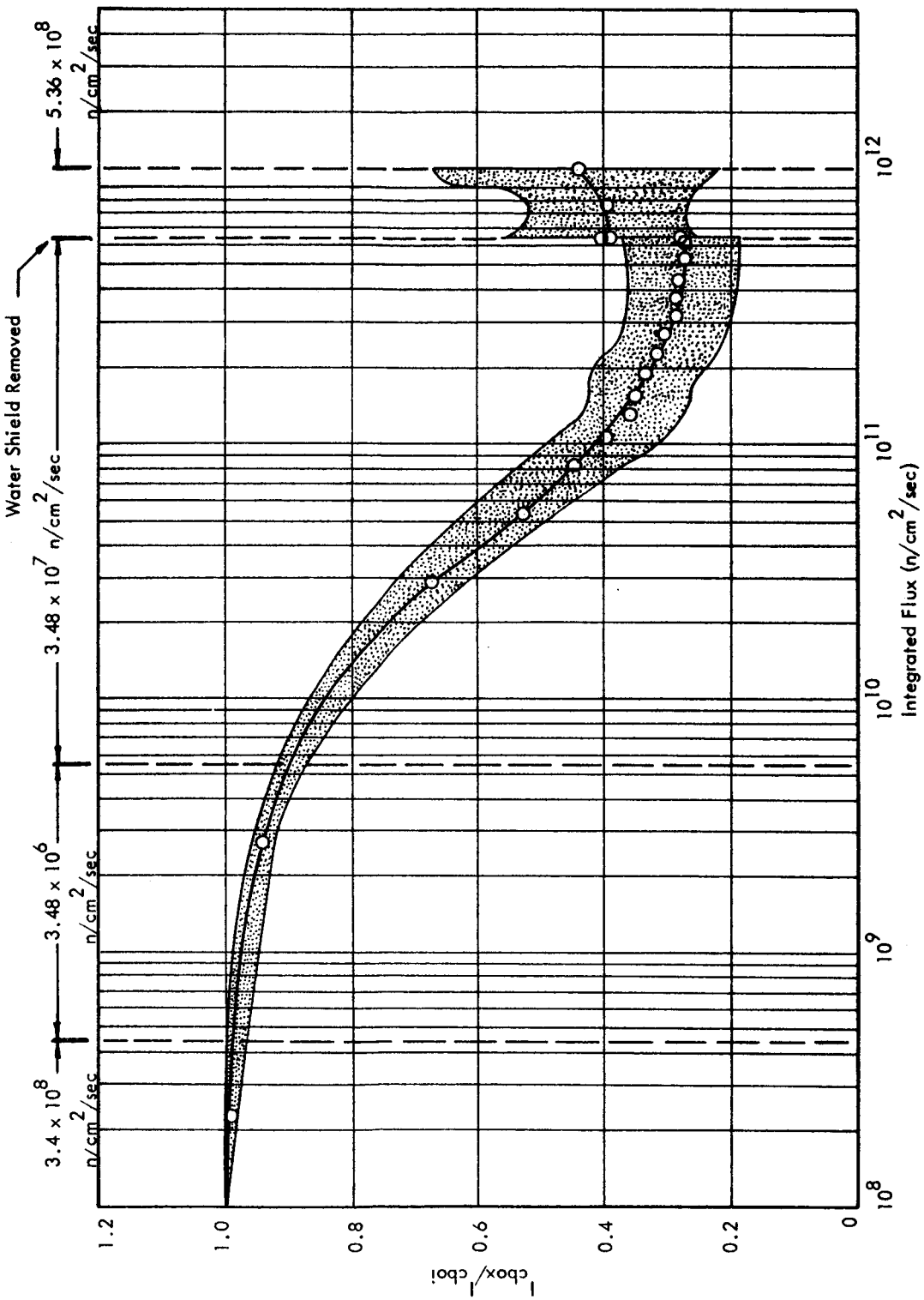

FIGURE 47 2N1016D (USED)-NORMALIZED LEAKAGE CURRENT (COLLECTOR TO BASE) VS. INTEGRATED FLUX

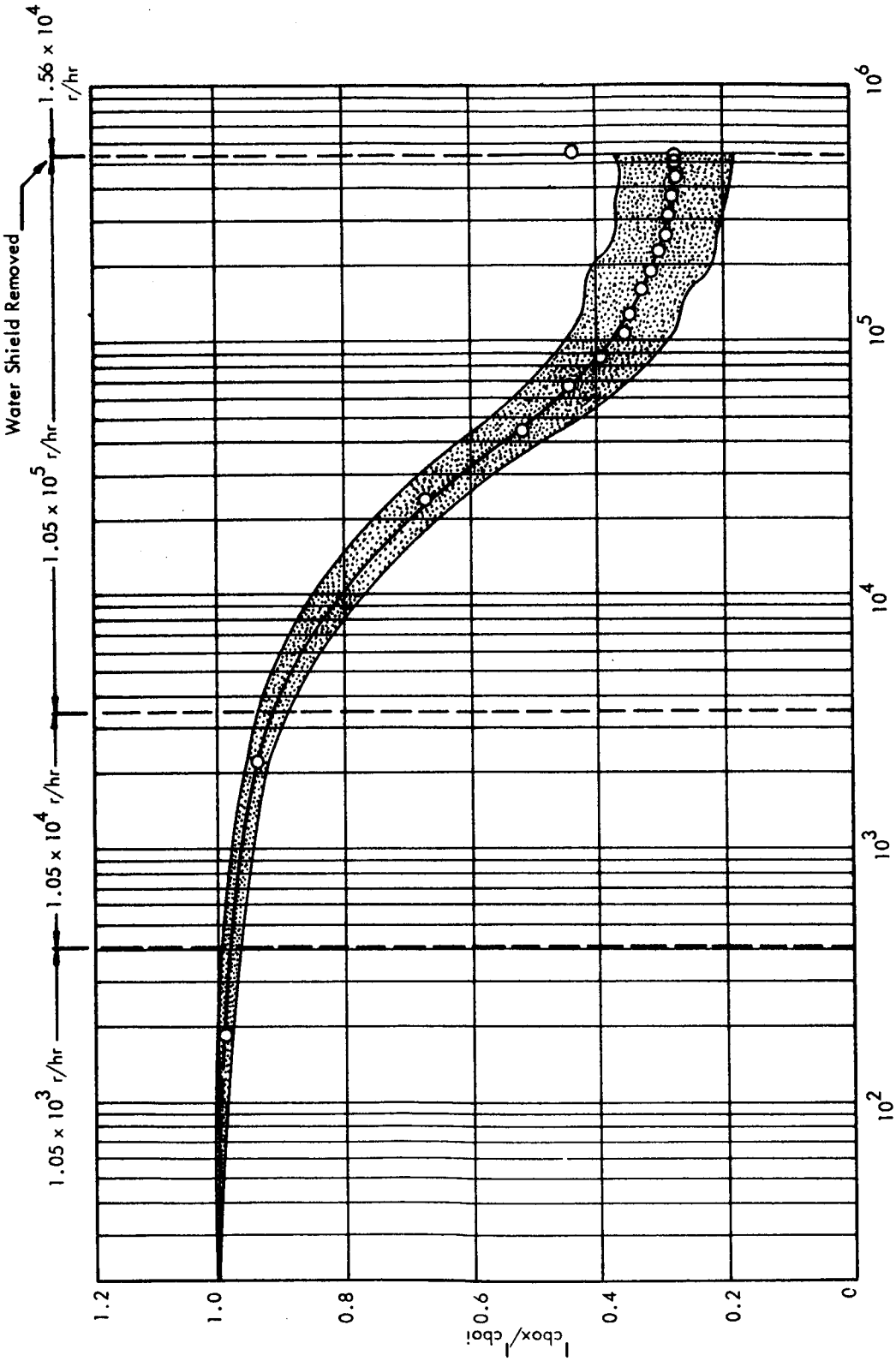

FIGURE 48 2N1016D (USED)-NORMALIZED LEAKAGE CURRENT (COLLECTOR TO BASE) VS. GAMMA DOSE

APPENDIX A

APPENDIX A

A possible alternative method of data analysis and presentation is referenced below. This method may offer certain advantages, once failure criteria are stated.

Volume NS-10, Number 1, January, 1963, of the IEEE Transactions on Nuclear Science contains an article by Mr. Frank W. Poblenz entitled "Analysis of Transistor Failure in a Nuclear Environment." Figures 1 through 7 have been prepared from normalized h_{FE} data for the four types of transistors and the one type SCR in the manner described by Mr. Poblenz. This was done to investigate whether or not the data obtained in this test lends itself to this treatment. It appears that it does.

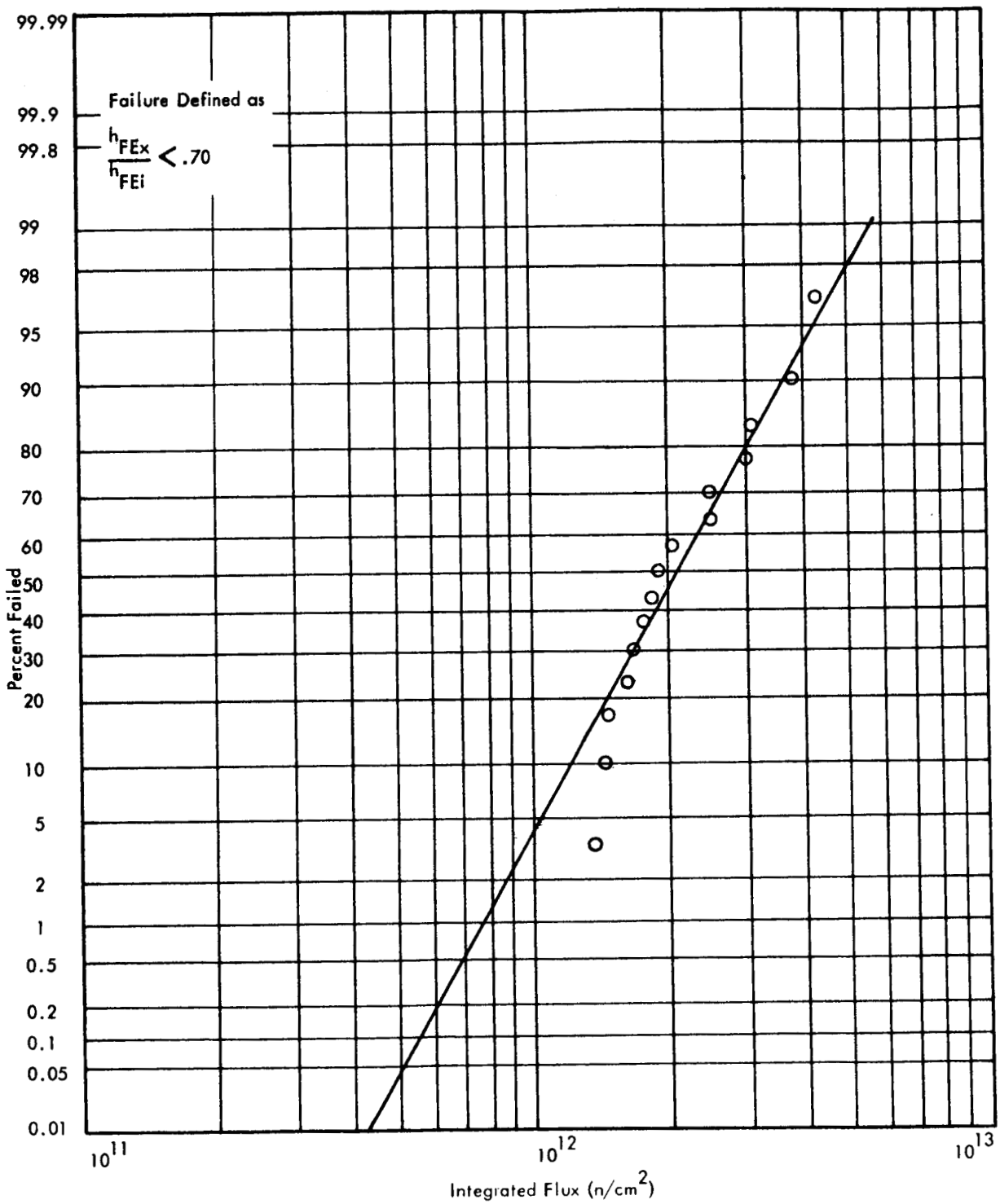

FIGURE 1 2N697 - PERCENT FAILED VS. INTEGRATED FLUX

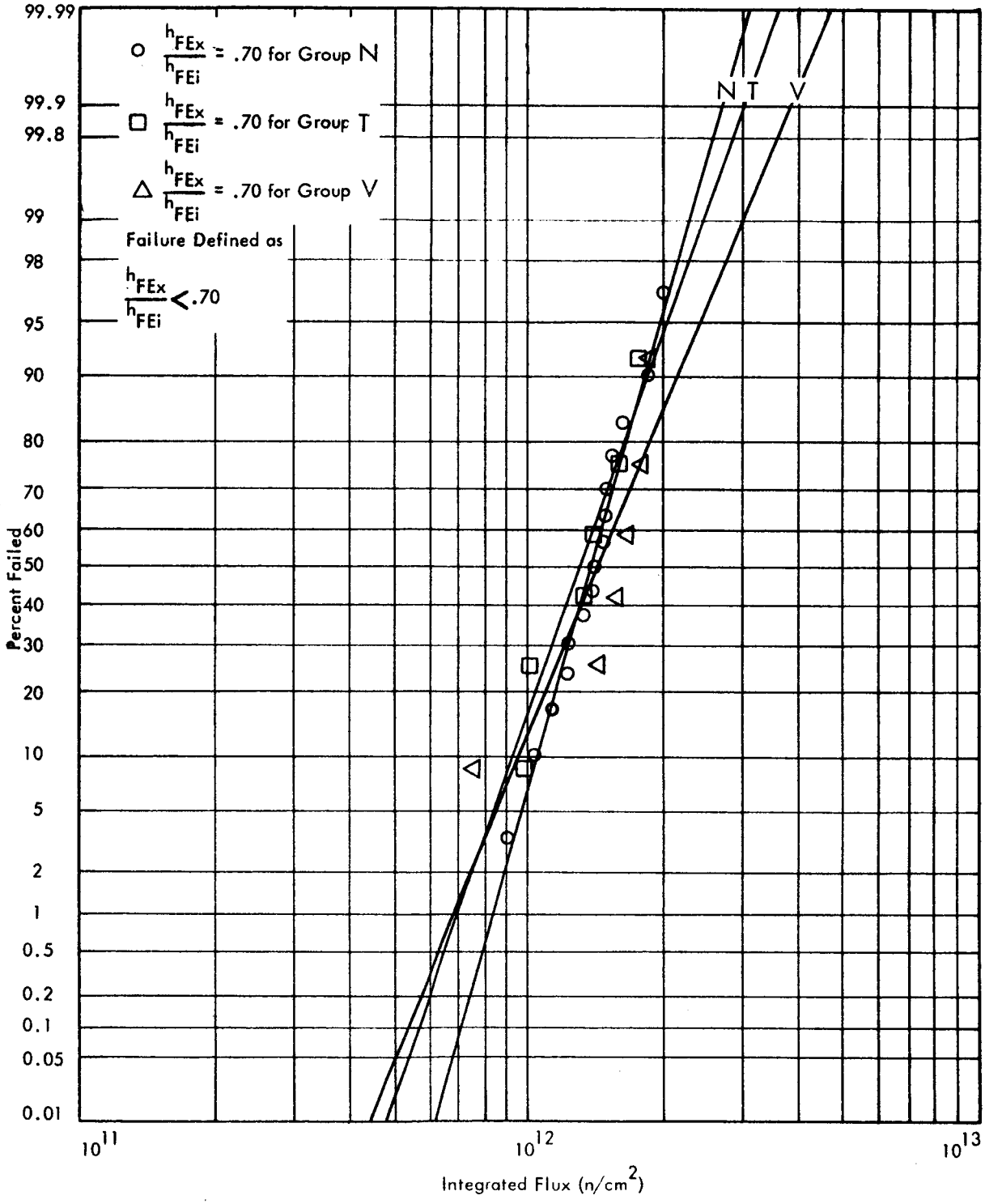

FIGURE 2 2N722 - PERCENT FAILED VS. INTEGRATED FLUX

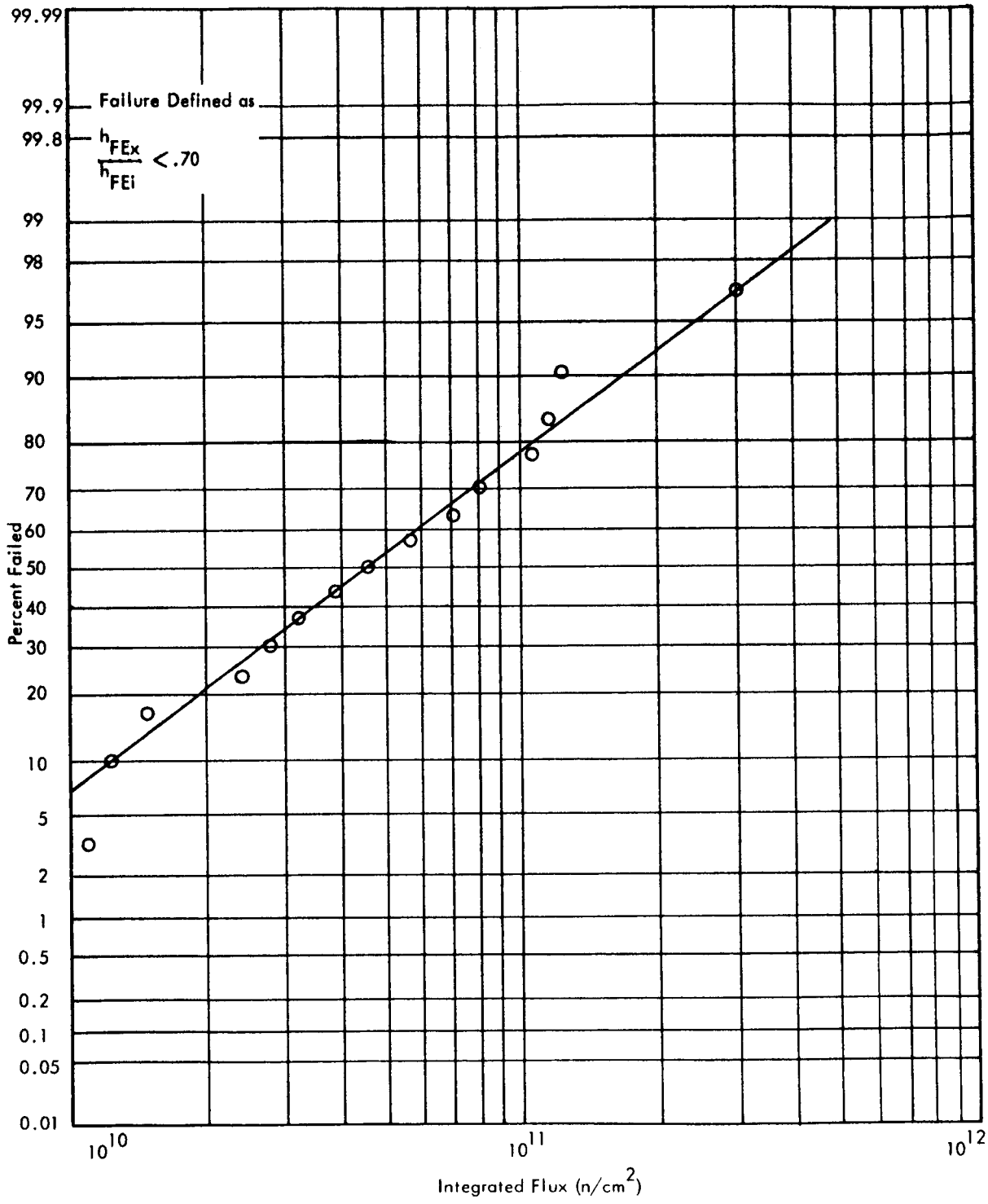

FIGURE 3 2N657A - PERCENT FAILED VS. INTEGRATED FLUX

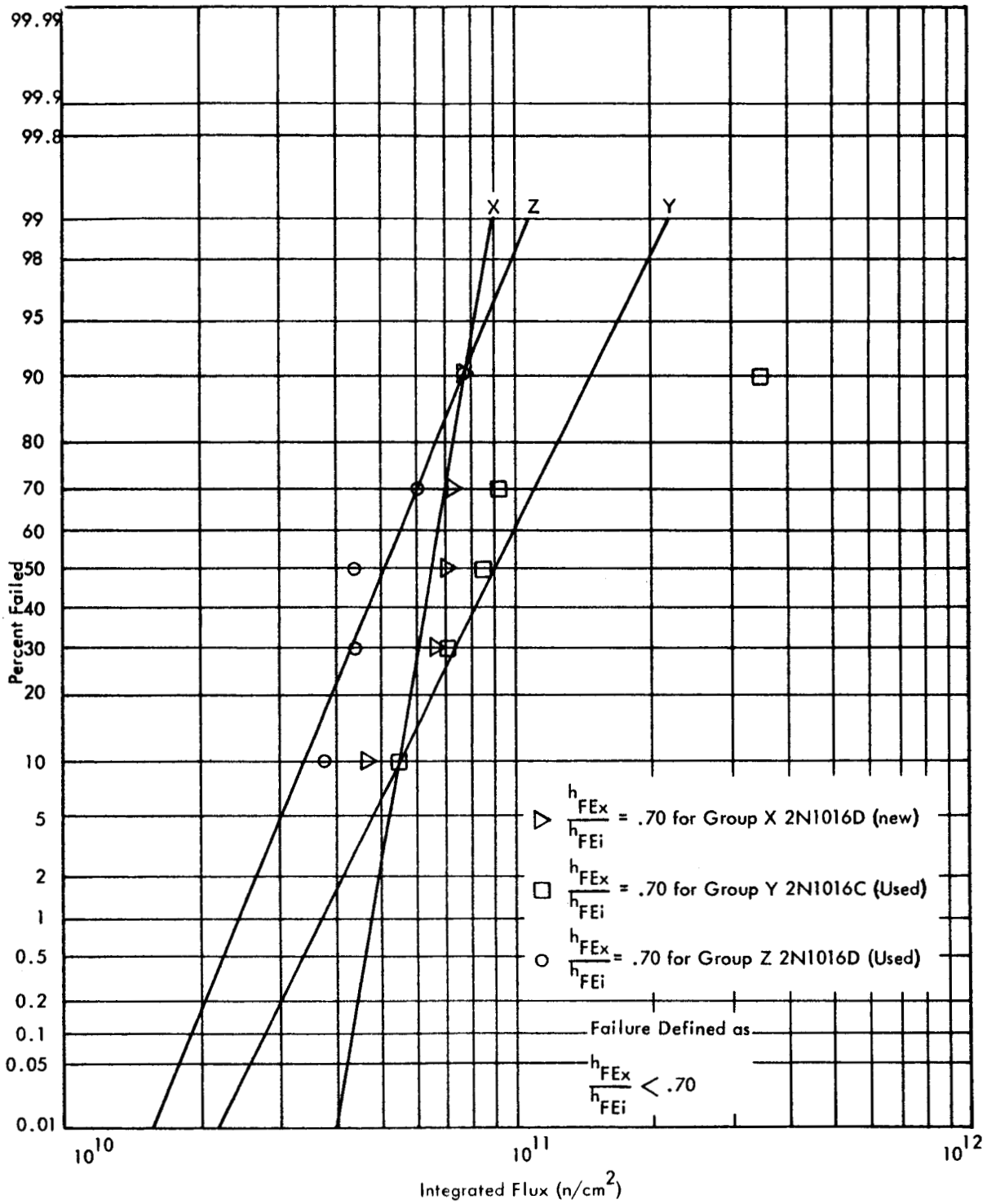

FIGURE 4 2N1016 - PERCENT FAILED VS. INTEGRATED FLUX

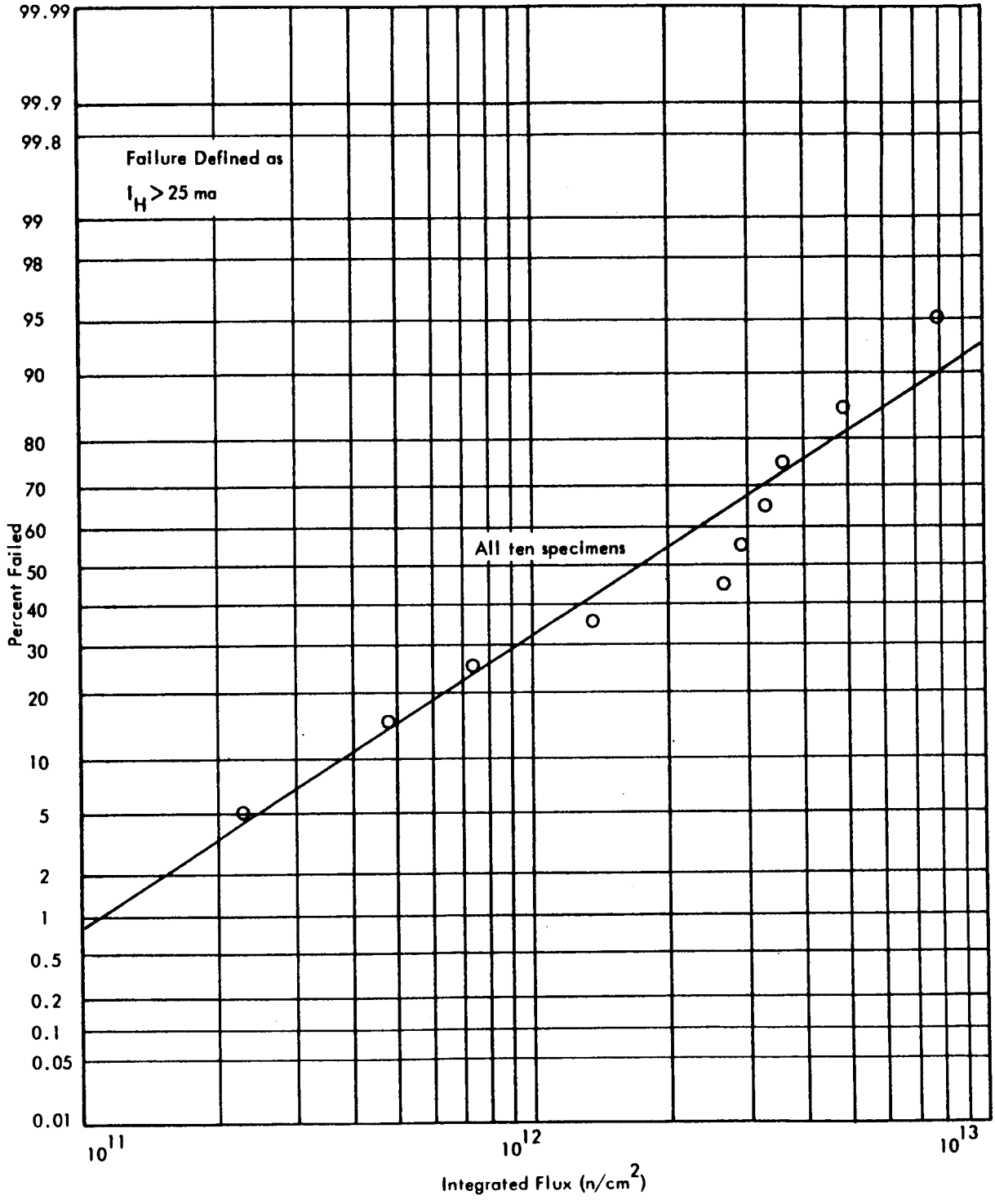

FIGURE 5 SCR 2N1774 - PERCENT FAILED VS. INTEGRATED FLUX

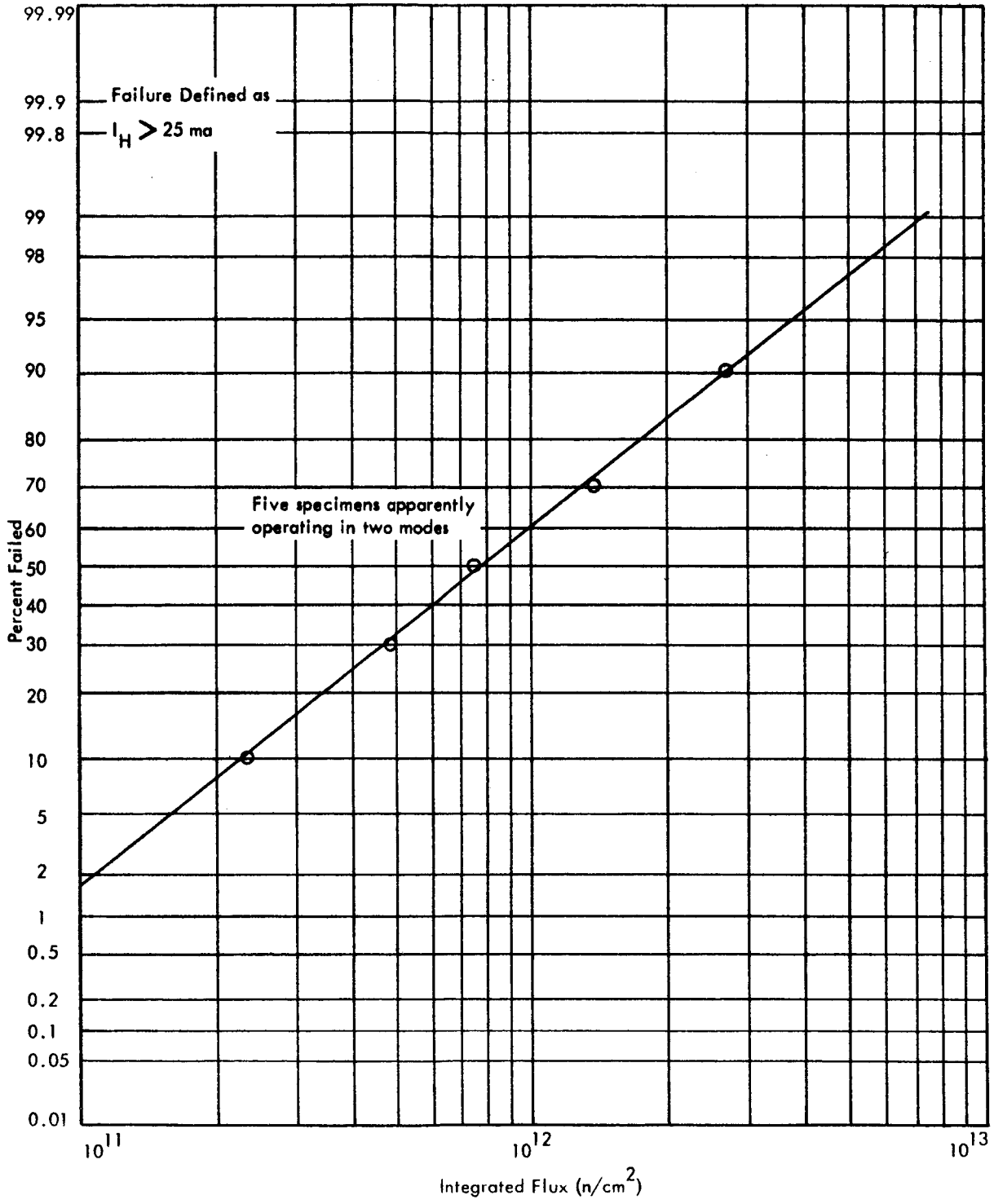

FIGURE 6 SCR 2N1774 - PERCENT FAILED VS. INTEGRATED FLUX

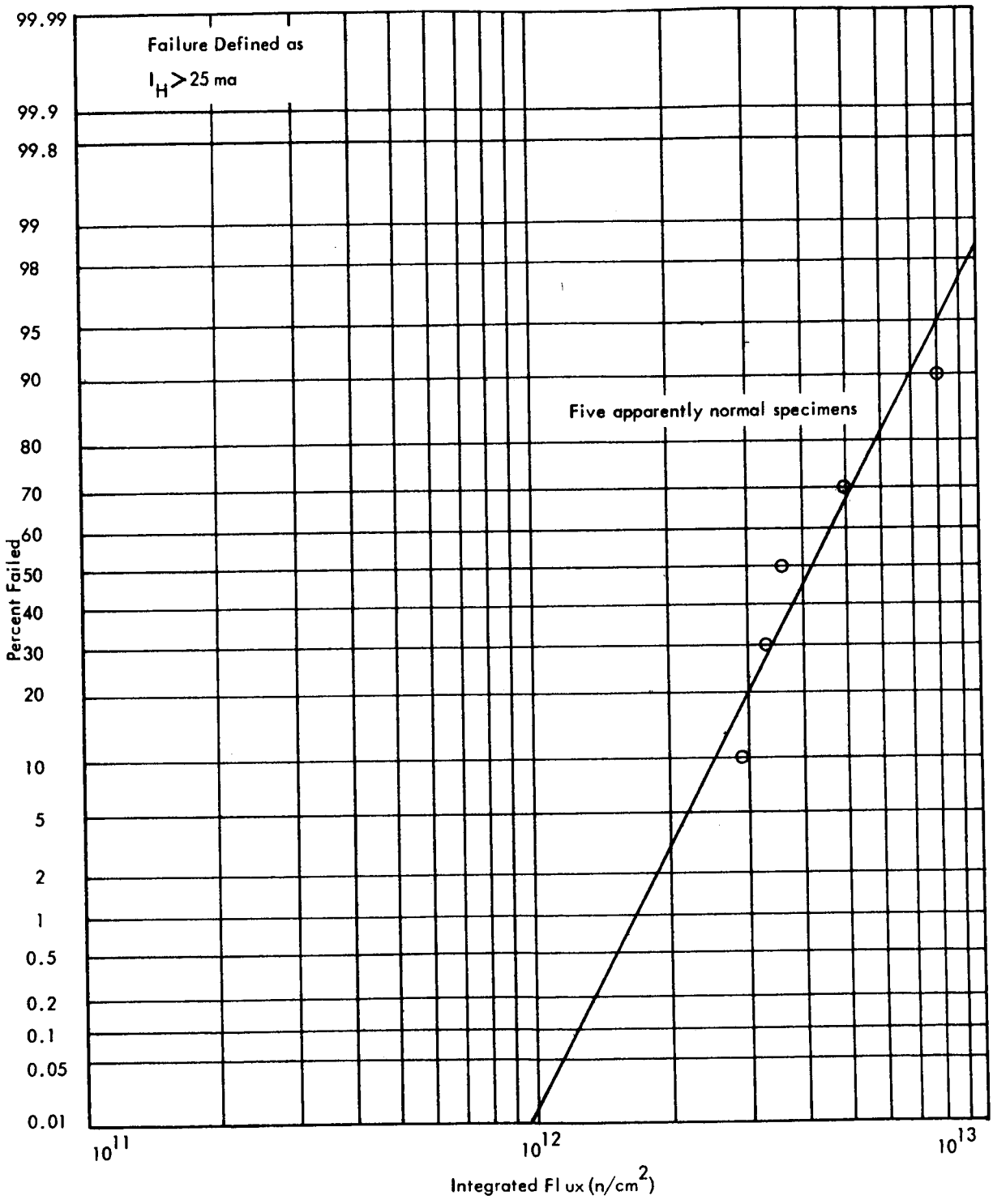

FIGURE 7 SCR 2N1774 - PERCENT FAILED VS. INTEGRATED FLUX

APPENDIX B

FACILITY DESCRIPTION

INTRODUCTION

The Georgia Nuclear Laboratories near Dawsonville, Georgia (Figure 1) area a $15,000,000 research and development complex located on 11,000 acres in the mountains of North Georgia, and are operated by the Lockheed-Georgia Company, A Division of Lockheed Aircraft Corporation. The facility is easily accessible by transportation facilities available at Gainesville, Georgia, 20 miles away, and Atlanta, Georgia, 50 miles distant. Figure 2 shows locations of various major facilities on site.

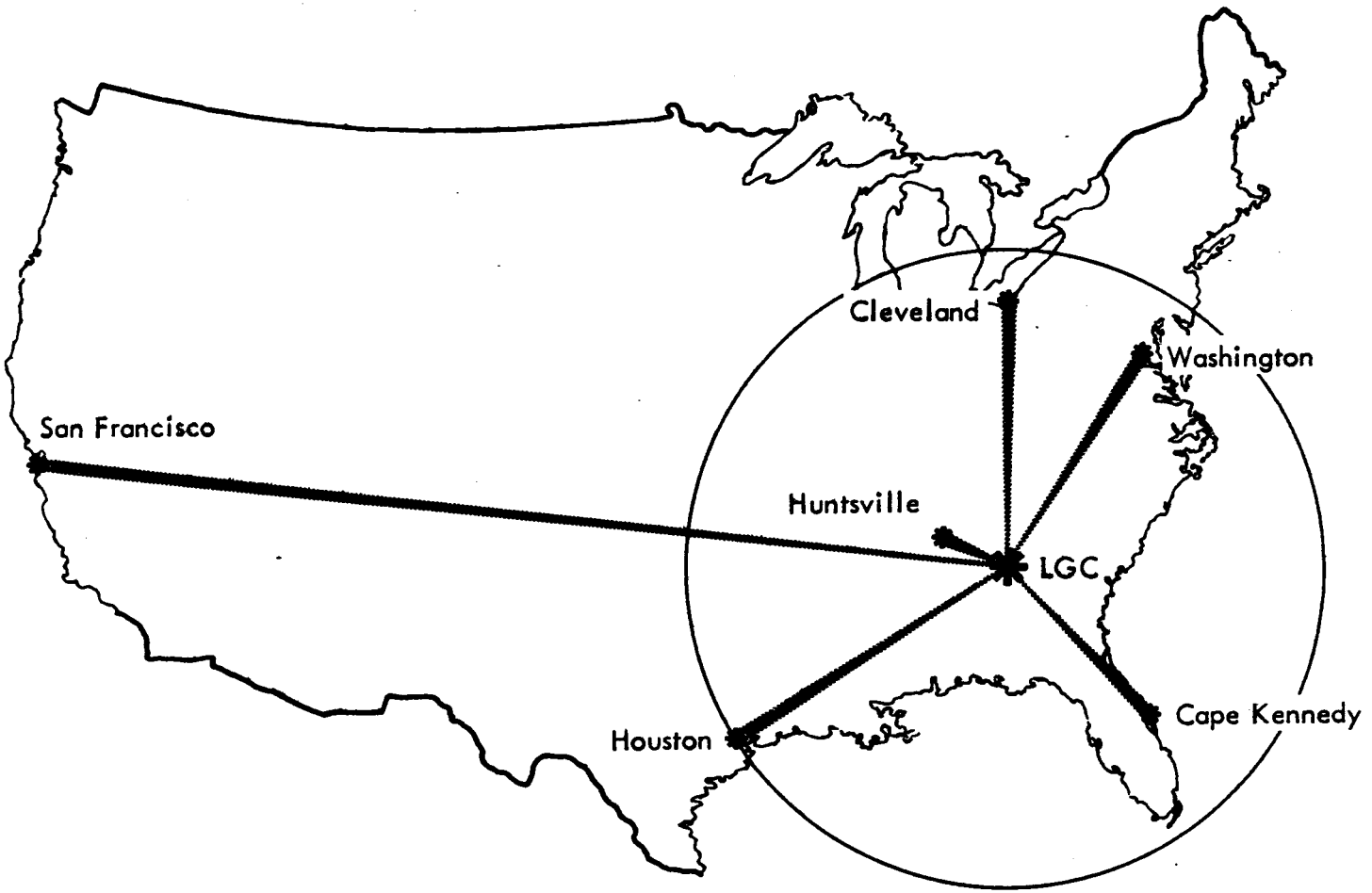

FIGURE 1 SITE LOCATION - LOCKHEED-GEORGIA NUCLEAR LABORATORIES

Georgia Nuclear Laboratories

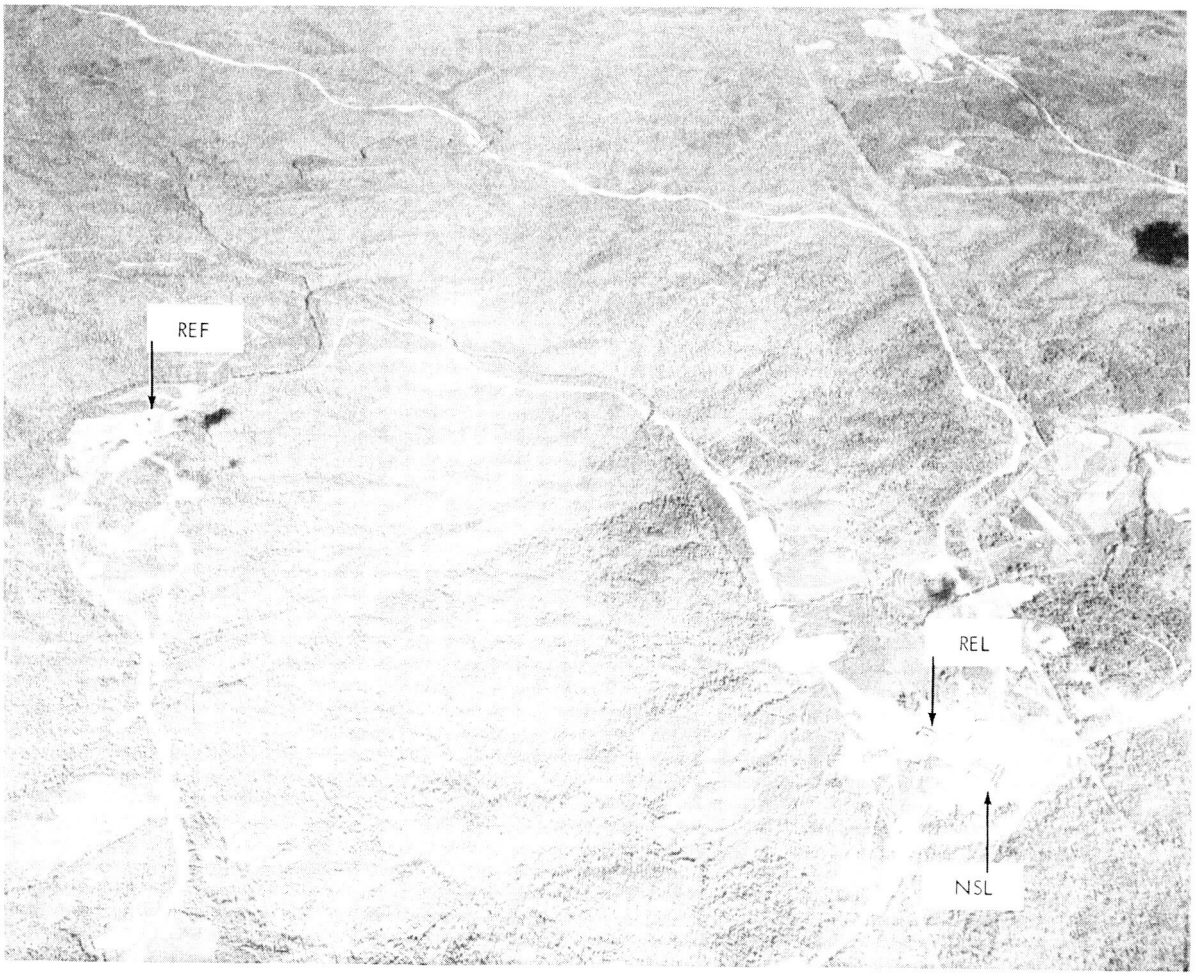

FIGURE 2 GEORGIA NUCLEAR LABORATORIES

LABORATORY FACILITIES

Lockheed facilities at (GNL) Georgia Nuclear Laboratories include a (REL) Radiation Effects Laboratory (Figure 3) and a (NIL) Nuclear Instrumentation Laboratory (Figure 4).

Physical and chemical testing laboratories located in the Radiation Effects Laboratory are capable of handling most present-day radiation effects testing problems both of a routine and research and development nature. Appropriate engineering parameters can be measured to permit definition of the exact nature and extent of radiation-induced degradation.

Equipment located in the Physical Testing Laboratory (Figure 5) includes a 20,000-pound creep rupture tester, 20,000-pound automatic tensile testing machine, Brinell and Rockwell hardness testers, Chemtron microhardness tester, Scott Model L-6 plastic and elastomer tester, B & L metallograph, and others. Environmental equipment available to support the Physical Test Laboratory is shown in Figure 6. The Spectroscopy Laboratory (Figure 7) contains spectrophotometers covering the wave length range from .190 to 25 microns. X-ray diffraction and X-ray spectroscopy equipment are also located there.

Also located in the Radiation Effects Laboratory is a completely enclosed and segragated test area specially designed and constructed to conduct qualification and reliability testing of missile components and parts. The laboratory is environmentally controlled to provide constant temperature and humidity conditions necessary for adherence to present day military testing specifications. Environmental equipment (Figures 8 and 9) is located in a manner conducive to production line testing of a multitude of components simultaneously. Electrical characteristics tests are performed in conformance with MIL Standard 202B. Below are listed some typical environments available within the laboratory.

X-Ray	Shock
Acceleration	Temperature Cycling
Flammability	Temperature Rise
Humidity	Terminal Strength
Moisture Resistance	Thermal Shock
Pressure	Vibration

Laboratory Facilities

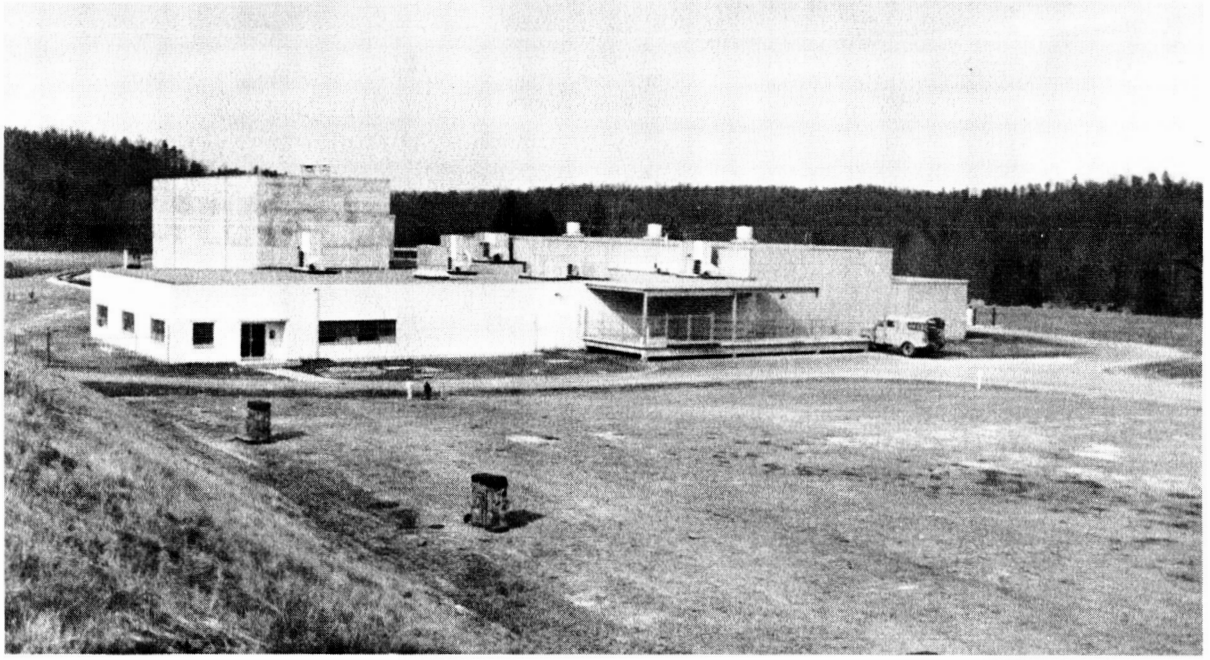

FIGURE 3 RADIATION EFFECTS LABORATORY

FIGURE 4 NUCLEAR INSTRUMENTATION LABORATORY

Physical Testing Facilities

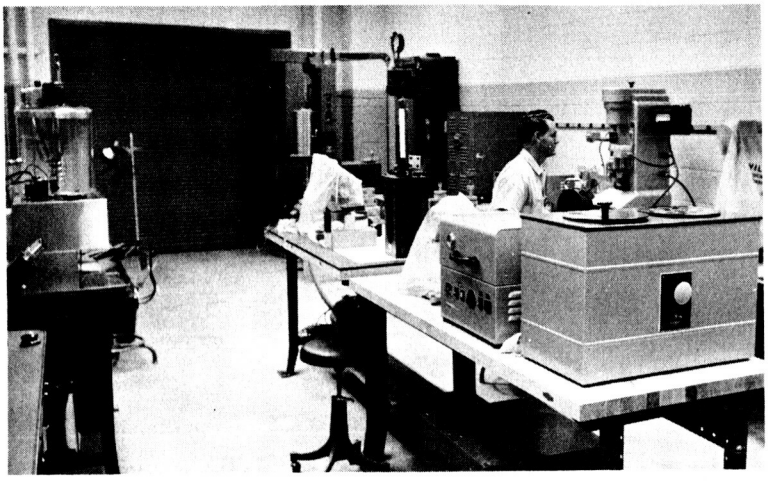

FIGURE 5
PHYSICAL TESTING
LABORATORY

FIGURE 6
PHYSICAL TESTING
SUPPORT LABORATORY

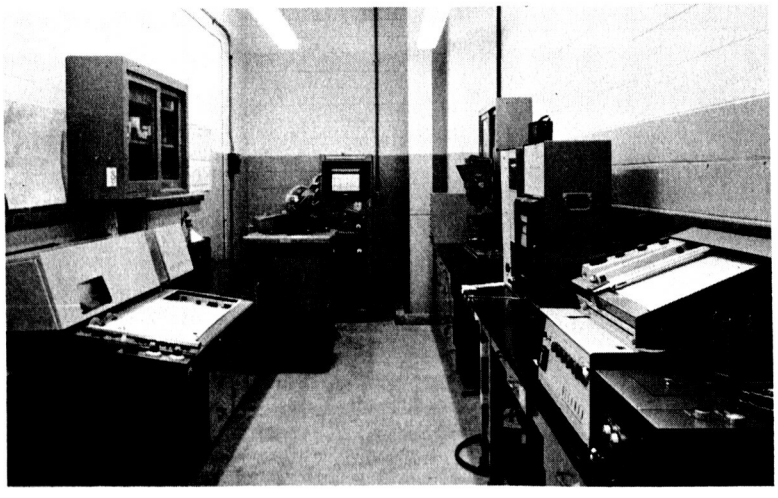

FIGURE 7
SPECTROSCOPY AND
X-RAY LABORATORY

Environmental Testing Laboratory

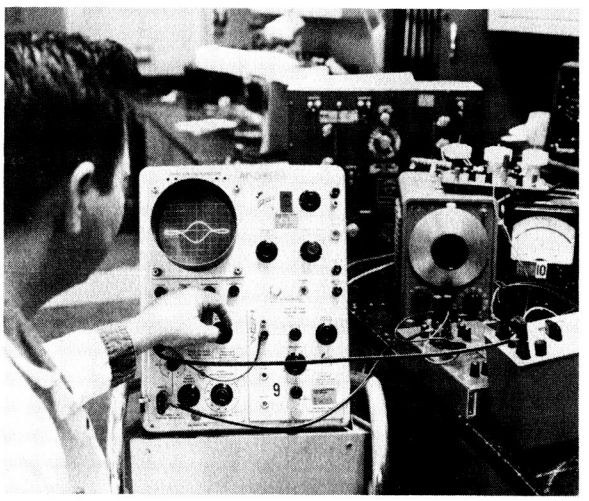

PARAMETRIC MEASUREMENTS AREA

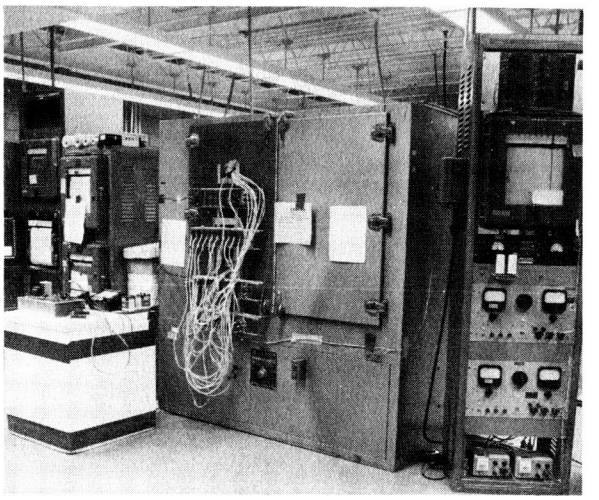

LIFE TEST AREA

FIGURE 8

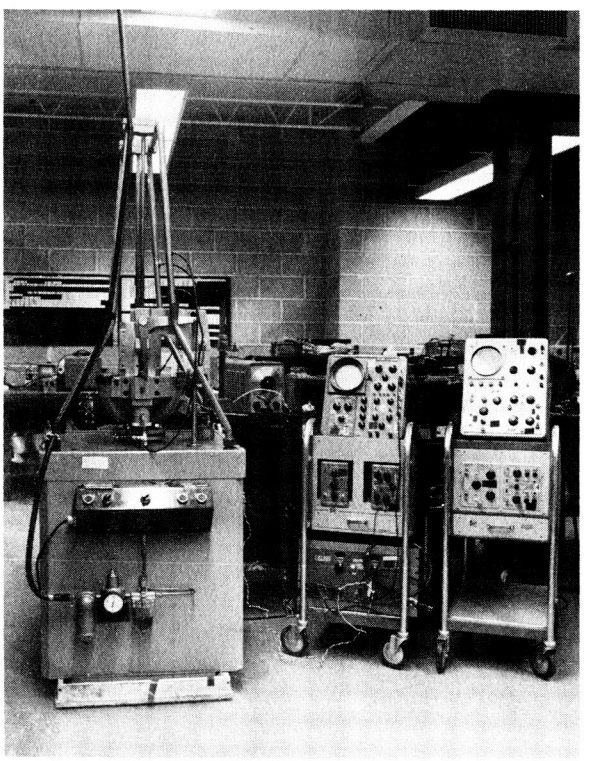

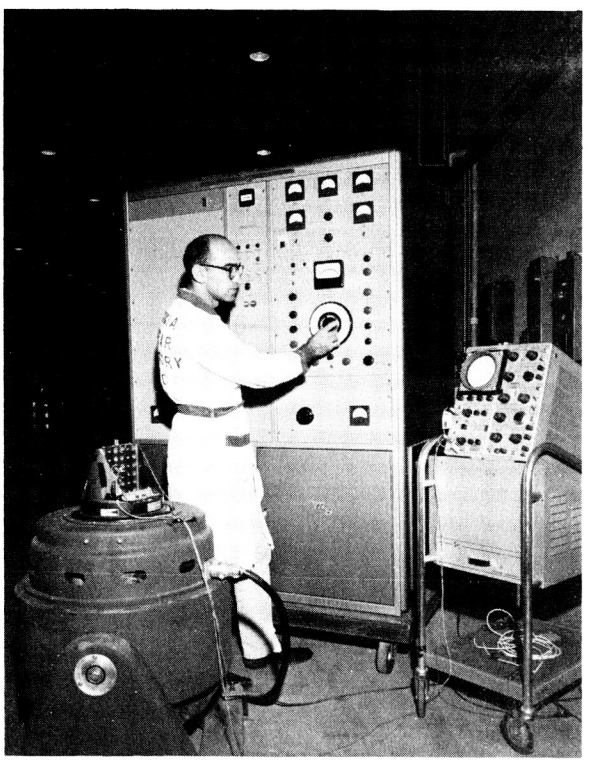

FIGURE 9 VIBRATION, SHOCK AND ACCELERATION TEST AREA

Machine shop facilities in the Radiation Effects Laboratory include a Warm Machine Shop (Figure 10) designed and equipped to perform machining operations on radioactive materials as well as cold machining work. Typical equipment includes lathes, saws, a brake, a shear, and a press. Normal welding equipment is available and in addition many specialized welding jobs can be performed in the shop. Two other small machine shops are available, one in the Nuclear Instrumentation Laboratory and the other at the Radiation Effects Facility.

Electronic and mechanical support facilities are also available in the Radiation Effects Laboratory. These include an Electrical/Electronics Laboratory (Figure 11) which is especially well equipped with diagnostic instrumentation consisting of a wide range of meters, generators, power supplies, amplifiers, and servo devices. The laboratory serves as a means for calibrating instrumentation and test specimens and determining reference parameters for electrical/electronic devices prior to irradiation. This laboratory is complemented by a Mechanical Laboratory (Figure 12) which is located nearby. Development and checkout of control and measuring devices for liquid and gaseous components are performed here. Equipment available consists of a hydraulic test bench, two pneumatic test benches, a flow meter system, pressure gauges, and a number of other pieces of related equipment.

Supporting analytical laboratory facilities available and located in the Radiation Effects Laboratory include: a well equipped Chemistry Laboratory (Figure 13); a High-Level Counting Facility equipped for counting alpha, beta, and gamma emitting isotopes (Figure 14); a Calibration Laboratory (Figure 15); a Standards Laboratory (Figure 16); and a Photographic Laboratory (Figure 17).

Electronic-Mechanical Laboratories

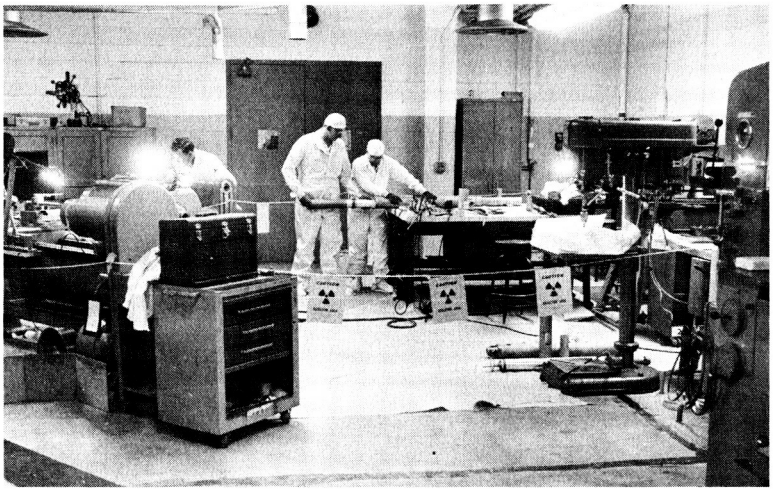

FIGURE 10
WARM MACHINE SHOP

FIGURE 11
WARM ELECTRONICS
LABORATORY

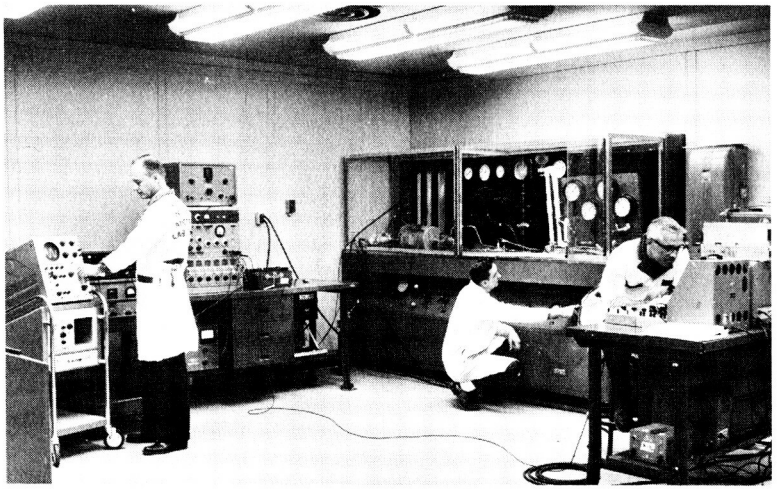

FIGURE 12
WARM MECHANICAL
LABORATORY

Analytical Support Laboratories

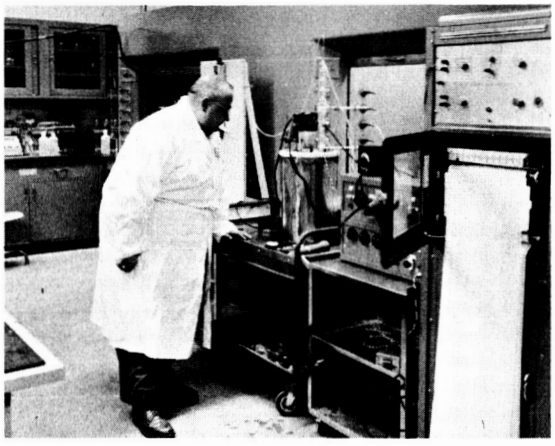

FIGURE 13 CHEMISTRY LABORATORY

FIGURE 14 HIGH LEVEL COUNTING ROOM

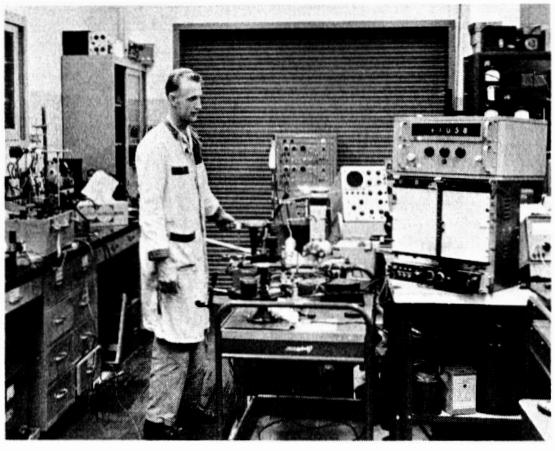

FIGURE 15 INSTRUMENT CALIBRATION LAB

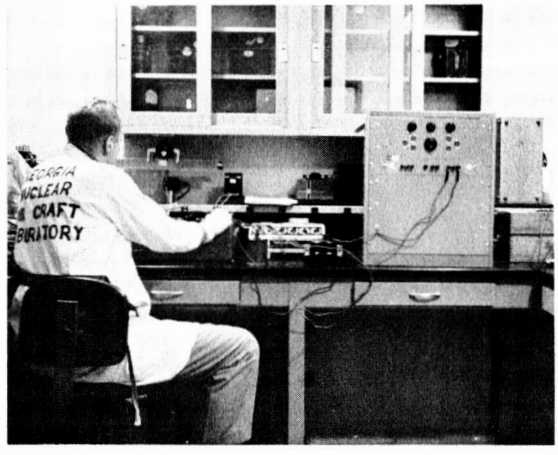

FIGURE 16 STANDARDS LABORATORY

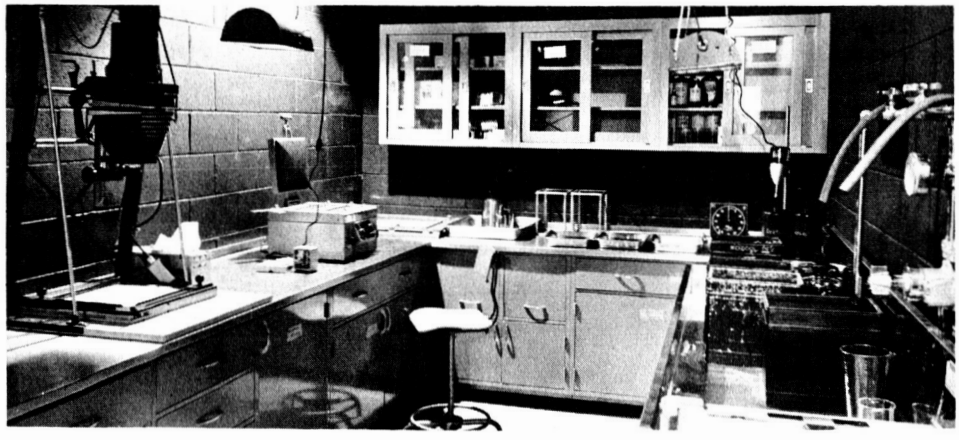

FIGURE 17 RESEARCH PHOTOGRAPHIC LABORATORY

REMOTE HANDLING FACILITIES

Remote handling facilities located in the Radiation Effects Laboratory provide the capability of handling extremely large or small irradiated test systems, components, or materials. The Hot Cell Complex (Figure 18) serves for the remote disassembly, maintenance, reassembly, and testing of irradiated test items and consists of the hot work area (Figure 19), a warm work area, and four hot cells. Removable partition blocks enable one large cell 12 feet wide and 88 feet long to be utilized.

The shielding walls permit safe handling of a source equivalent to 33,000 curies of cobalt-60. The physical size of the cells (approximately 15,000 cubic feet) and services available are compatible with the handling of large or small test articles. The hot cells are equipped with cable and plumbing access to Warm Laboratory hydraulic and pneumatic test equipment. A multitude of wall penetrations will permit the performance of most any type of anticipated experiment.

Remote Handling Facilities

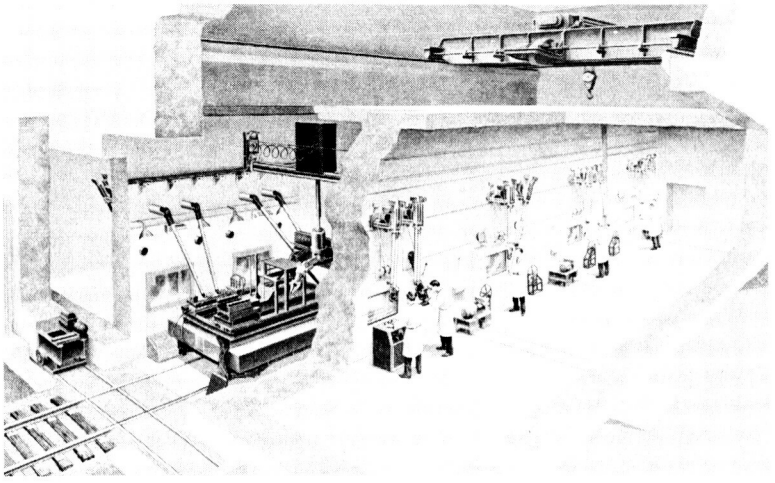

FIGURE 18
HOT CELL COMPLEX

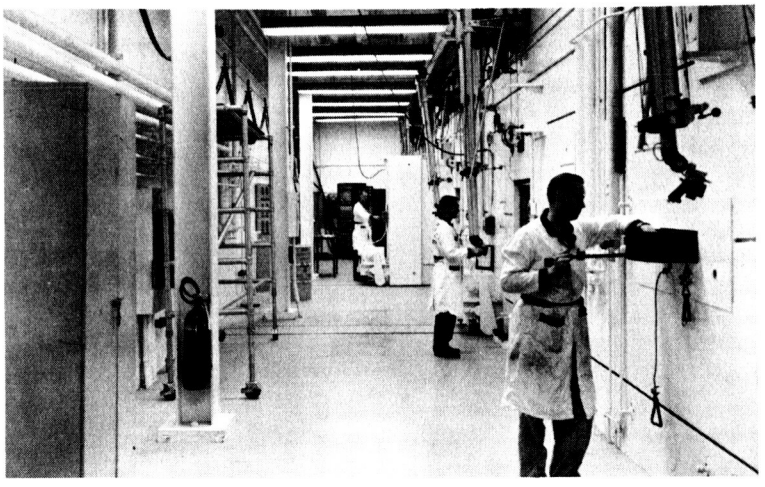

FIGURE 19
HOT WORK AREA

RADIATION TESTING FACILITIES

Reactor facilities at Georgia Nuclear Laboratories include the Radiation Effects Reactor (RER) and the Critical Experiment Reactor (CER). Centrally located in the center of the Georgia Nuclear Laboratories site is the Radiation Effects Facility (Figure 20) where the Radiation Effects Reactor is located along with the underground reactor operations building and other support facilities. A cutaway view of this facility is shown in Figure 22. This area is inter-connected with the Radiation Effects Laboratory and the Nuclear Instrumentation Laboratory by a paved road and a Hot Materials Transport System (Figure 21). The Radiation Effects Reactor (Figure 23) is located in a pool of demineralized water in the center of five test car positions and is raised to an operating position by means of a hydraulic lift. Test irradiation volumes are such that full scale operating systems may be irradiated. Experimental services including electrical and fluid power, test instrumentation, and emergency systems are connected to the test cars through the mating boards located below each test car position. For smaller test specimens, space can be made available inside the pressure vessel.

The underground Operations Building of the Radiation Effects Facility contains all the controls and instrumentation equipment for reactor and the experiment. A reactor control room (Figure 24) is located adjacent to the data acquisition-reduction area (Figures 25 & 26). Data acquisition equipment has the capability of acquiring test data from 700 test points, converting d-c analog, digitizing, performing computations, and presenting plotted and tabulated parameters for engineering evaluation. Nuclear parameters are also cabled from the test article to the data acquisition area.

DESCRIPTION OF TEST CAR POSITIONS RELATIVE TO THE RADIATION EFFECTS REACTOR

Since the Radiation Effects Reactor was designed and constructed principally for radiation effects testing on systems and subsystems, specimens to be irradiated are usually located outside the reactor pressure vessel; however, relatively small specimens have been irradiated inside the pressure vessel immediately adjacent to the active core. The reactor

Radiation Testing Facilities

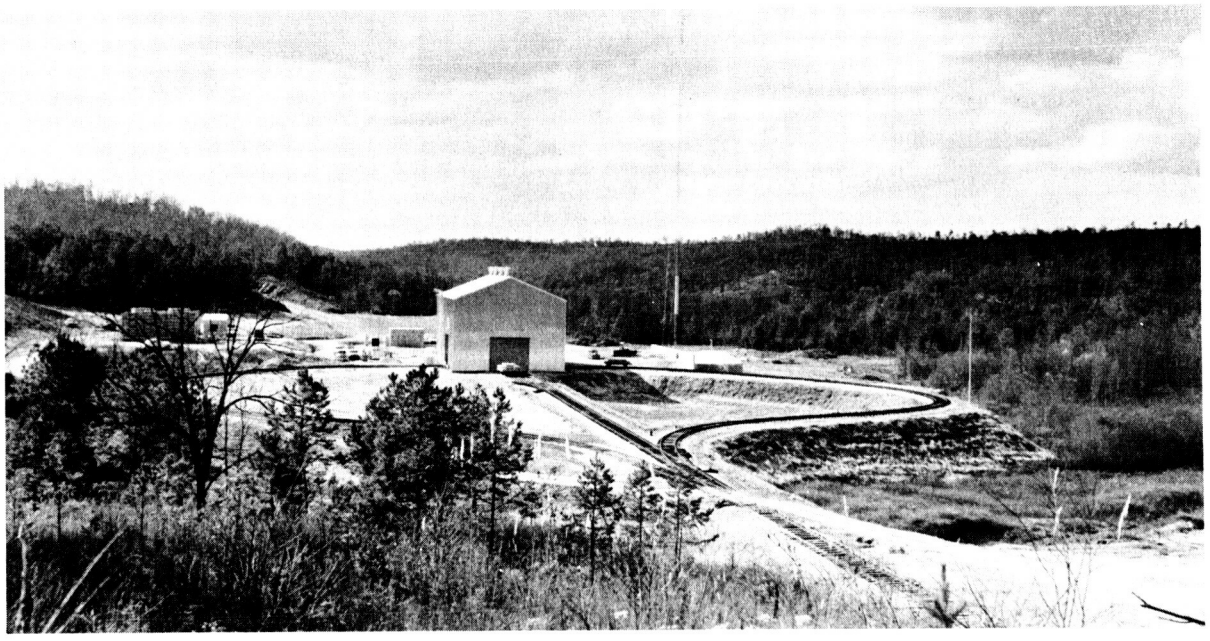

FIGURE 20 RADIATION EFFECTS FACILITIES

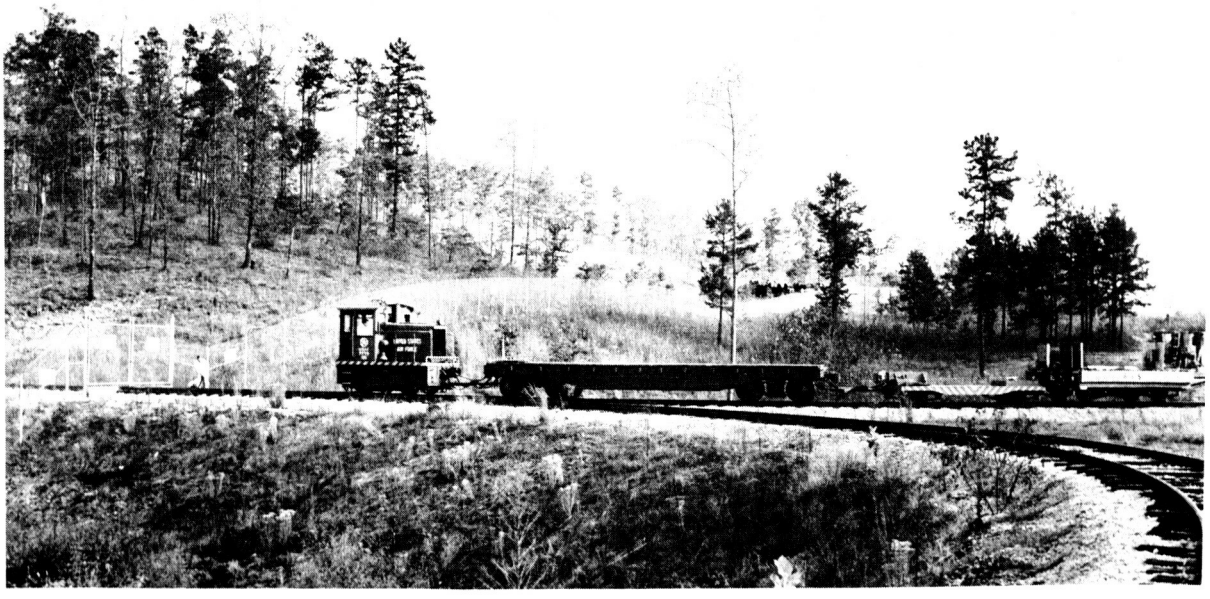

FIGURE 21 HOT MATERIAL TRANSPORT SYSTEM

Radiation Effects Facility

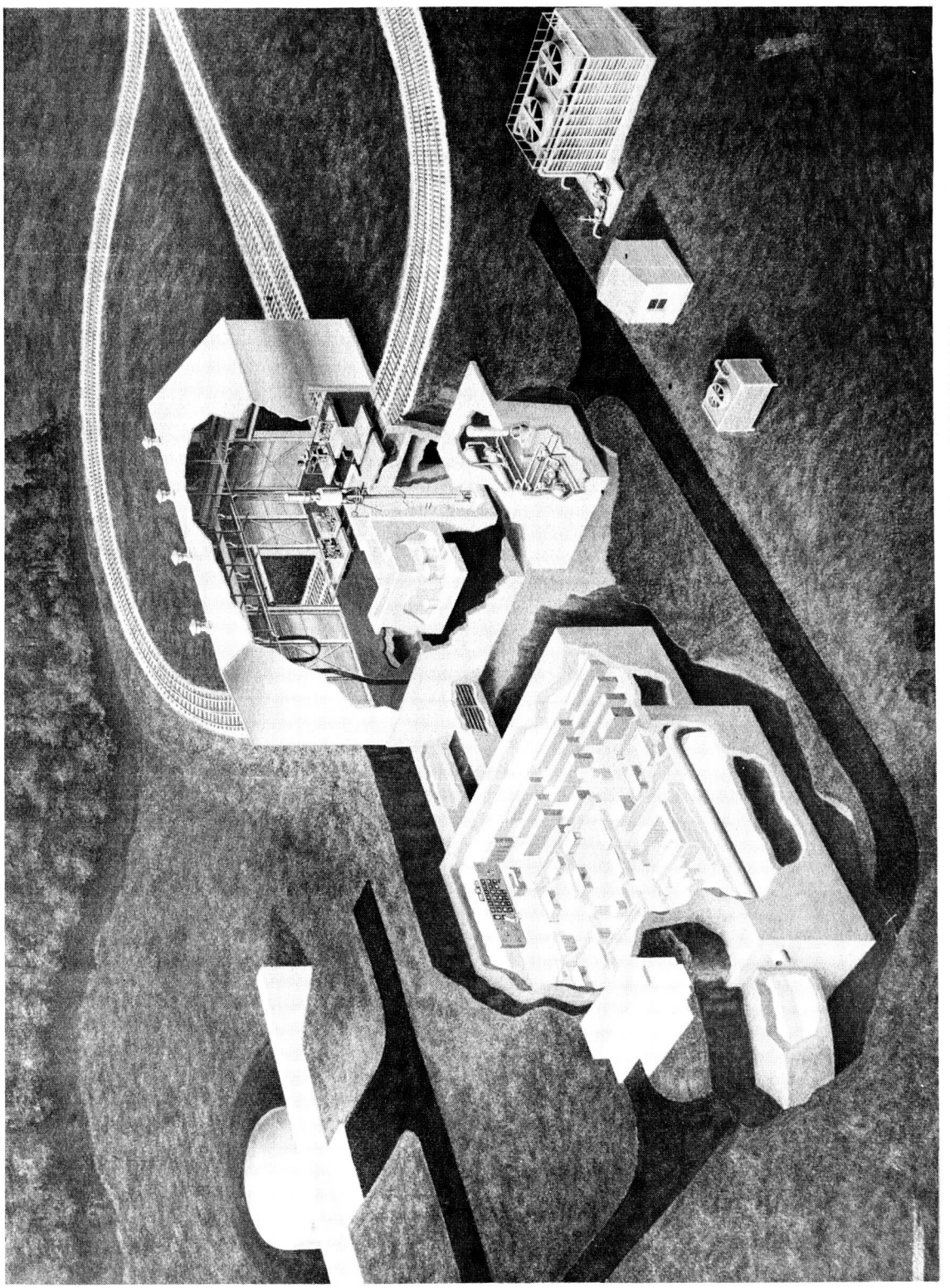

FIGURE 22 RADIATION EFFECTS FACILITY CUTAWAY

Radiation Testing Facilities

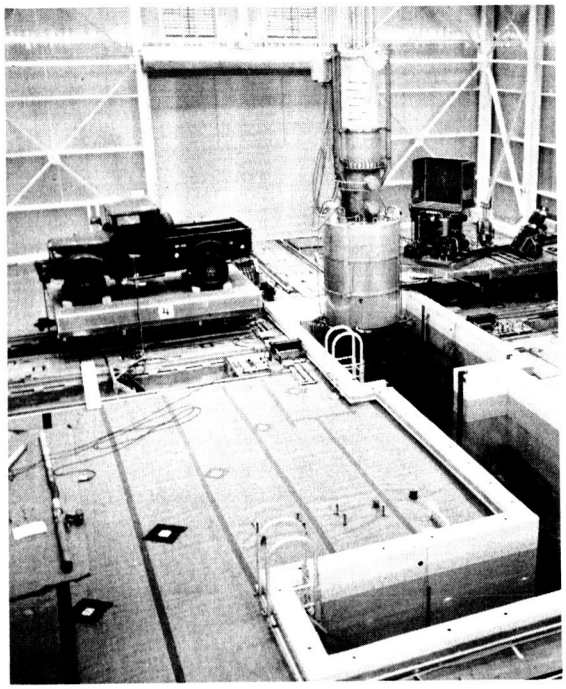

FIGURE 23 RADIATION EFFECTS REACTOR

FIGURE 24 REACTOR CONTROL ROOM

FIGURE 25 DATA ACQUISITION CENTER

FIGURE 26 DATA REDUCTION CENTER

pressure vessel which has a diameter of 33" is surrounded by a shield tank assembly. The outside diameter of the shield tank is 73", thus providing approximately 20" for water shielding if desired. This shielding is normally utilized to alter the neutron to gamma dose rate ratio. The shield tanks are lined with a 1/4" boral liner which is easily removable in front of car positions 5 and 6. The boral liner is used for the purpose of restricting neutron activation as much as possible when high thermal neutron fluxes are not desired on the test specimens. The boral liner decreases the thermal neutron flux approximately a factor of 100. A plan view of the reactor with a perspective showing relative test car positions is shown in Figures 27 and 28 respectively.

Some dimensions of concern are as follows:

Distance from reactor vertical centerline to the front of car extension at Positions 1, 2, 5, and 6 . . . 49"

Distance from reactor vertical centerline to the front of car extension at Positions 3-4 . . . . . 26"

NEUTRON AND GAMMA RAY LEAKAGE FLUXES AVAILABLE

Detailed neutron and gamma ray flux and dose rate data have been obtained in the 5 irradiation volumes above the flat cars, and in smaller volumes around the pressure vessel. Figure 29 presents flux data up to the pressure vessel.

With the shield tanks empty the tissue rad neutron to gamma ratio is approximately 1:5, and with shield tanks full this ratio is approximately 1:30.

Lockheed Report NR-100, available upon request, presents data obtained during a neutron spectral measurement program. It is worthwhile to note that the neutron spectra obtained with RER shield tanks empty are very similar to the pure Watt fission spectrum; however, when the shield tanks are filled, the spectrum is slightly shifted to the lower energy region. Measurements reported in NR-100 were made several feet from the reactor; however, additional fast neutron

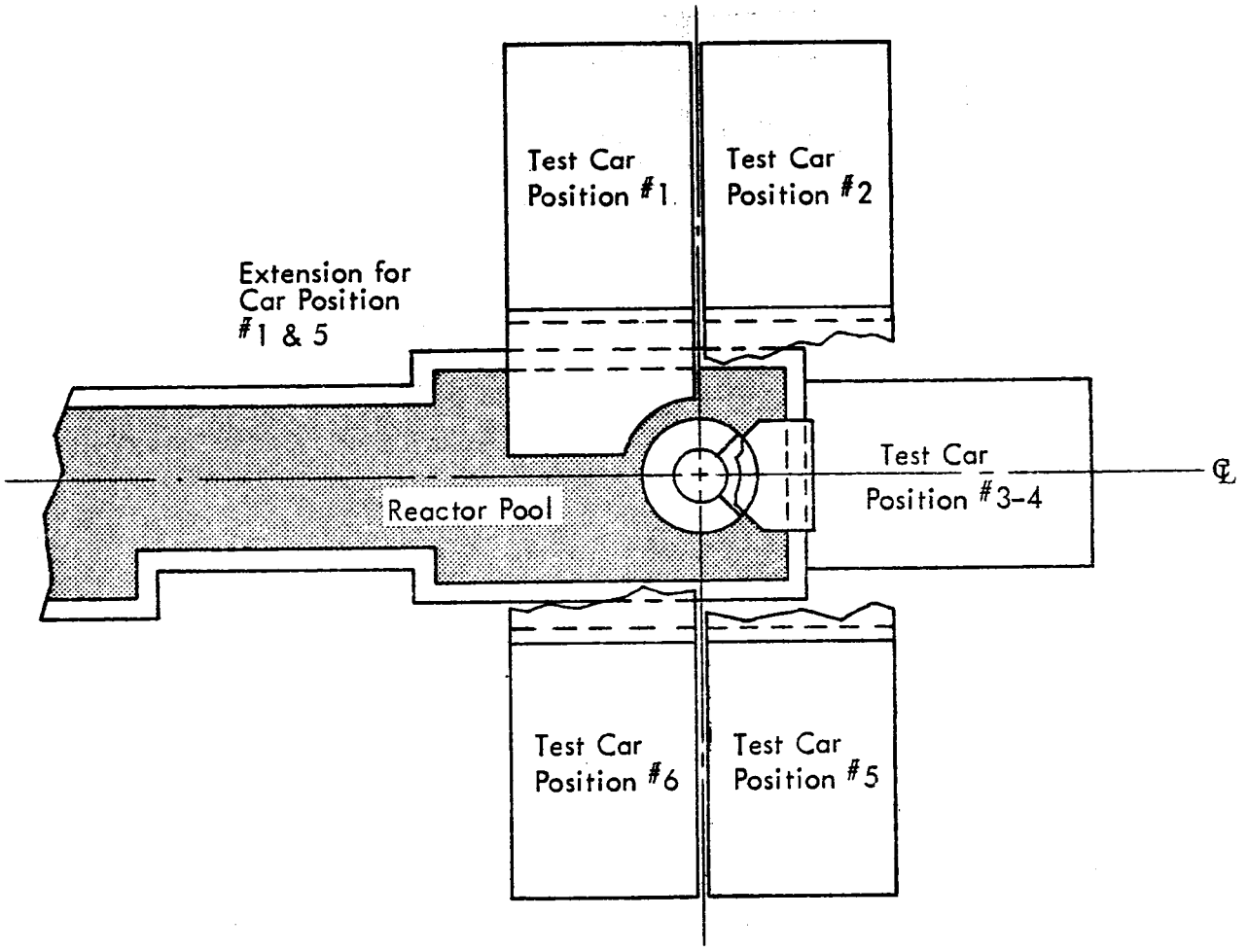

FIGURE 27 RADIATION EFFECTS REACTOR (PLAN VIEW)

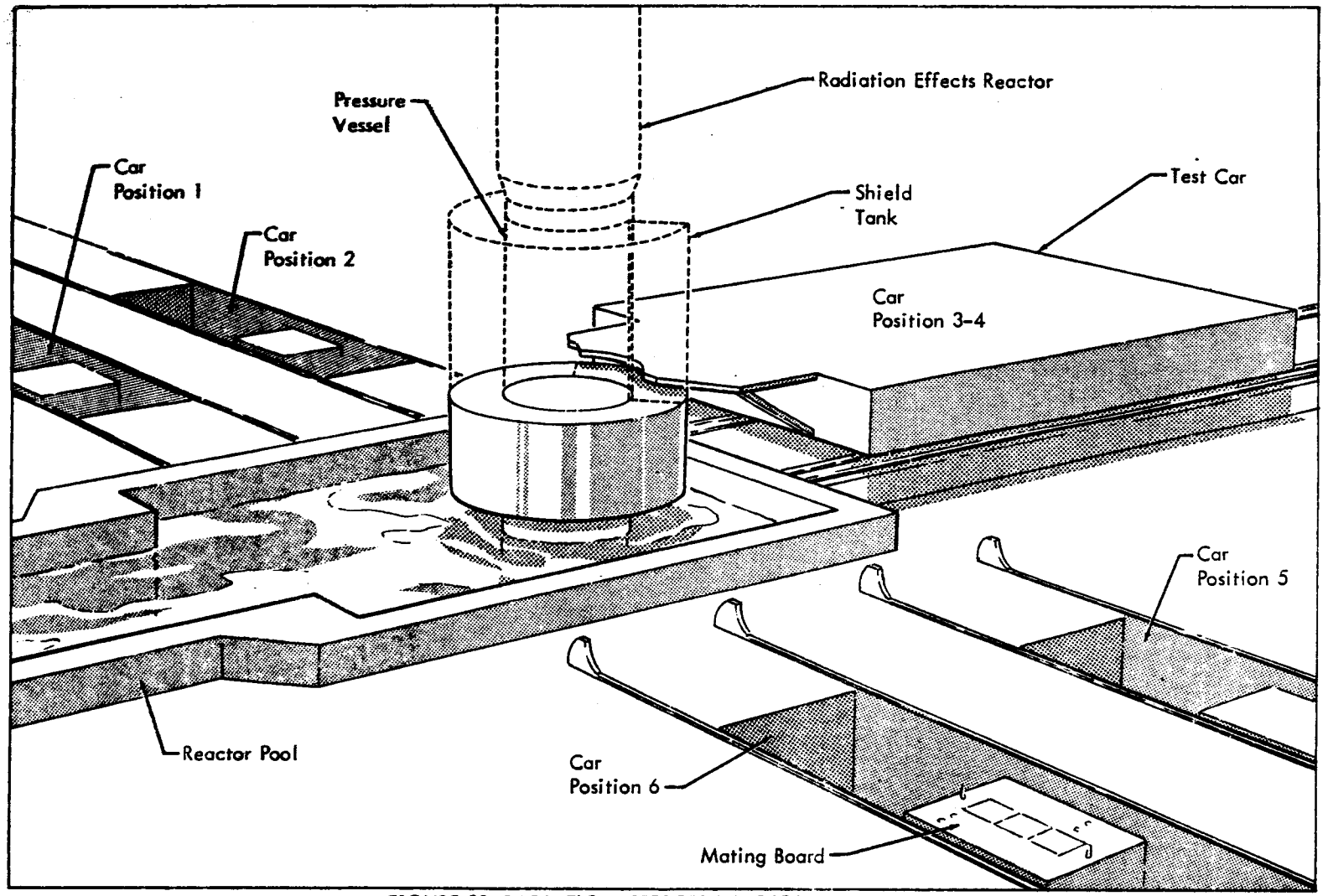

FIGURE 28 RADIATION EFFECTS REACTOR

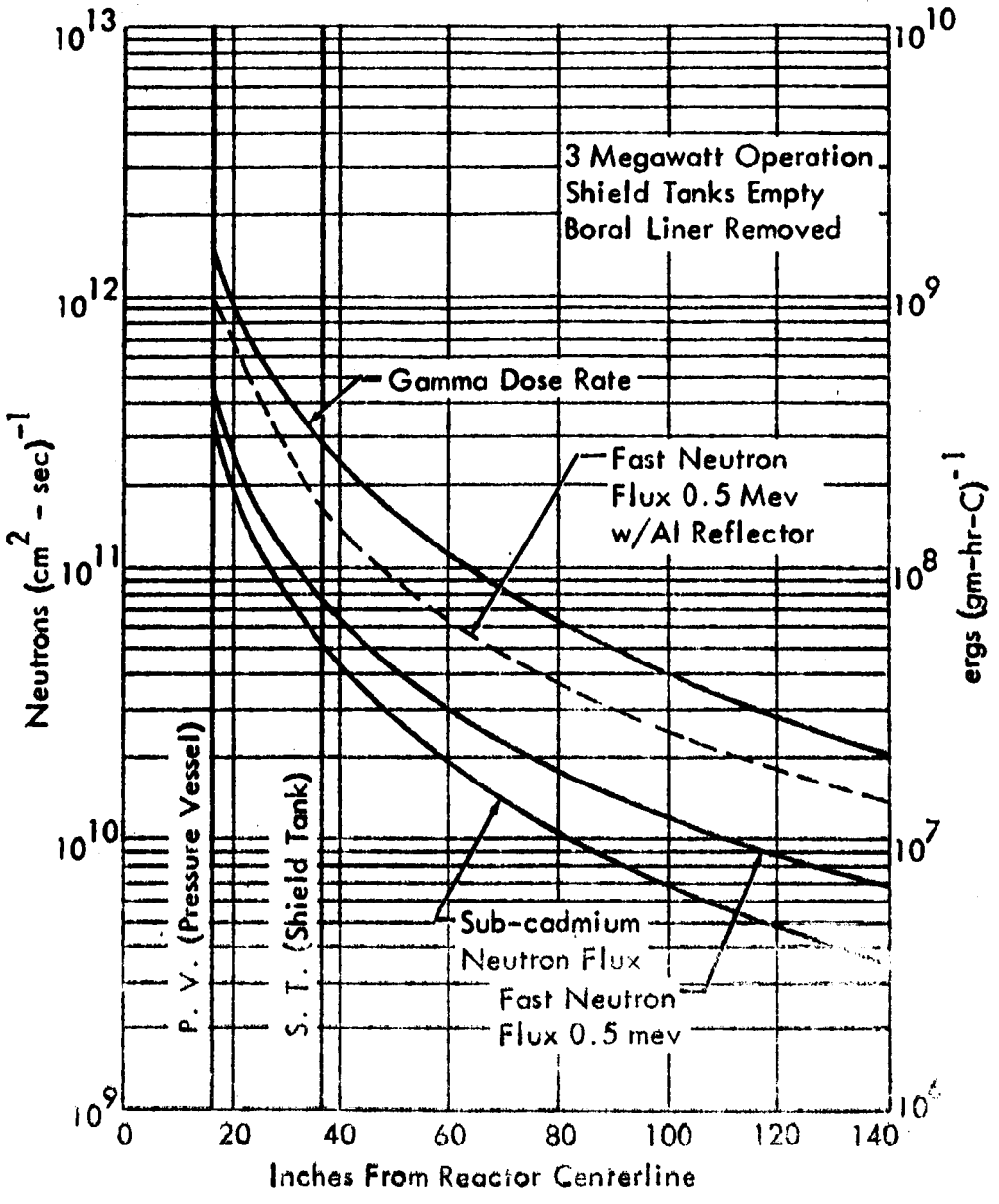

FIGURE 29 GNL - RER FLUX

spectral measurements were made immediately adjacent to the pressure vessel. As shown in Figure 30, this spectrum is also very similar to the Watt fission spectrum. The reactor can be operated on a very short power cycle or on cycles of extended periods of time. Above 10 KW it can be held to within $\pm$ 2% of the desired power level for extended periods. The reactor power can be carried from an insignificant level to 3 MW in less than 1 minute. In general, the Radiation Effects Reactor is very versatile and can be used for many types of irradiations under many varying conditions.

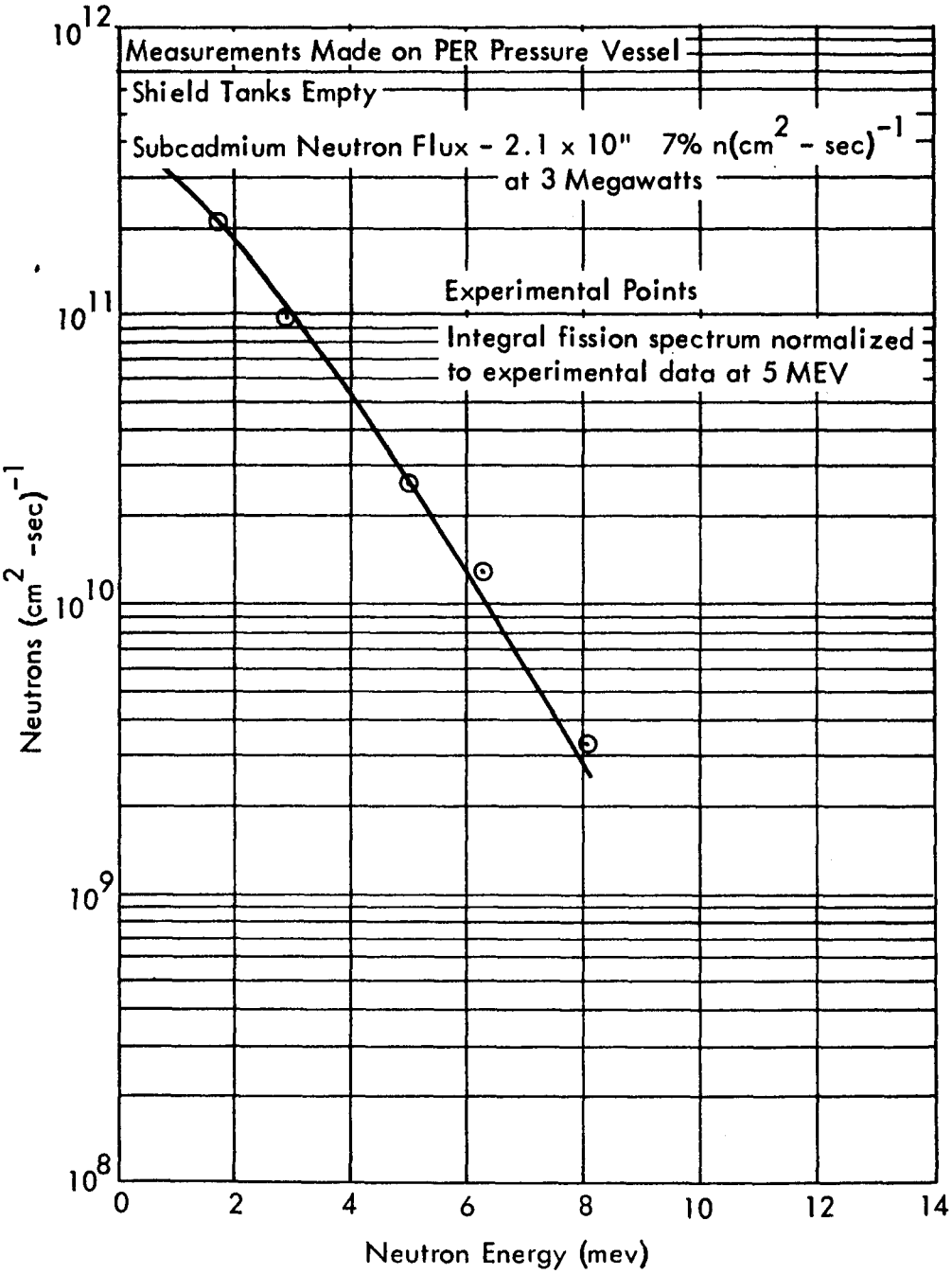

FIGURE 30 FAST NEUTRON FLUX ABOVE EFFECTIVE THRESHOLD ENERGY

SUPPORT FACILITIES

The Mathematical Analysis Department at the Marietta Plant furnishes high speed digital and analog computational services. The digital equipment consists of an IBM 7090 and a Bendix Digital Differential Analyzer. The analog facilities include a Beckman EASE electronic analog computer and a Computer Engineering Associates' direct analogy electric analog computer.

To facilitate maximal use of the Marietta Plant computational equipment by the Georgia Nuclear Laboratories an extensive data reduction center includes such equipment as an IBM 407 Accounting Machine, a reproducing punch, a tape to card converter, a card punch, a sorter, and a Mosley Tape Converter. A graphic presentation showing data flow through the center is presented in Figure 31.

Supporting all these facilities is the Engineering Scientific and Technical Information Center. There, an integrated and continuous scientific and technical information program is planned, developed, and maintained. A comprehensive radiation effects literature file is maintained in order that the most up to date state-of-the-art information is available to engineering personnel. Consultant services are provided on current and anticipated information problems and requirements. Direct affiliations are maintained with AEC, ASTIA, NASA, the Library of Congress, Army, Navy, Air Force, and other governmental and industrial information centers.

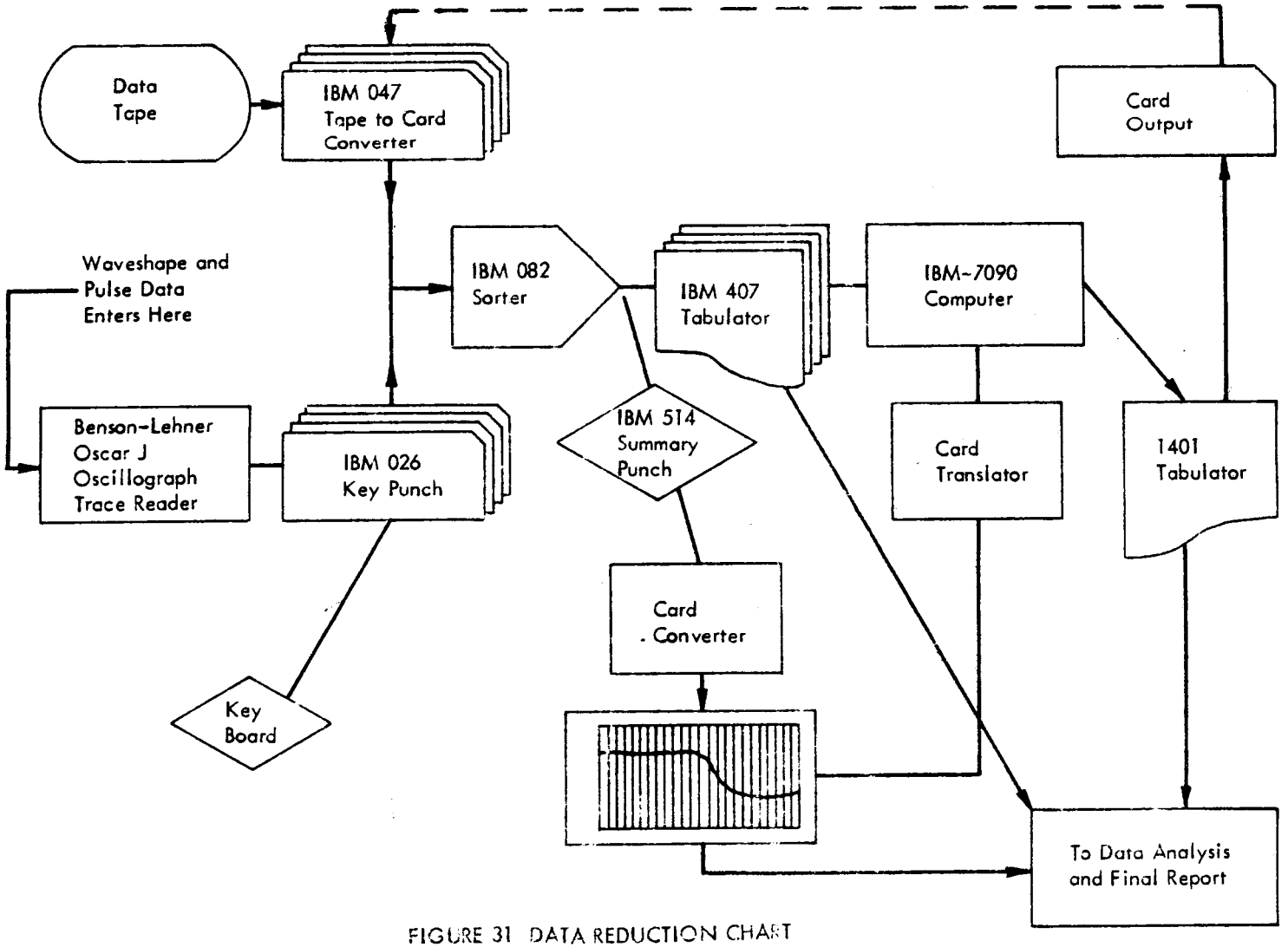

FIGURE 31 DATA REDUCTION CHART